Role of the nasal septal cartilage in midfacial development

Ayman Al Dayeh

A dissertation submitted in partial fulfillment of the requirements for the degree of

Doctor of Philosophy

University of Washington

2012

Reading committee

Susan W. Herring, Chair

Anne Marie Bollen

Tracy Popowics

Program Authorized to Offer Degree:

Oral Health Sciences

University of Washington

Abstract

Role of the nasal septal cartilage in midfacial development

Ayman Al Dayeh

Chair of the Supervisory Committee:

Professor Susan W. Herring

Department of Orthodontics

The role of the nasal septal cartilage in midfacial growth has been an ongoing intellectual dilemma. While some authors believe that the septal cartilage is the driving force for midfacial growth, others believe that the cartilage role in midfacial growth is passive and it acts as a vertical strut that supports the midface against masticatory loads. This dissertation evaluated the above hypotheses using a pig animal model to measure the in vivo growth and the mechanical deformation of the nasal septal cartilage during mastication.

The in vivo growth of the nasal septal cartilage and nasofrontal suture was measured in real time using linear displacement transducers. In addition, cellular proliferation of the septal chondrocytes was evaluated. The results showed that the growth strain rate of the nasal septal cartilage (0.07 ± 0.03 % length/hour) was significantly higher than that of the nasofrontal suture (0.03 ± 0.02% length/hour) and that the growth of the cartilage tended to precede the separation of the suture. In

addition, cellular proliferation analysis revealed that the septal chondrocytes are proliferating at a relatively high rate (22 ± 5.0% /24 hours).

Deformation of the septal cartilage and nasofrontal suture during mastication was assessed utilizing linear displacement transducers. The results showed that the septal cartilage and the nasofrontal suture are compressed in an anteroposterior direction during mastication with the magnitude of deformation of the septal cartilage (1000 to 2700 με) comparable to the deformation of the suture (2000 to 4000 με).

The mechanical properties of the septal cartilage were evaluated. The results revealed that the septal cartilage is highly adaptable to compressive loading and that its stiffness is much lower than stiffness of surrounding bones.

In conclusion, the results of this thesis support the hypothesized active role of the nasal septal cartilage in midfacial growth. On the other hand, the hypothesis that the septal cartilage acts as a vertical strut during mastication was not supported.

Table of contents

List of Figures

List of Tables

Acknowledgments

I would like to express my sicere appreciation to my advisor, Dr. Sue Herring for her constant patience, guidance and support throughout this journey. Her devotion and enthusiasm for scientific knowledge will strongly impress my future career.

I would also like to express my deep appreciation for my supervisory committee: Drs. Anne Marie Bollen, Ariel Raigrodski, David Eyre, Greg King and Tracy popowics for their insightful comments throughout different stages of this research

I would like to extend my appreciation to Drs. Katherine Rafferty and Mark Egbert for their enormous help in this research especially in conducting the complicated pig surgeries. I would also like to thank Dr. Karl Kiyala for his valuable input in the statisitcal analysis of the second chapter of the study.

I wish also to extend my thanks to the students and assistants working in Dr. Herring lab: Ms. Patricia Emry taught me the basics of tissue preparation and sectioning, Tori Mathys assisted me in histologic analysis, Alice Nunes and Adam Veitschegger for their help in the mechanical testing, Terrence Laurence and Isabel Hujoel for their help in histology.

My great appreciation goes to the faculty and staff of Oral Health Sciences for their constant guidance throughout the last seven years. Special thank to Ms Jennifer Kohn and Ms Eileen Kakida for their constant assistance and help.

I especially thank the faculty and staff in the Department of Orthodontics for their constant help and support as I was studying concurrently in the Departments of Oral Health Sciences and Orthodontics for two and half years.

Special Thanks goes to my classmates and fellow residents in the Departments of Oral Health Sciences and Orthodontics for their friendship throughout my graduate study.

My deepest gratitude and appreciation goes to my mother, father and brothers for their unconditioned love and support. Their constant belief and encouragement throughout my life is the greatest gift that helped me throughout my past, current and future career and life.

Chapter I: Introduction

Craniofacial sutures serve as major postnatal growth sites (Opperman 2000). However, studies showed that extirpation of sutures does not result in retardation of craniofacial growth (Babler et al. 1982), indicating that sutures lack intrinsic growth potential (Enlow and Hans 1996). Rather, they grow in response to forces that tense the sutural tissue, resulting in bone formation at the sutural edges (Scott 1953; Persson et al. 1979; Rönning 1995; Thilander 1995; Opperman 2000). Using external forces to distract sutures and thus modify facial growth is common in orthodontic practice, such as using a palatal expander to distract the midpalatal suture (Garrett et al. 2008). The identity of physiologic forces that distract sutures has been addressed extensively in literature; most studies support the idea that growth of internal soft tissue is the major source of such force. For example, growth of the brain tenses the calvarial sutures (Persing et al. 1991; Huggare and Rönning 1995; Opperman 2000; Ogle et al. 2004) and expansion of the eyeball tenses the orbital sutures (Sarnat 1980). The source of the force that separates midfacial sutures has been an intellectual dilemma. Scott (1951, 1953), suggested that the expansion of the nasal septal cartilage stretches the midfacial sutures including the nasofrontal suture. This theory was refuted by Moss (1968), who suggested that the growth of the nasal septal cartilage is passive and it is simply one aspect of midfacial growth that increases the size of the nasal cavity and nasal capsule in response to increased functional demands such as breathing. Evidence for an active role of the nasal septal cartilage in midfacial growth comes mainly from extirpation

experiments. As will be explained in greater details below, partial or total extirpation of the septal cartilage resulted in retardation of growth in different groups of animals (Sarnat and Wexler 1966; Kvinnsland 1974; Verwoerd et al. 1980). However, these findings were not universal. Some extirpation experiments have shown that the resultant changes after septal cartilage extirpation are truly a collapse of the nasal bone rather than retardation of anteroposterior growth (Moss et al. 1968; Stenström and Thilander 1970). Furthermore, Moss (1968) offered an alternative "biomechanical explanation" that the nasal septum acts as a vertical strut preventing the collapse of the nasal cavity and keeping the airway patent. Extirpating of the septal cartilage deprived the nasal cavity of this "vertical strut" and resulted in the collapse of the nasal bones, giving the appearance of anteroposterior shortening, but not actually retarding growth. Such controversy raises the need to further investigate the role of the nasal septal cartilage in midfacial growth and in facial integrity.

The central goal of this thesis, therefore, is to study the role of the nasal septal cartilage in midfacial growth and in facial integrity to determine if the septal cartilage plays an active role in midfacial growth and to determine if it acts as a vertical strut preventing the collapse of the nasal bones.

Relation of the nasal septal cartilage to growth of the midface

The active role of the nasal septal cartilage in powering midfacial growth was popularized by Scott (Scott 1953), who described the septal cartilage as a primary cartilage that is the extension of the cranial base. He theorized, because of that origin, that the septal cartilage "in its growth, it separates the facial bones from one another

and from the cranial portion of the skull and allows growth to take place at the sutures" (Scott 1953). Evidence supporting an active role of the septal cartilage in midfacial growth comes mainly from two types of experiments: studying the growth of the cartilage in vitro and observing the resultant midfacial growth after septal cartilage extirpation. Copray (1986) reported that the septal cartilage of 4 day-old rats is capable of growing independently in organ culture while retaining its shape and generating growth pressure, especially in the anteroposterior direction. He concluded that because of its independent growth potential and ability to generate growth pressure, the cartilage acts as a growth center separating the facial sutures. Species in which partial extirpation of the septum retarded midfacial growth included rabbits (Sarnat and Wexler 1966; Wong et al. 2010) and rats (Kvinnsland 1974). However, conflicting results were seen in rats (Moss et al. 1968) and in guinea pigs (Stenström and Thilander 1970), where extirpation of septal cartilage resulted in collapse of the nasal bone with minimal effect on the anteroposterior facial growth.

Both types of experimental approaches have limitations. Organ culture is clearly not representative of the in vivo situation. Extirpation of the septal cartilage is associated with surgical trauma that might alter the normal cartilage growth. In addition, variability in extirpation sites is unavoidable. Above all, both culture and extirpation experiments lack the direct measurement and comparison of the growth of the cartilage to the sutures it is thought to separate. Finally, all previous studies involved species (rabbits and rodents) with evergrowing incisors. Any condition that interferes with occlusion or incisal wear (i.e., any surgical trauma) could itself affect midfacial growth.

One of the goals of this study is to improve on these experimental approaches by offering a direct measurement of the growth of the septal cartilage and the nasofrontal suture, in order to determine if growth of the cartilage leads to separation and growth of the suture. The studies utilized a species with rooted incisors, minipigs.

Contribution of chondrocytic proliferation to the overall growth of the cartilage

Cellular proliferation and chondrocytic hypertrophy together with matrix formation results in growth of the cartilage(Seinsheimer and Sledge 1981). Cellularity and proliferation were chosen for study, considering that the cells are also the source of the enlargement due to hypertrophy and matrix synthesis. The cartilaginous nasal septum is continuous posteriorly with the perpendicular plate of the ethmoid and with the cranial base at the presphenoid bone. Histologically, the arrangement of the chondrocytes at these two locations is similar to that of a growth plate, at least in very young animals, cell division followed by endochondral bone formation has been observed at these two sites (Stenström and Thilander 1972; Wealthall and Herring 2006), indicating that they are contributing to anteroposterior midfacial growth by pushing the septal cartilage forward. This raises the question whether the growth power of the cartilage is a result of interstitial expansion or an anterior thrusting of the cartilage as a result of cartilage growth at its junctions with presphenoid and ethmoid bones. Wealthall and Herring (2006) measured the endochondral mineralization at the posterior end of the septum in 0 to 15 day- old mice and reported that the observed growth cannot account for the much larger increase in length of the septum, supporting the existence of other mechanisms of growth such as cellular proliferation and matrix formation in more

anterior locations of the septum. Searls' work on albino rats (Searls 1977; Searls 1979) showed that the septal chondrocytes of 0, 5 and 10 day-old animals are proliferating and possibly contributing to the growth of the septal cartilage. Furthermore, he reported regional variability within the septum that altered from 0-15 days of age. Such regional variability was also reported in rabbits (Long et al. 1968). This variability might partially explain the inconsistent outcome of extirpation. If various parts of the cartilage are growing at different rates, then extirpation of the fastest growing sites will result in a more detrimental effect on the growth compared to slower growing sites. I used pigs of similar age (4-6 months) in all the in vivo parts of this thesis, including the examination of cellular proliferation. This eliminated age as a variable in the study, although regional variation still had to be assessed.

Nasal septal cartilage and facial integrity

The bony rostrum is formed dorsally by the nasal bones and laterally by the maxillary bones. Its floor is formed by the palatine processes of the maxillary bones and palatine bones. The rostrum houses the nasal cavity, which is divided by the nasal septum stretching from the ethmoid bone posteriorly to the external nose. Badoux (1966, 1968) visualized the rostrum as a framed structure with the surrounding bones forming the bars and the sutures acting as joints. He postulated that the arrangement of the bones of the rostrum renders it an "imperfect framed structure" that is weak and prone to collapse under loads. This is especially important since the nasal cavity is in close proximity to the dentition and thus subject to heavy loading during mastication. He suggested that the nasal septum acts as a vertical strut reinforcing the weak structure of the rostrum, preventing its collapse under masticatory loading. This reasoning was cited

to explain the collapse of the nasal dorsum after extirpation of nasal septal cartilage in young guinea pigs (Stenström and Thilander, 1970) and in rats (Moss et al., 1968). Nevertheless, this explanation seems less than compelling, given that the septum is comprised of cartilage, not bone. Cartilage is usually weaker and more flexible than bone which challenges the hypothesized strut role of the septal cartilage. Cartilage in the body is typically thought of serving rapid growth in juveniles and serving for shock absorption in adults.

Mastication is the major source of the physiologic loading of the skull (Kiliaridis 1995; Katsaros 2001; Kiliaridis 2006). The snout especially, due to its proximity to the dentition is heavily loaded during mastication (Rafferty and Herring 2002). Despite the great body of knowledge regarding the physiologic strain in various facial bones and sutures (Rafferty and Herring 1999; Herring and Teng 2000; Herring et al. 2001; Rafferty et al. 2003), there are no previous data on the in vivo loading of the nasal septal cartilage. This can be attributed to the deep location of the cartilage that makes surgical access difficult. In addition, the strain gages traditionally used to measure bone and sutural strain cannot be glued to the septal cartilage.

In this study I use a novel approach to measure the strains generated on the septal cartilage during mastication in order to determine the mechanical importance of the septal cartilage for the integrity of the face and to assess whether the septal cartilage acts as a vertical strut during mastication as suggested by Badoux (1966, 1968) and Moss (1968).

.

Mechanical properties of the cartilage

The notions that septal cartilage growth separates the facial sutures and that the cartilage supports the nasal cavity, dictate that the cartilage of the septum is mechanically capable of withstanding such loads. If the septum thrusts the facial bones apart, then the resistance of the facial sutures will place the septum under compression, both vertically and anteroposteriorly. If the cartilage acts as a strut, then it should be rigid enough under vertical compression to support the nasal cavity. If the septal cartilage is adapted to any of these loading regimes, then a directional difference in its strength and stiffness is expected. Therefore understanding the mechanical properties of the septal cartilage will help to support or refute the above hypotheses.

Cartilage is a viscoelastic tissue with both solid (matrix) and liquid phases. The solid phase is composed predominately of collagen fibers and proteglycans. The matrix has a high negative charge and absorbs and retains water (Mathews and Decker 1977). This complex composition gives rise to a well documented nonlinear response to tensile and compressive loads (Huang et al. 2001). The intrinsic compressive properties are dictated by the interaction between proteoglycan and water content while the tensile properties are dictated by the collagen content (Huang et al., 2001). In addition, because of the charged nature of the matrix, the loading rate is an important determinant of the mechanical properties of the cartilage. Although mechanical properties of nasal septal cartilage have been studied previously (Wong et al. 2001; Naumann et al. 2002; Rotter et al. 2002; Chao et al. 2003; Gaon et al. 2003; Richmon et

al. 2005; Grellmann et al. 2006; Richmon et al. 2006; Westreich et al. 2007), these studies were carried out under varying sample preparation testing protocols and loading speeds that generally differed from physiological conditions. In this thesis, I assess the tensile and compressive mechanical properties of porcine septal cartilage under loading rates and experimental settings that help to test the in vivo role of the septal cartilage in facial growth and integrity.

Research goals

The septal cartilage is postulated to play an active role in midfacial growth, stretching the facial sutures and resulting in bone formation at the suture edges. In addition, it is theorized that the cartilage acts as a vertical strut, supporting the nasal cavity, preventing the collapse of the nasal bone under masticatory loads. The overall research goal of this study was to determine if the septal cartilage plays an active role in the growth of the midface and whether it functions as a mechanical strut supporting the nasal cavity.

The overall research goals were approached through four immediate goals. The first goal was to measure the in vivo expansion of the nasal septal cartilage and nasofrontal suture. The second goal was to determine the location and rate of cellular proliferation in the septal cartilage. The third goal was to measure the deformation of the septal cartilage and the overlying nasofrontal suture during mastication and during masseter stimulation. The fourth goal was to assess the mechanical properties of the septal cartilage under compression and tension.

In chapter II, the first goal of the study is addressed. Differential variable reluctance transducers (DVRT, a type of linear displacement transducer), were used to provide a detailed measurement of the growth of the septal cartilage and the nasofrontal suture. Two differential variable reluctance transducers (DVRTs) were implanted in different locations in the septal cartilage. A third DVRT was implanted across the nasofrontal suture. The DVRTs were connected to a wireless transmitter and the growth of the cartilage (change in length of the cartilage DVRTs) and expansion of the nasofrontal suture (change in length of the sutural DVRT) were monitored, minute by minute for period of several days. If growth of the septal cartilage leads to separation of the suture as hypothesized, then the growth of the cartilage should (1) exceed that of the suture and/or (2) precede it in time. In addition, comparison of the two cartilage sites could reveal regional variation in septal growth.

The second goal of the study is addressed in chapter III. Animals received 5'-bromo-deoxyuridine (BrdU) injection 24 hours before sacrifice. BrdU is a thymidine analogue that is picked up by the cells in the DNA synthesis phase of the cell cycle (S phase). Immunohistochemical methods were used to characterize the proliferation in various parts of the septal cartilage. The general hypothesis predicts that the chondrocytic proliferation occurs throughout the septum and contributes to overall growth. In addition this chapter will supplement the results of chapter II by providing a more detailed assessment of regional variation in septal growth.

In chapter IV, the biomechanical role of the septal cartilage in preserving the integrity of the midface is tested by measuring the deformation of the nasal septal cartilage and nasofrontal suture during function. Utilizing differential variable reluctance

transducers and strain gages, I measured the magnitude of strain generated on the septal cartilage and nasofrontal suture during mastication and masseter stimulation. Two groups were used in this part of the study. In one group two DVRTs were implanted anteroposteriorly (horizontally) at the septoethmoid junction and the anterior part of the cartilage. The second group consisted of the pigs used in chapter II, in which the two DVRTs were both implanted horizontally at intermediate positions in the cartilage. In both groups, strain across the nasofrontal suture was also recorded. The results of group 1 have been published (Al Dayeh et al. 2009). Assessing in vivo functional strain helped to test whether the septal cartilage acts as a vertical strut during mastication. If so, vertical compression should be associated with horizontal tension (because of a Poisson effect) during mastication. Furthermore, if the septum is stiff, then the magnitude of strain should be relatively low. In addition in this chapter, briefly, I discuss the anatomy and histology of the nasal septal cartilage with special focus on its relation to neighboring structures. This will help to understand the mechanical role of the cartilage.

The focus of the fourth goal of this study was on the mechanical properties of the septal cartilage. This goal is presented in chapter V. This is the only part of the study that used standard pigs rather than minipigs. In addition, age could not be controlled, although most specimens were probably about 6 months old, the upper extreme of the minipigs sample. Nasal septa were harvested and tested under compression or tension. This chapter helped to determine if the mechanical properties of the septal cartilage support an active role in midfacial growth (chapter II) and/or in preserving the integrity of the midface (chapter IV). If the cartilage is acting as a growth center as hypothesized,

then the stiffness of the cartilage under anteroposterior compression should be higher than the stiffness of nasofrontal suture under anteroposterior tension. The results of this chapter are compared to a previous publication from our lab concerning the mechanical properties of the nasofrontal suture (Popowics and Herring 2007). If the septal cartilage is acting as a strut, then the cartilage should be stiff enough to bear masticatory loads. Further, if the cartilage is compressed vertically as suggested by Moss (1968), then it should be especially stiff and strong under vertical compression.

Chapter II: Growth of the nasal septal cartilage

Background

It has been hypothesized that the major determinants of the anteroposterior growth of the mammalian skull are three cartilaginous zones: the cranial base synchondroses (Ingervall and Thilander 1972; Sirianni and Goy 1987; Persing et al. 1991; Kasai et al. 1995; Rosenberg et al. 1997; Nie 2005), the condylar cartilage of the mandible (Rönning 1995), and the nasal septal cartilage. Of these zones, the nasal septal cartilage is the most controversial; while some researchers (Moss et al. 1968; Babula et al. 1970; Stenström and Thilander 1970) state that the septal cartilage is a supportive structure with minimal role in midfacial development, others hypothesize that it is the driving force for midfacial growth (Scott 1953; Sarnat and Wexler 1966; Sarnat and Wexler 1968; Kvinnsland 1973; Kvinnsland 1974; Kvinnsland 1974; Kvinnsland 1988). Craniofacial sutures serve as major postnatal growth sites. However, it is generally agreed that sutures have no intrinsic growth potential (Enlow and Hans 1996); they respond to forces that tense the tissue of the suture, resulting in bone formation at the bone edges (Scott 1953; Persson et al. 1979; Rönning 1995; Thilander 1995; Opperman 2000). Most studies support the idea that growth of internal soft tissue is the major source of such force. For example, growth of the brain tenses the calvarial sutures (Persing et al. 1991; Huggare and Rönning 1995; Opperman 2000; Ogle et al. 2004) and expansion of the eyeball tenses the orbital sutures (Sarnat 1980). The

nasofrontal suture is a suture of the midface that is heavily compressed by mastication, yet it is rapidly growing (Rafferty and Herring 1999). The source of the force that separates this suture has been an intellectual dilemma. While many authors believe that the expansion of the nasal septal cartilage stretches the midfacial sutures including the nasofrontal suture (Scott 1953; Sarnat and Wexler 1966; Verwoerd et al. 1980), others believe that the growth at this suture is in response to functional demands, such as increase in the nasal airway size and expansion of the nasal capsule as described by the functional matrix theory (Moss 1964; Moss et al. 1968; Stenström and Thilander 1970). The role of the septal cartilage in powering midfacial growth was popularized by Scott (Scott 1951; Scott 1953), who described the septal cartilage as a primary cartilage representing the anterior extension of the cranial base. He suggested that this origin makes the cartilage act as a growth center separating the facial sutures. Scott's suggestion has been supported by various findings such as: (1) the septal cartilage's ability to grow in organ culture (Copray 1986; Kvinnsland 1988) and as an allograft (Kvinnsland 1973), (2) its response to growth factors and hormones (Takigawa et al. 1984; Vetter et al. 1984; Vetter et al. 1984; Vetter et al. 1985; Bujia et al. 1996; Tokimasa et al. 2000), and (3) midfacial retrognathia in rats injected with nasal septal cartilage antisera (Hans et al. 1996). In addition, midfacial retrognathia associated with some anomalies such as Binder's syndrome, achondroplasia and arhinencephaly has been attributed, in part, to defects in the nasal septal cartilage (Delaire and Precious 1987). Support for the role of nasal cartilage in powering midfacial growth mainly comes from extirpation experiments; partial and/or total extirpation of the nasal cartilage resulted in retardation of facial growth in rabbits (Sarnat and Wexler 1966) and in rats

(Kvinnsland 1974). However, these findings were challenged by Moss (Moss et al. 1968) and Stenström (Stenström and Thilander 1970), who reported that extirpation of the septal cartilage in rats and in guinea pigs resulted in collapse of the nasal bone, with minimal effects on the anteroposterior growth of the midface. They concluded that the septal cartilage is a passive structure that follows rather than drives facial growth. This chapter is designed to determine if the septal cartilage plays an active role in midfacial growth as suggested by Scott (1953).

In vitro studies in rats indicate that growth of the septal cartilage is not uniform. Ventral segments show higher growth rates compared to dorsal segments (Copray 1986). This can be attributed to the fact that cellular proliferation and matrix formation – major contributors to the growth of nasal septal cartilage – are not uniform. For example, Searls' work on albino rats showed that the septal chondrocytic proliferation rate varies not only with age, but also with region, with the posterior area being more active (Searls and Kinser 1972; Searls 1976; Searls 1977; Searls 1979). In another study on 3-week-old Dutch rabbits, the highest proliferative activity was found in the anterior tip and the most posterior part of the septal cartilage (Long et al. 1968). In humans, age and location are also strong determinants of chondrocytic proliferation (Vetter et al. 1984) with the anterior and posterior areas showing the fastest proliferation rates. Similarly, matrix formation rate varied with location in rats (Copray 1986). These studies illustrate the importance of location, age and species in determining the growth of the septal cartilage. This could partially explain the variable outcomes of extirpation experiments; if different parts of the septal cartilage are growing at different rates then

the location of the extirpated segment will have a profound effect on the outcome of the experiments.

Septal cartilage growth in vivo and in vitro is stimulated by growth hormone and growth factors (Vetter et al. 1985; Tokimasa et al. 2000). Growth hormone deficiency results in decrease of the anteroposterior dimension of the cranial base including the nasal septum (Pirinen 1995). On the contrary, acromegaly patients (increased GH) are characterized by increased facial dimensions attributed in part to the stimulation of the nasal septum (Pirinen et al. 1994). The cartilage response to growth hormone suggests that cartilage growth may correspond with the secretion of GH. Since GH secretion in mammals is episodic (Arbona et al. 1988) growth of the septal cartilage may also be episodic.

Another question that arises when discussing the role of the nasal septum in midfacial growth is how the expansion force of the septum is transmitted to the facial sutures. Many studies claim that the septum is attached to the premaxillary bone through a thick fibrous tissue layer known as the septopremaxillary ligament (SPL). Since the SPL is located anterior to the facial sutures, the expansion of the septum will place all of the facial sutures except those in the midline under a tensile load, by pulling forward on the premaxilla. This will result in bone apposition and growth at the sutures. Retardation of midfacial growth following resection of the SPL was seen in chimpanzee (Siegel et al. 1992). Several authors attribute the midfacial retrognathia seen in cleft lip and palate patients to lack of integrity of the SPL (Delaire and Precious 1986; McComb and Salyer 1990). They suggested that early correction of the SPL is needed in order to

reestablish the continuity of force transmission between the nasal septum and the midface.

The controversy around the role of the nasal septal cartilage in midfacial growth can be attributed, in part, to limitations associated with experimental approaches, such as measuring the growth of the cartilage in vitro and extirpating portions of the septum. Organ culture growth is clearly not comparable to the in vivo situation. The surgical extirpation model is associated with unavoidable trauma and variability in extirpation location. In addition, both culture and extirpation studies suffer from lack of direct comparison between the growth of the septal cartilage and that of the sutures it is thought to expand.

The present chapter is designed to improve on these experimental approaches by making telemetric, continuous and simultaneous measurements of the anteroposterior growth of the septal cartilage (at two sites) and the nasofrontal suture. Pigs were used as a study model because of the space requirements for instrumenting the nasal cavity and to allow a comparison with previous studies on nasofrontal suture growth (Rafferty and Herring 1999), and mechanical deformation of the septal cartilage, in vivo (Chapter IV) and in vitro (Gaon et al. 2003).

Monitoring the growth of the septal cartilage assessed its interstitial growth. Comparison of the cartilage growth at two sites allowed a determination of whether septal growth is uniform. Comparing real time growth of the septal cartilage and nasofrontal suture tested my hypothesis that the septal cartilage growth leads to growth of the nasofrontal suture. I hypothesized that if growth of the septal cartilage is powering

midfacial growth, then it should precede that of the nasofrontal suture or exceed it in amount. In addition, because the recording was continuous, the presence of circadian variation was also investigated by measuring and comparing the growth during day and night time hours. An understanding of the contribution of the nasal septal cartilage to normal midfacial growth will help elucidate the etiology, clinical presentation and treatment approaches for craniofacial malformations involving midfacial hypoplasia.

Materials and Methods

Animal model

Subjects used for this study were 10 female Hanford minipigs (*Sus scrofa*), ranging in age from 3.5 to 4.5 months and weighing 12–27 kg. Pigs were obtained from Sinclair Research Farms (Columbia, MO). All the procedures were approved by the Institutional Animal Care and Use Committee of the University of Washington, and were carried out in Seattle in 2007–2009. Details of animal age, sex and weight on the day of the experiment are given in Table II-1.

Instrumentation

Differential variable reluctance transducers (DVRT, Microstrain, VT) were used to measure growth and masticatory strain at the septal cartilage and the nasofrontal suture. This linear displacement transducer is comprised of two parts, a rod and a coiled core (Figure II-1B), each fixed in the tissue by a barb or screw. The rod is free to slide within the core, and its position is detected by measuring the coil's differential reluctance using a sine-wave excitation and synchronous demodulator. This differential

detection method provides a very sensitive measure of rod movement (±1 μm). The linear displacement of the rod over time was the measure of growth. While the pig was feeding, the displacement of the rod could also be used to assess functional deformation during mastication (chapter IV).

DVRT signals were conditioned and amplified, then telemetered to a nearby computer with a USB Base Station (Microstrain) where the signals were captured. For growth measurement signals were collected at one minute intervals, and for masticatory strain signals were captured at a higher frequency (32, 64 or 638 Hz).

Surgical procedure

Instruments were implanted under aseptic conditions in a dedicated surgical suite. Pigs were premedicated by intramuscular injection of oxymorphone (0.1mg/kg, analgesic) acepromazine (0.5mg/Kg, sedative), glycopyrolate (0.01 mg/Kg, anti-sialagogue) and buprenorphine (0.01 mg/Kg, analgesic). Pigs were then mask-anesthetized using isoflurane/nitrous oxide and intubated. Following intubation, 2 ml of 2% lidocaine with 1:200000 epinephrine was injected subcutaneously on the dorsal surface of the nose.

The following procedure was used with a few exceptions (Table II-1). A 5-cm supra-periosteal midline incision was made to expose the dorsal surface of the nasal and frontal bones and the nasofrontal suture. An oscillating saw (Stryker, MI) was used to cut two 2-cm windows in the left nasal bone (Figure II-1A). The posterior window was positioned 5 mm in front of the nasofrontal suture while the anterior window was about 2 cm more rostral. The lateral periosteum of each window was kept intact to ensure

adequate blood supply. Bone was reflected to expose the underlying parietotectal cartilage. Electrosurgery was used to cut through the parietotectal cartilage to reach the nasal cavity. Bone wax and Gelfoam (Pfeizer, NY) were used when needed to control bleeding. In each window a DVRT was implanted horizontally in the dorsal half of the lateral surface of the cartilaginous nasal septum (Figure II-1). A 19-gauge needle was used to create holes on the intact side of the nasal and frontal bones and a third DVRT was implanted into the right nasal and frontal bones spanning the nasofrontal suture. The distance between the barbs of each DVRT was measured and used to calculate strain during mastication and to standardize growth measurements. The bony windows were replaced and fixed using mini-plates and screws (Stryker, MI). The lead DVRT wires were fixed to the surrounding tissue using silk sutures. A subcutaneous tunnel was made at the posterior limit of the incision to emerge at the back of the neck. A 2-ml Alzet osmotic pump (Cupertino, CA) loaded with amikacin (250mg/ml) or gentamicin (40mg/ml) was implanted near the exit site in the back of the neck. Incisions were sutured. A lateral cephalogram was taken to measure the orientation of the DVRTs to the long axis of the nasal bone. A fentanyl patch (25 or 50 mcg/hr) (Duragesic, NJ) was then applied. Animals were allowed to awaken; following recovery buprenorphine was injected (0.01 mg/Kg) to provide analgesia until the fentanyl took effect. Throughout the survival time after the surgery, animal were constantly monitored for any signs of infection or discomfort. Analgesics (buprenorphine) and/or antibiotics (trimethoprim or Clavamox) were administered when needed.

DVRT wires were connected to a signal demodulator (DEMOD-DC2, Microstrain) attached to a three-channel wireless transmitter (V-link, Microstrain) that broadcast at a

frequency of 915 MHz The demodulator and transmitter were housed in a jacket worn by the animal and powered by a long-life 19 mA battery to insure continuous recording of the DVRT lengths. Data were collected every minute from the three locations via the USB base station receiver, connected to a computer running Agile-link software (Microstrain). The original study design was to record growth of the 3 sites continuously for 10 days. However, due to instrument failure, monitoring time and location varied. Table II-2 summarizes the number of hours recorded from each location for all the animals studied. When the instruments had stopped recording (usually because of breakage), the animals were anesthesized by isoflurane and were sacrificed by intracardiac perfusion or by a lethal dose of pentobarbital in an ear vein. After sacrifice, the head was dissected and DVRTs were visually inspected to check for positioning.

Data capture

The continuous 1 sample/min recording was briefly interrupted for two daily feedings (roughly around 11 am and 5 pm). During feeding, the DVRT signals were recorded at 32, 64 or 638 Hz using the same wireless apparatus. In 4 animals, DVRT wires were unplugged from the wireless demodulator and plugged into another demodulator (MB-STD4, Microstrain), which allowed simultaneous recording and digitization with EMG signals (MEC 100 and MP 100A, BIOPAC systems, Santa Barbara, CA). These data are presented in chapter IV.

Data analysis

DVRT voltage was converted to displacement using a calibration procedure conducted prior to each experiment. The displacement was added to the initial DVRT

length (as recorded during the surgery) to calculate DVRT length for each minute interval recorded. Masticatory strain was calculated by dividing the DVRT displacement during mastication by initial DVRT length. The DVRT lengths at the three locations were plotted against real time (as recorded by the computer clock). The difference between the initial (average of first 2 hours) and final (average of last 2 hours) DVRT length was taken as the total growth at each location and this was converted to growth strain by dividing by initial DVRT length in mm. Total growth strain was divided by total monitoring time (in hours) to calculate the growth strain per hour. DVRTs measure linear dimensions, and it had been intended for each of them to be identically parallel to the snout dorsum to measure the anteroposterior growth. However, surgical access issues prevented perfect parallelism. In order to standardize the direction of growth, the angle between the long axis of each DVRT and the nasal bone was calculated from the x-ray. The anteroposterior component (horizontal) of growth strain was calculated as: growth strain per hour*cos θ where θ is the angle between the long axis of the DVRT and the long axis of the nasal bone. The vertical component of the growth strain was calculated as: growth strain per hour *sin θ but was not analyzed further as the study was focused on the anteroposterior growth of the cartilage in comparison to the separation of the nasofrontal suture.

The existence of a regional difference in the growth of the cartilage was tested using a paired-t test. Growth of the septal cartilage and the nasofrontal suture were compared to test the hypothesis that the septal cartilage grows faster than the nasofrontal suture, using ANOVA and paired-t test as appropriate. Statistics were performed using Excel (Microsoft, WA) and SPSS (SPSS Inc., IL). The growth data

were explored for evidence of a circadian rhythm by comparing growth recorded at night (when lights are turned off in animal housing facility, 6p.m to 6a.m) to that during the day (6 am to 6 pm) for each location. The hypothesis that the septal cartilage and nasofrontal suture grew more at night was tested using paired t-tests.

The growth patterns of the septal cartilage and the nasofrontal suture were examined by plotting DVRT lengths against recording time in 24 hourly increments using Kaleidagraph (Synergy, PA). Since data were gathered in 1-minute intervals, each increment in the plot was 1/60 hr (approximately 0.01667 hr). Each plot started at 6pm in real time (as indicated by computer clock). In some cases, data acquisition was interrupted (for example, a DVRT was accidentally unplugged overnight), thus full-day data were not always present. However in most animals I was able to record at least one 24-hour cycle in at least one location. Table II-2 lists the available 24-hour datasets. Sequences less than 24 hrs long were analyzed separately. The graph was plotted (Kaleidagraph, Synergy PA) and a 10% weighting algorithm (LOWESS: locally weighted scatterplot smoothing) was applied. This algorithm fits simple models to localized subsets of the data to build up a function that describes the variation in the data, point by point. The weighted data were used to calculate the derivative of growth (i.e. growth speed). These growth speeds were used to compare the cartilage and the suture locations. In addition, these data were used to determine whether the growth pattern better fit a saltational or a continuous model. If growth is continuous, then little variation in growth speed should be observed, whereas saltatory growth should show bursts. Bursts were defined as time intervals longer than one hour during which growth speed was at least 3 times the average growth speed over the total time of recording. The

number and duration of bursts in the 24-hr periods and during day and night time were counted and averaged. In addition, the number of “growing” hours (derivative >0) and “non-growing” hours (derivative ≤0) were calculated. Values were compared to test if there was any variation in growth between day and night.

Cross-correlation analysis for time series (Statistica, OK) was used in order to compare the timing of growth at the three sites. This was done in two ways. First, correlations between raw growth curves at the three sites were calculated and compared at different time lags (± 150 minutes). This was intended to assess whether the growth of the cartilage preceded that of the suture. Second, the same procedure was performed on the growth speed curves (derivative of the growth data) in order to test if growth bursts of the septal cartilage preceded bursts of growth at the nasofrontal suture.

Results

Growth strain rate

All locations showed growth as evidenced by increases in DVRT length. (Table II- 3, Figures II- 2 and -3). The highest average horizontal growth strain rate was seen in the anterior cartilage (0.07 ± 0.03 %/hr, n=9) followed by the posterior cartilage (0.06 ± 0.04 %/hr, n=6) and the nasofrontal suture (0.03 ± 0.02 %/hr, n=8). Cartilage values were averaged to allow comparison of the septal cartilage and nasofrontal suture. The cartilage was found to grow faster (p=0.007, paired-t) in the 6 animals with both values and in the total sample (p=0.004, 2 sample t-test). ANOVA was performed for a more detailed examination of the three locations; the marginally significant results (p=0.05)

were found by post hoc testing to be due to the higher growth rate of the anterior septal cartilage compared to the nasofrontal suture ($p=0.04$). The other differences did not reach statistical significance.

Growth pattern

The pattern of growth, as shown by the derivative function of the growth curve, was always saltatory at all locations with alternating periods of active growth bursts and periods of no or negative growth (shrinkage) (Figure II-2B). The duration, amplitude and number of peaks are listed in Table II-4. The three locations were statistically undistinguishable in the amplitude as well as in the duration of growth bursts ($p>0.3$, ANOVA). The total duration of active growth (growth speed>0) ranged from 55% - 61% with about 5 bursts/ 24-hr cycle, each lasting about 3 hours (Table II-4). The amplitude of growth bursts relative to average growth rate per hour ranged from 5 times in the posterior cartilage, to 7 times in the nasofrontal suture and 10 times in the anterior cartilage ($p>0.4$, ANOVA). The total duration of no growth (growth speed=0) and negative growth (growth speed<0) averaged around 20% each, in all of the three locations. Although the periodicity of the bursts is clear, there was substantial variability among pigs, within pigs and among locations. The timing of each peak in real-time is illustrated in Figure II-4 and in Table II-5.

Diurnal variation

Day and night time growth is displayed in Table II-6. No significant difference was found between averaged growth strain rates at any location. In order to test further for possible differences in growth between day and night, the number and amplitude of

peaks were compared (Table II-7). The number of peaks per 12 hrs did not differ between night and day for any location. For the two cartilage locations, peak amplitude was similar during night and day, However, for the nasofrontal suture, the amplitude of growth bursts was significantly higher during the daytime ($p=0.03$, paired-t).

Cross-correlation analysis

Relatively high cross-correlation coefficients were found to occur between growth of the anterior septal cartilage and the nasofrontal suture ($R= 0.7 \pm 0.1$, $n=6$). In 5 of these 6 animals, the highest correlation was with no time lag (lag=0) and in the sixth animal (417) the growth of the suture lagged the growth of the anterior septal cartilage by 30 minutes. Only 3 animals had data from the posterior septal cartilage and the nasofrontal suture. Two of these had the highest correlation ($R=0.8 \pm 0.2$) at time lag 0. The third animal (417), the same pig that showed non-zero lag between the anterior cartilage and the suture, showed a weaker highest correlation ($R=0.4$) which occurred when the growth of the suture lagged that of the cartilage by 100 minutes. Moderate correlations ($R=0.6 \pm 0.1$, $n=3$) were also found between the growth of the anterior and posterior septal cartilage. These correlations were found at lags of -7 to 4 minutes.

When the cross-correlation analysis was conducted on growth bursts rather than the original growth curve (i.e. the derivative function), coefficients were lower ($R=0.3$-0.6) and lags were more variable (Table II-8). Growth bursts of the suture lagged the anterior cartilage by 0-120 minutes and the posterior cartilage by 0-30 minutes. It is notable that there were no examples of cartilage growth lagging that of the suture.

Discussion

Limitations

Initially it was intended to monitor the growth of the cartilage and the suture continuously and simultaneously for period of 7 days. However, in several animals some of the DVRTs broke prematurely. The sensors that remained unbroken gave consistent and precise measurements as evidenced by the overall increase in DVRT length. In addition, gross examination of the DVRTs after animal sacrifice did not reveal any significant signs of damage in the cartilage and the suture. Therefore, the resultant data from the functioning sensors is reliable and offer a precise insight into the real-time growth of the cartilage and the suture.

Growth strain

The change in DVRT length was my measure of growth, but it is important to mention that DVRT separation may not be entirely due to growth in the sense of cellular proliferation and matrix formation. In addition to the post-surgical settling of the devices, the septal cartilage could change size by absorbing or losing water. Cartilage extracellular matrix is rich in proteoglycans and the resulting negative charge of the matrix causes high affinity for cations and water (Mathews and Decker 1977). On the other hand, compressive strains can force water out of the matrix (Mow and Wang 1999; Mosher et al. 2001). This behavior might have resulted in intermittent expansion or contraction of the cartilage with concomitant increase or decrease in DVRT length.

However, since growth was recorded for a long period of time, I believe that the total DVRT separation is a reasonably accurate estimate of the growth.

Growth of the septal cartilage

The results from both septal locations show unequivocally that the nasal septal cartilage expands interstitially during postnatal growth. Of course, this finding does not demonstrate that the septum is the driving force of midfacial growth. Nevertheless, it does indicate that internal expansion of the septum is a real phenomenon, and periods of growth as short as few hours are sufficient for measurable elongation to occur in juvenile animals, roughly equivalent in dental age to a 6 year-old human. On average, the septum grows at about 0.07% per hour. This value compare favorably with rates reported for organ culture of 4-day-old albino rat septal fragments (0.08-0.13%, calculated from Copray 1986), especially considering that the material in the culture study was unrestrained from attachment to the skull and was much younger.

Because previous studies indicated some regional variation in chondrocytic proliferation (Long et al. 1968; Searls 1977), non-uniform growth of the cartilage was expected. Comparing the growth recorded by both cartilage DVRTs showed no such difference. This might due to the fact that only two locations of the cartilage were compared. Also the small sample size could have been responsible for this result. In chapter III, the proliferation of septal chondrocytes is compared in order to determine if the uniformity noticed is reflected at the cellular level. In addition, cartilage growth is a product of matrix formation, and cellular enlargement as well as proliferation (Abad et

al., 2002, Seincheimer et. 1981). Thus a parallel relation between growth and chondrocytic proliferation may not be present.

Growth of the nasofrontal suture

The average separation of the nasofrontal suture measured around 90 ± 60 µm/day. This exceeds the mineral apposition rate measured previously at the suture (one-side estimate of 27-30 µm/day, yielding an estimate of 50-60 ±15-20 µm/day for the entire suture; calculated from Rafferty and Herring, 1999), however, the difference is not statistically significant. This possible difference in values suggests that the separation of the suture (DVRT measure) is faster than the rate of hard tissue deposit. If real, this finding would support the idea of growth of the sutures being related to separation of their bony elements (Scott 1956). Since sutures have no intrinsic separating growth power (Babler et al. 1982; reviewed by Persson 1995), the separation measured at the nasofrontal suture must be the result of an external force.

While separation of the nasofrontal suture was rapid, it was significantly less than the growth recorded at the cartilage (0.03%/hr vs. 0.07%/ hr, Table II-3). Considering that the nasal septal cartilage volume is bigger than the suture's and that it expands rather uniformly, a higher growth rate than the suture is consistent with the notion that the nasal septum drives sutural growth. Thus, the idea that the cartilage generates enough pressure to separate the nasofrontal suture, resulting in bone formation at the suture, is supported. A higher growth rate at the cartilage raises the question of how the bone of the snout maintains a constant size relationship with the septum. Presumably,

additional growth occurs at the anterior border of the nasal bones and the bone of the snout may also enlarge by internal resorption and external deposition, possibilities that will require future studies.

Growth pattern

The growth pattern at all sites showed clear signs of pulsation, characterized by periods of fast growth followed by periods of minimal, no or negative growth. Overall, active growth was taking place around half of the time.

The number of bursts averaged around 5 per 24 hours at all sites, suggesting underlying systemic phenomena. This number is similar to the number of pulses of growth hormone reported in previously in adult pigs of similar strain (Claus et al. 1990) and slightly smaller than the number reported in growing pigs (8 pulses/day, Dubreuil et al. 1988). Thus it is conceivable that growth of the cartilage and the suture follows a pattern similar to that of growth hormone secretion. Unfortunately, growth hormone secretion could not be monitored in this study. Further indirect evidence of a possible association between growth and growth hormone secretion comes from consideration of the timing of bursts.

The finding of “negative growth rate” (i.e. shrinkage) was unexpected. This occasional finding (about 20% of the recording time) may be simply the jitter imposed by the high sensitivity and resolution of DVRT recording (one-minute intervals). Values could vary with animal behavior, such as mastication, and these intervals could appear as shrinkage. Certain postures or general dehydration might cause fluid to exit from the cartilage or suture space, which also appear as shrinkage. The surgical attachment of

the instrument might also have caused the appearance of occasional shrinkage. The DVRTs were attached to the cartilage using barbs and to the nasal and frontal bones using screws. The force of growth will tend to widen the holes, which could result in play at the junction, resulting in noise and possible shrinkage until new tissue fills the hole.

Diurnal variation

In humans, the growth hormone release is higher during the night (Alford et al. 1973; Van Cauter et al. 1992), but this pattern does not apply to pigs. Previous studies on diurnal variation of growth hormone secretion in pigs suggest a pattern other than nocturnal release. Depending on age and gender, various authors report either higher frequency or amplitude of growth hormone pulses during the day or no diurnal variation (Dubreuil et al. 1988; Claus et al. 1990). Thus, there seems to be a tendency for greater day-time growth hormone release, but it is only a trend. In the present study, there was no diurnal variation in frequency of growth bursts. The amplitude of growth bursts in the cartilage was similar in day and night, but the nasofrontal suture had higher daytime amplitude (Table II-7). This very slight trend toward the greater daytime growth is in the expected direction. Thus the association of growth of the septum with growth hormone secretion is still a viable option.

Cross-correlation

Cross correlation analysis was employed to test if the growth of the septal cartilage precedes the growth at the nasofrontal suture. The results do not refute the hypothesis, since the cartilage growth never lagged that of the suture, but the suture often lagged the cartilage. However, the data were also consistent with the idea that

both tissues grow simultaneously, because most often the lag was 0. In retrospect, this simultaneity should have been expected; growth of the septal cartilage and separation of the nasofrontal suture must occur in association. Nevertheless, the one-way deviation from a lag of 0 suggests a strong tendency for the cartilage to grow first, followed by the separation of the suture. This is the result expected if, as Scott (1953) proposed, growth of the septal cartilage drives sutural growth.

Growth correlation coefficients were generally higher when the overall growth curves were compared, and lower for the derivative curves with the growth bursts. This suggests that the overall expansion of the septum is the dominant feature of the cartilage-suture association rather than the brief pulses of accelerated growth.

Summary

In this chapter the real-time growth of the nasal septal cartilage and nasofrontal sutures was monitored, simultaneously and continuously at high resolution in one-minute intervals. Returning to the hypotheses posed at the beginning of this chapter, I found that growth of the cartilage exceeds that of the suture and is simultaneous with the separation of the suture. These results indicate that the growth of the septal cartilage is causing the separation of the nasofrontal suture. In addition, my results suggest that the growth of the septal cartilage is uniform, since no difference was found between the two monitored locations.

Table II-1: Age and weight of the pigs on the surgery day

Animal ID	Age (months)	Weight (Kg)	Modifications from protocol
411	4	18	
412	3.5	14	One window
413	4.5	19	One window, right nasal bone
417	4	12	One window
422	3.5	18	
427	4.5	18	
428	4.5	20	One bone plate was not replaced
429	4.5	27	
430	4.5	27	
431	4	20	
Average ± SD	**4.2 ± 0.4**	**19.3 ± 4.8**	

Table II-2: Total number of hours recorded from each DVRT and number of 24-hour cycles available for analysis

Animal ID	Total hours of growth recorded			Number of 24-hour cycles		
	Anterior septal cartilage	***Posterior septal cartilage***	***Nasofrontal Suture***	***Anterior septal cartilage***	***Posterior septal cartilage***	***Nasofrontal Suture***
411	110	120	160	3	2	0
412	23	0	0	0	0	0
413	30	0	0	1	0	0
417	127	99	165	3	3	3
422	47	37	47	1	0	1
427	86	50	48	0	1	1
428	0	0	40	0	0	1
429	20	0	80	0	0	2
430	272	80	272	11	4	7
431	40	67	53	1	2	2

Table II-3: Average anteroposterior growth strain rate of the septal cartilage and nasofrontal suture over the entire recording period (%DVRT length per hour)

Animal ID	Anterior cartilage	Posterior cartilage	Nasofrontal suture	Averaged cartilage
411	0.04	0.13	0.03	0.09
412	0.11	NA	NA	0.10
413	0.10	NA	NA	0.10
417	0.07	0.05	0.04	0.06
422	0.04	0.07	0.02	0.06
427	0.07	0.03	0.03	0.05
428	NA	NA	0.05	NA
429	0.10	NA	0.06	0.10
430	0.05	0.02	0.01	0.03
431	0.05	0.02	0.01	0.04
Average ± SD	**0.07 ± 0.03***	**0.06 ± 0.04**	**0.03 ± 0.02***	**0.07 ± 0.03†**

** The anterior septal cartilage grew significantly faster than the nasofrontal suture (p=0.04, ANOVA with post hoc analysis).*

† The averaged cartilage growth strain rate was significantly higher than the nasofrontal suture (p=0.004, 2 sample t-test).

Table II-4: Number, duration and amplitude of growth bursts and the total number of growth hours recorded by the DVRTs

Location	Number of peaks in 24 hrs	Peak duration (hrs)	Amplitude relative to the averaged growth speed (fold difference)	Growth hours as a percentage of a 24-hr cycle	Non growing hours as a percentage of a 24-hr cycle	Negative growing hours as a percentage of a 24-hr cycle
Anterior septal cartilage (n=6)	5.6 ± 0.6	2.6 ± 0.4	10 ± 5X	55 ± 17%	21 ± 5%	23 ± 8%
Posterior septal cartilage (n=5)	4.6 ± 1.5	3.1 ± 0.8	5 ± 3X	57 ± 33%	21 ± 6%	21 ± 7%
Nasofrontal suture (n=7)	4.8 ± 0.7	3.0 ± 0.7	7 ± 5X	61 ± 27%	20 ± 6%	18 ± 6%

Values are expressed as mean ± SD, n: number of pigs

Table II-5: Timing of growth bursts at the three regions

	1	2	3	4	5	6
Anterior septal DVRT						
411	4pm- 8:30pm	10pm-12:30am	2am-6 am	8am-10am		4pm-6pm
417	5 pm-7:30pm	11:30pm-1:30am	4am -7am	8am-11:30am	3pm -4pm	5pm-6:30pm
422	4:30pm-8pm	10pm-1am	2:30am-4:20am	7:30am-9am	11am-2:30pm	4pm-6pm
430	4pm-7:30pm	9:30pm-12:30am	4am -5:40am	9am-10:30am	12:30pm-2:30pm	4pm-6pm
431	5pm-10pm	12:30am-2:30am	3am-5:30am	7:30 am-8:30am	1pm-4:30pm	
Posterior septal DVRT						
411	10pm-2am		3am-4:30a.m	8:30am-11am		12pm-3pm
417	10pm-12am	1:30am-4am	6am -9am	9:30am-11am	12:30pm -3pm	4pm-6 pm
427	4pm-10:30pm		3am-6am	6:30am-10am	1pm-3pm	4pm-6pm
430	5pm-7pm	10pm-1am	1:30am -4am	5am-7am	7:30am-9am	10 am-2pm
431		10pm-2am	3:30am-5:30am	7:30am-9:30am	10:30am-12:30pm	
Nasofrontal suture DVRT						
417	8 pm-10:30pm	11pm-2am	2:30am -4am	5am-6am	7am -10am	11:30am-1pm
422	4pm-11pm	1:30am-3am	5am-6:30am	8:30am-11am	1pm-6pm	
427	4pm-12am		5am-6:30am	9am-10:30am	11:30am-1p.m	1:30pm-3pm
428	4pm-8:30pm	10:30pm-1am	2:30am -8am	8:30am-11:00am	12am-2pm	
429	4pm-11pm	12am-3am	3:30am-6am	9am-2pm		
430	5pm-8pm	8:30pm-10:30pm	11:30am -1am	2am-5:30am	7:30am-10am	
431	8pm-9:30pm	1am-3am	4am-5:30am	6 am-7am	11:30 pm-2:30pm	

Table II-6: Average growth strain rate (%DVRT length/hr) of each DVRT during daytime (6a.m-6p.m) and night-time (6p.m-6a.m) cycles

Animal ID	Anterior		N	Posterior		N	Suture		N
	Day	***Night***		***Day***	***Night***		***Day***	***Night***	
411	0.04	0.03	5	0.19	0.09	5	NA	NA	
413	0.12	0.01	3	NA	NA		NA	NA	
417	0.03	0.04	4	0.02	0.09	4	0.09	0.07	6
422	0.03	0.05	1	0.08	0.18	2	NA	NA	
427	0.14	0.02	3	0.03	0.030	2	0.04	0.02	2
428	NA	NA		NA	NA		0.02	0.07	2
429	NA	NA		NA	NA		0.03	0.07	5
430	0.05	0.03	11	0.02	0.01	4	0.05	0.01	8
431	0.03	0.03	2	0.03	0.02	3	0.01	0.01	3
Average ± SD	**0.06 ± 0.05**	**0.03 ± 0.01**		**0.06 ± 0.06**	**0.07 ± 0.06**		**0.04 ± 0.03**	**0.04 ± 0.03**	

N= number of 12-hr periods recorded

Table II-7: Growth pattern (derivative function of the growth curve) compared for day vs. night

Location	Night		Day	
	#Growth bursts	***Amplitude relative to average speed (folds)***	***#Growth bursts***	***Amplitude relative to average speed (folds)***
Anterior septal cartilage	2.9 ± 0.9	10.2 ± 4.9	2.9 ± 0.2	8.0 ± 0.9
Posterior septal cartilage	2.3 ± 1.3	5.6 ± 3.2	2.3 ± 1.2	5.2 ± 2.9
Nasofrontal suture	2.1 ± 0.9	5.0 ± 3.8	2.5 ± 0.9	8.1 ± 5.3*

**The amplitude of growth bursts for the nasofrontal suture during the day was significantly higher than night-time (p=0.03, paired-t)*

Table II-8: Timing of raw growth and growth speed for each location from cross-correlation analysis

Animal	Nasofrontal suture vs. Anterior septal cartilage		Nasofrontal suture vs. Posterior septal cartilage		Anterior septal cartilage vs. Posterior septal cartilage	
	Cross-correlation coefficient	Time lag (min)[a]	Cross-correlation coefficient	Time lag (min)[a]	Cross-correlation coefficient	Time lag (min)[a]
Raw growth						
411	0.8	0	ND	ND	ND	ND
417	0.6	30	0.4	100	0.6	-7
422	0.6	0	ND	ND	ND	ND
427	0.7	0	ND	ND	ND	ND
430	0.7	0	0.9	0	0.6	0
431	0.8	0	0.7	0	0.7	4
Average ± SD	**0.7 ± 0.1**	**12 ± 11**	**0. 8 ± 0.2**	**33 ± 58**	**0.6 ± 0.1**	**1 ± 1**
Growth speed (derivative of raw growth)						
411	0.6	60	ND	ND	ND	ND
417	0.4	50	0.3	30	0.3	5
422	0.5	80	ND	ND	ND	ND
427	0.4	120	ND	ND	ND	ND
430	0.5	0	0.6	30	0.5	10
431	0.5	0	0.5	0	0.5	-4
Average ± SD	**0.5 ± 0.1**	**52 ± 47**	**0.4 ± 0.1**	**20 ± 17**	**0.4 ± 0.1**	**4 ± 7**

ND, no data

[a] *Positive lags indicate that the septal cartilage growth (burst) preceded that of the nasofrontal suture or the posterior septal cartilage growth (burst) preceded that of the anterior septal cartilage*

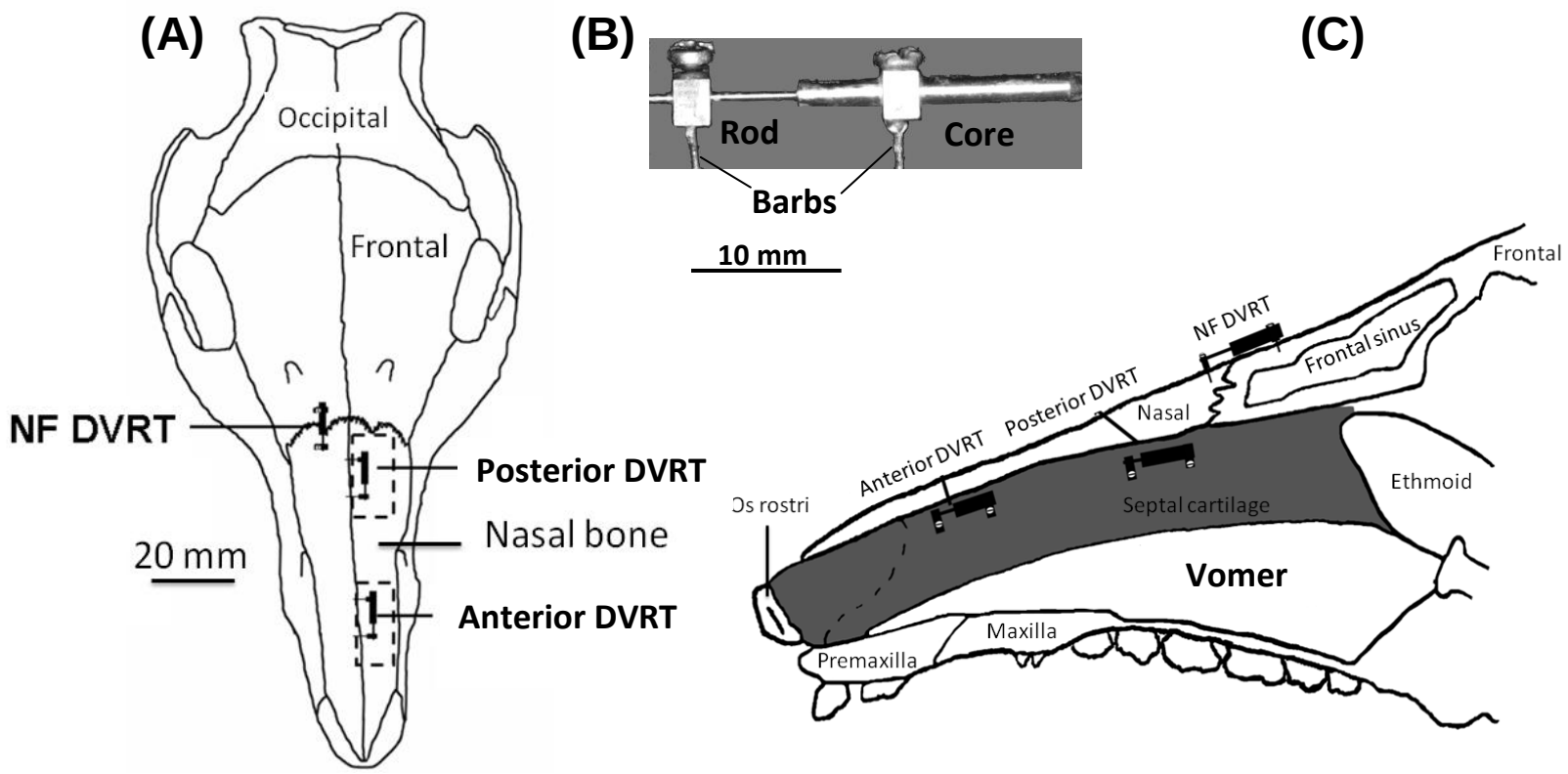

Figure II-1: (A) Dorsal view of the skull illustrating surgical access windows (dashed boxes) and DVRT positions. (B) DVRT showing the rod, coiled core and the barbs. (C) Sagittal section showing the positions of the DVRTs. The vomerine groove houses the ventral part of the septal cartilage. NF DVRT: nasofrontal suture DVRT

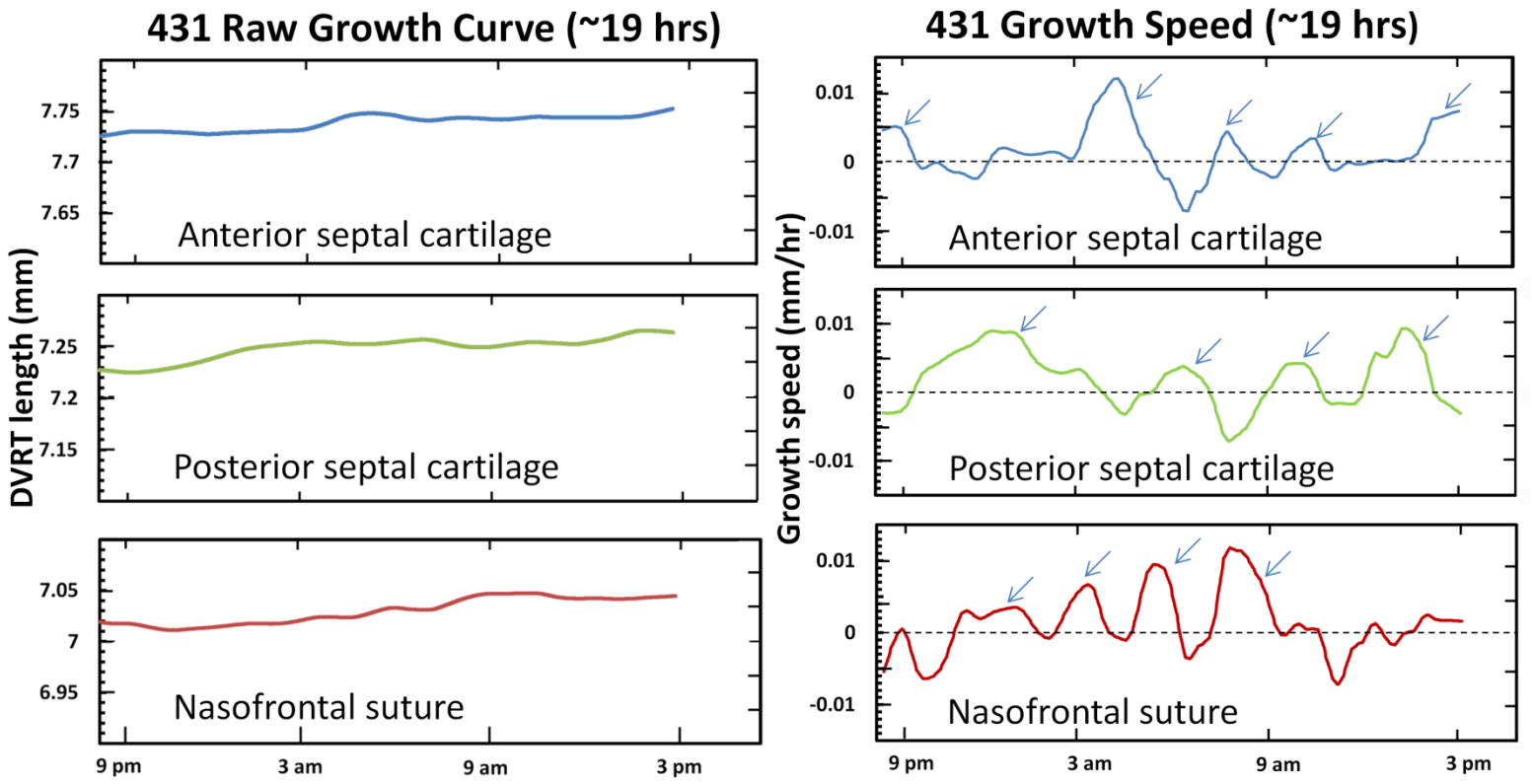

Figure II-2: Examples of growth curves (animal 431, day 1). Left: Raw growth curves of DVRT length (smoothed data). Right: Growth speed curves (derivative functions of the raw growth curves on the left) showing episodic bursts (arrows). The dashed line at 0 indicates stasis. Each location shows 3-4 growth bursts and at least one episode of shrinkage, but these are not simultaneous in the different locations

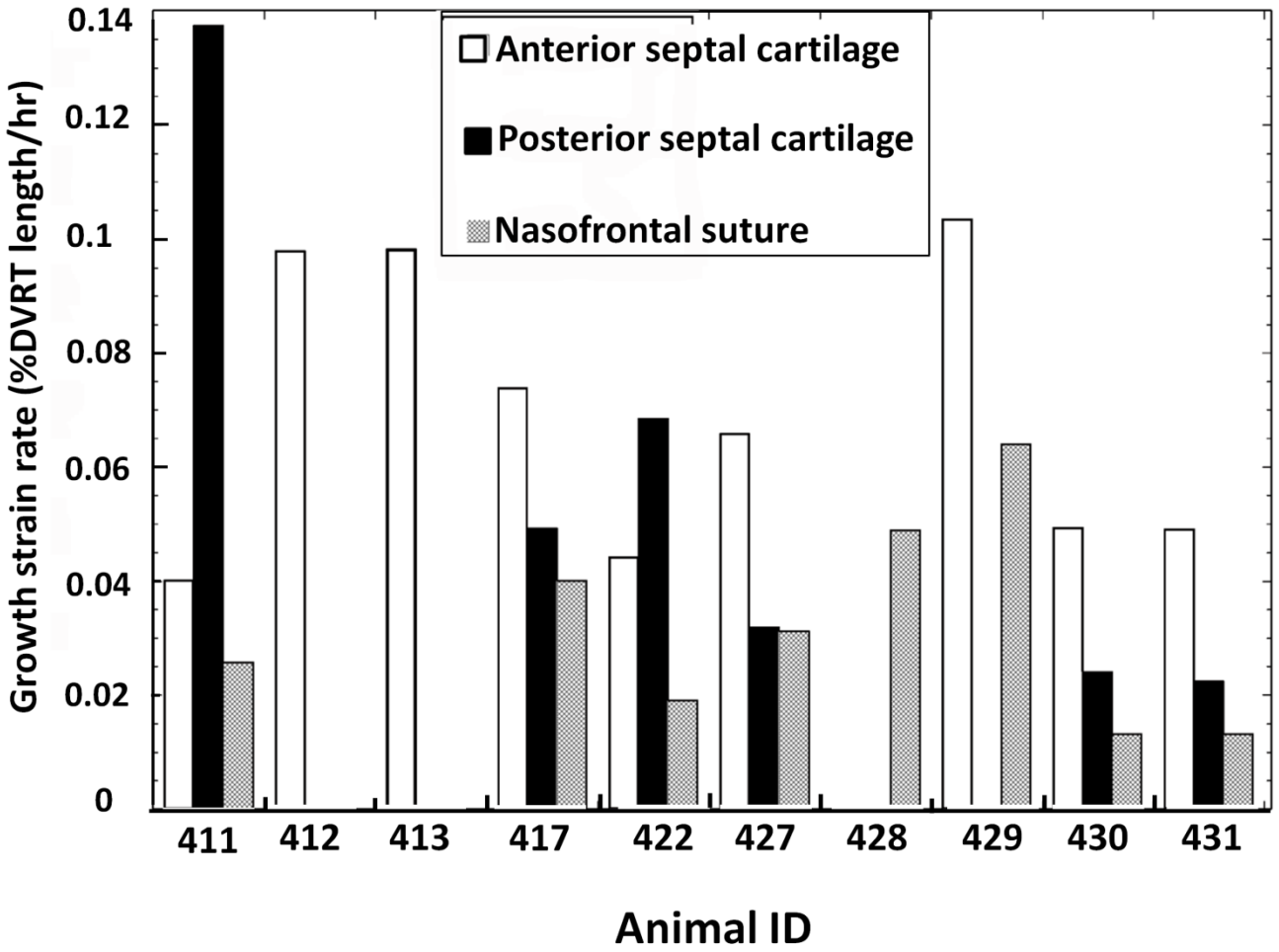

Figure II-3: Growth strain rates of different locations in individual animals for the entire recording period

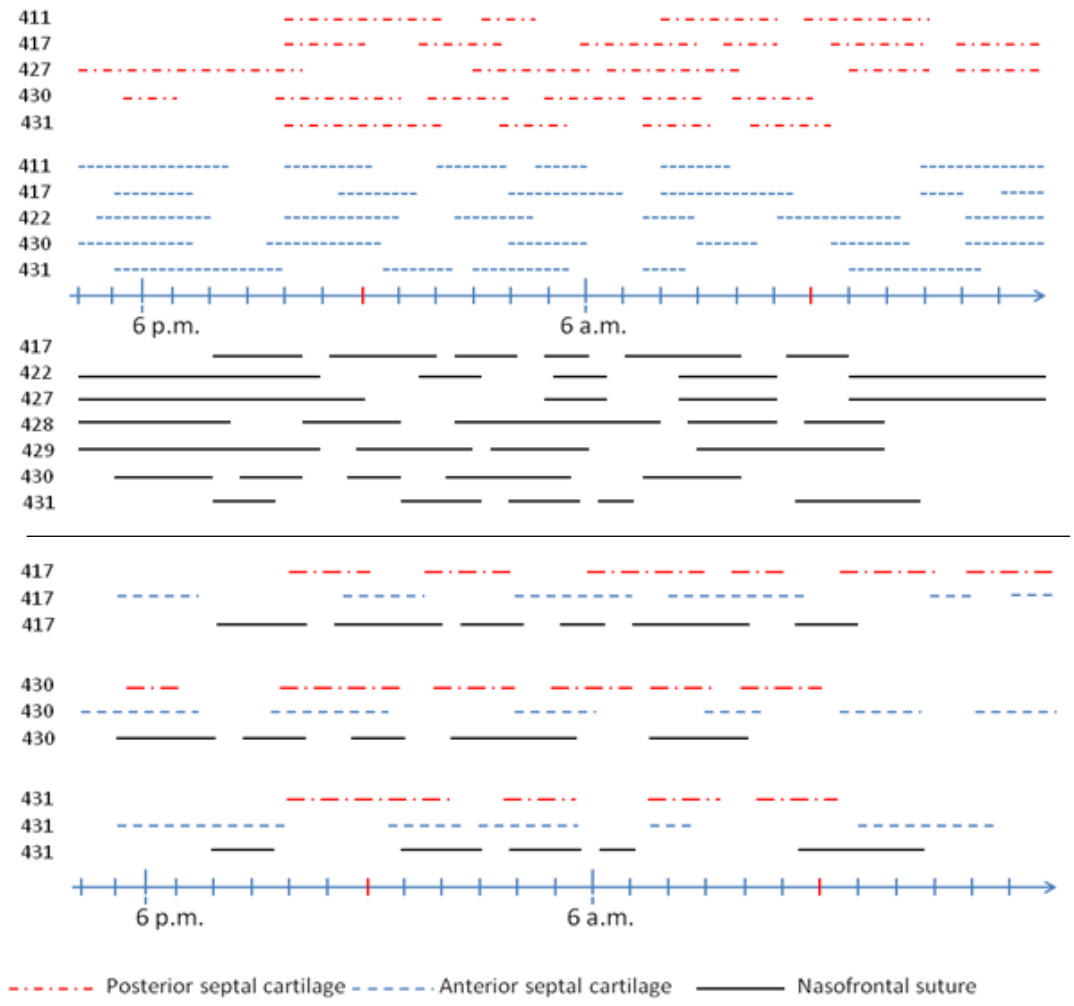

Figure II-4: The timing of growth bursts in each pig. Only locations with complete 24-hour cycles are shown. A: arranged by location, B: arranged by pig for the three animals with complete data

Chapter III: Proliferation of the septal cartilage chondrocytes

Background

The role of the nasal septal cartilage in midfacial growth has been the subject of extensive discussion (Scott 1951; Moss et al. 1968; Sarnat and Wexler 1968; Stenström and Thilander 1970; Kvinnsland 1973; Kvinnsland 1974; Kvinnsland 1974; Copray 1986; Hans et al. 1996; Cupero et al. 2001). Observing the resultant changes in midfacial growth after extirpating the septal cartilage has been the experimental approach most frequently used (Moss et al. 1968; Sarnat and Wexler 1968; Stenström and Thilander 1970; Kvinnsland 1974; Wong et al. 2010). As discussed in chapter II, the findings are not consistent, with some authors reporting retardation of midfacial growth ; (Sarnat and Wexler 1968; Kvinnsland 1974; Wong et al. 2010) and others minimal effects (Moss et al. 1968; Stenström and Thilander 1970). Such controversy may be partially attributed to variations in sites of cartilage extirpation. If various parts of the septal cartilage are growing at different rates, then extirpation of the rapidly growing parts will result in more detrimental effects on midfacial growth, while extirpation of the more slowly growing parts will result in minimal retardation of midfacial growth. Thus assessing the uniformity of growth of the septal cartilage might help to explain the variable outcomes of septal cartilage extirpation.

In chapter II, I attempted to address the uniformity of growth of the septal cartilage by directly measuring the expansion of the septal cartilage. However, because of surgical accessibility, I was only able to compare the interstitial growth of the septal

cartilage at two sites, both close to the dorsal border of the septum. My findings indicated that the septal cartilage expanded anteroposteriorly at both sites and did not show a regional difference at these two locations. The limited number of sites in which growth was monitored and their relative proximity necessitate a more comprehensive investigation of the growth of the entire septal cartilage. The goal of this chapter is to assess the uniformity of growth of the septal cartilage by measuring and comparing chondrocytic proliferation in various regions of the cartilage.

The proliferation and hypertrophy of chondrocytes together with matrix formation result in growth of cartilage (Seinsheimer and Sledge 1981). Previous studies on rat nasal septal cartilage have reported inconsistent findings on rates of proliferation in different parts of the cartilage. While Kvinnsland (1977) reported that the highest proliferation rate was in the anterior followed by middle and posterior parts of the cartilage, Searls (1972) found the highest rate in the sphenoidal tail followed by posterior, middle and anterior cartilage. Both studies used tritiated thymidine in animals of similar age. As might be expected, no consistent pattern of chondrocytic proliferation in the septum among different species and among different age groups in the same species has been found (Long et al. 1968; Searls 1975; Kvinnsland 1977; Searls 1977; Searls 1979; Wealthall and Herring 2006). This inconsistency may imply stochastic variations around an underlying similarity among all regions, but also raises the need for more thorough and modern approaches to investigate the chondrocytic proliferation in the nasal septum. In this study, I use Hanford miniature pigs of similar age to the ones used in the growth study (Chapter II).

Assessing DNA synthesis is a good measure of cellular proliferation. Immunohistochemical detection of bromodeoxyuridine (BrdU), a synthetic analogue of thymidine, has largely replaced tritiated thymidine as a means to identify cells in the S-phase of the cell cycle (Muskhelishvili et al. 2003; Rabie et al. 2003; Sun et al. 2007) and was employed in the present study.

Chondrocytic proliferation in the cartilage can be divided into proliferation of chondroblasts or stem cells located in the perichondrium and chondrocytes embedded in the matrix. Previous reports (Luder 1994) have shown that the contribution of these two parameters to the growth of the condylar cartilage of the mandible is dependent on age. In young rats with rapidly growing condylar cartilage, the proliferation and enlargement of the intramatrix chondrocytes together with matrix formation is the major contributor to the growth of the cartilage (around 80%). However, in older animals, with decreased growth rate, the main contributor to the growth of the cartilage is the proliferation of the perichondrial chondrocytes (around 75%). These findings suggest that in the septal cartilage, the intra-matrix and perichondrial chondrocytes might be proliferating at different rates.

The major purpose of this study is to measure the chondrocytic proliferation rate in different locations of the septal cartilage. Comparing the resultant values will help to (1) determine if cellular proliferation is contributing to the growth of the cartilage growth; (2) determine if chondrocytic proliferation varies regionally, which could lead to reinterpretation of results of chapter II; and (3) assess whether the proliferating chondrocytes are from a perichondrial or intra-matrix (central) origin.

Materials and Methods

Animals and tissue processing

The subjects used for this study were six Hanford minipigs (*Sus scrofa*, Sinclair Research Farms, MO), both sexes, ranging in age between 4 to 6 months (4.4 ± 1 months) and weighing 17 to 32 Kg (23 ± 6 Kg). Animals were injected IV with 40 mg/Kg of 5'-bromo-2'-deoxyuridine (BrdU, Sigma, St Louis, MO) 24 hours before they were sacrificed by intra-cardiac perfusion with Prefer® fixative (Anatech Ltd, Battle Creek, MI). Both procedures were carried out under isoflurane anesthesia and were approved by the IACUC at University of Washington under protocol 2331-01. Following sacrifice, the head was removed and the snout was cut into 7-9 coronal blocks using a band saw (Figure III-1). Blocks were decalcified in 10% formic acid/sodium formate. Decalcified blocks were embedded in paraffin, and 7 μm coronal sections were obtained and mounted on positively charged slides (Sigma-Aldrich, St Louis, MO). Sections were deparaffinized using the Xylene substitute Clearene® (Surgipath Medical Industries, Richmond, IL) and then rehydrated using three consecutive washes of 100, 100 and 70% ethanol. Antigen retrieval was performed by incubating the sections with 1% trypsin and 1% CaCl2 at 37°C for 20 min. Endogenous peroxidases were blocked by incubation with 3% hydrogen peroxide at room temperature for 20 min. Endogenous biotin and non-specific binding proteins were blocked by incubation with avidin (Vector Labs, CA) and 1% bovine serum albumin (BSA) (Vector Labs) for 15 min, followed by incubation with biotin (Vector Labs) and 1% BSA for 15 minutes. Sections were washed using phosphate buffered saline after each step. Sections were then reacted with 0.5%

mouse monoclonal BrdU antibody (Vector Labs), in 1% BSA at room temperature for 1 hour. Negative controls were incubated with BSA without BrdU antibody. The nasal epithelial cells in each section were used as positive control. After washing in PBS, sections were treated with biotin-conjugated secondary antibody for 30 min (Vector Labs), washed again in PBS, and incubated with tertiary antibody (avidin-labeled peroxidase, Vector Labs) for another 30 min. Chromogen development was performed by means of the peroxidase substrate diaminobenzidine (DAB, Vector Labs) for 30 seconds and stopped by thorough rinsing with water. Slides were then counterstained by methyl green for 10-30 seconds, dehydrated using 100 % ethanol followed by Clearene, and coverslipped.

Image capture and analysis

Sections were examined by light microscopy (Nikon Eclipse E400, Tokyo, Japan) and one slide from each block was used for further analysis. Blocks at or posterior to the nasofrontal suture were considered the posterior portion, all other blocks were considered the anterior portion (Figure III-1). The most anterior block (block 0 in Figure III-1) was omitted because of its irregular shape and partial ossification as the *os rostri*. The block closest to the nasofrontal suture was omitted to provide a clear division between anterior and posterior locations. To account for regional differences within a block, the cartilage sections were divided by 2 imaginary planes into dorsal, middle and ventral thirds (Figure III-2). The parietotectal cartilages, which represent the bifurcation of the dorsal septum to form a cartilaginous roofing of the nasal cavity, were considered to be a fourth cartilage region. Images of the 4 cartilage (parietotectal and 3 central) and 3 perichondrial locations (Figure III-2) were captured digitally using a Coolsnap FX

camera (Image Processing Solutions, North Reading Inc., MA) attached to a computer running MetaVue (Universal Imaging, Downingtown, PA). The images of the four cartilage locations (parietotectal and dorsal, middle and ventral central) were captured using the 10X objective of the microscope and the resultant image area was around 0.59 mm^2 , while the three perichondrial locations (dorsal, lateral and ventral) were captured using the 20X objective and the resultant area of the image was around 0.15 mm^2. Captured images were assigned random numbers that do not reflect the image location in order to help blinding the examiner to section location.

Images were analyzed using METAMORPH software (Molecular Devices, PA). BrdU-positive cells and total cells in each region were counted. The number of labeled cells was divided by the total cell count in order to generate a proliferative index. The proliferative index of each section (block) was calculated by averaging the indices of various regions. Finally, the proliferative indices of the anterior and posterior portions were calculated by averaging the proliferative indices of each block from that portion. The grand proliferative indices of the anterior and posterior regions were compared using a paired t-test (Kaleidagraph) to determine if the chondrocyte proliferation in the cartilage is uniform. The proliferative indices of the central and perichondrial locations were compared to determine whether perichondrial proliferation is the major source of new cells in the cartilage. Individual regions among the perichondrial and central locations were compared using ANOVA for repeated measures. In case of significance, t-tests were used to determine its source. Additionally, cellular density was calculated as total cells per unit area, and compared to assess the cellularity of the different parts of the septal cartilage. Because sample size was small, comparable non-parametric

tests were also performed. Significant findings were identical using both parametric and non-parametric methods, so only the former are reported here. Statistical tests were performed using Kaleidagraph and SPSS as appropriate.

Results

Chondrocytic proliferation

Typical BrdU reacted cartilage images are shown in Figure III- 3 (A, C). No reaction was present in the negative controls (Figure III-3, B and D). The proliferative indices of the septal cartilage were surprisingly consistent, with averages of 0.14 (dorsal perichondrium, anterior) to 0.27 (ventral cartilage posterior) and a total range from 0.07 (parietotectal cartilage of animal 402) to 0.32 (lateral perichondrial location of animal 425) (Tables III-1 and 2).

First, an overall comparison of various regions (tectal, central cartilage and perichondrial) was carried out, followed by individual regions within the central and perichondrial category. Overall, the proliferative index of the central locations was significantly higher than the indices of the parietotectal and perichondrial locations ($p<0.04$, ANOVA for Repeated Measures with post hoc paired t-test). Among the central locations, the middle and ventral sites showed higher proliferative index than the dorsal site ($p <0.05$, ANOVA for Repeated Measures with post hoc paired t-test). Similarly, among the perichondrial locations the middle and ventral sites showed higher proliferative index than the dorsal site ($p <0.006$, ANOVA for Repeated Measures with post hoc paired t-test).

After the regional comparisons, the anterior (Blocks 1-5, Figure III-1) and posterior (Blocks 7-9) parts of the septum were compared, first overall and then by region. No significant difference was found between the grand proliferative indices of the anterior and posterior portions of the septum ($p=0.4$, paired t-test). Similarly, no difference was found between the proliferative indices of the anterior and posterior parietotectal, central and perichondrial locations, whether considered together ($p>0.3$, paired t-test) or separately ($p>0.2$, paired t-test).

Within the anterior portion, the differences among the parietotectal, central and perichondrial locations did not reach statistical significance ($p=0.1$, ANOVA for Repeated Measures). However, comparison of individual regions revealed that the proliferative index of the dorsal perichondrial location was significantly lower than the indices of the remaining locations except the parietotectal cartilage ($p<0.05$, ANOVA for Repeated Measures with post hoc paired t-test). Within the posterior portion, the overall proliferative index of the central cartilage locations was higher than the indices of the parietotectal and perichondrial locations ($p<0.02$, ANOVA for Repeated Measures with post hoc paired t-test). Again, the proliferative index of the dorsal perichondrial location was significantly lower than the indices of the remaining locations except the parietotectal cartilage ($p<0.01$, ANOVA for Repeated Measures with post hoc paired t-test) and the index of the parietotectal cartilage was significantly lower than the indices of the three central locations ($p<0.04$, ANOVA for Repeated Measures with post hoc paired t-test).

Cell density

The cellular density of various regions of the cartilage are illustrate in Tables III-3, 4. Considering the septum as a whole, the cellular density (expressed as number of cells per mm^2) of the central locations was significantly lower than the density of the parietotectal and perichondrial locations ($p<0.001$, ANOVA for Repeated Measures with post hoc paired t-test). Among the central locations, no significant difference between individual regions was found. Among the perichondrial locations the ventral location showed higher cellular density than the dorsal locations ($p<0.01$, ANOVA for Repeated Measures with post hoc paired t-test).

The anterior portion of the septum showed higher overall cellular density than the posterior portion in 5 of the 6 animals, however the difference did not reach statistical significance ($p=0.2$, paired t-test). When the central cartilage was examined separately, the trend for higher anterior than posterior cellularity was stronger but still did not reach statistical significance ($p=0.06$, paired t-test). Qualitatively, the chondrocytes in the central regions appeared bigger in the posterior portion of the cartilage (Figure III-4 A, B). No difference in cellular density was found between the anterior and posterior parietotectal and perichondrial regions.

Comparing the regions within the anterior portion, the perichondrial locations showed higher cellular density than the central locations ($p=0.003$, paired t-test). No difference was found between individual central and perichondrial regions. Within the posterior portion, not only the perichondrial but also parietotectal locations showed

higher cellular density than the central locations ($p<0.02$, ANOVA for Repeated Measures with post hoc paired t-test). Again, no difference was found among the individual central and perichondrial cartilage regions.

Discussion

Limitations

One examiner identified the BrdU positive cells and performed the cell counting procedure manually. This might have introduced errors to the results. In order to test the reproducibility of the results the intra examiner correlation was assessed. In one animal (402) the BrdU labeled cells and the total cells were counted on two separate occasions by the same examiner. The correlation between the two measures was calculated, the correlation coefficient was relatively high ($R^2=0.9$) indicating that cell counting was acceptably reproducible. Since the images were assigned random numbers, the examiner was blinded to the location of the image. Therefore the potential bias was minimal.

Cellular proliferation and growth of the septal cartilage

Searls and colleagues (Searls and Kinser 1972; Searls 1977; Searls 1979) studied the proliferation of the septal chondrocytes in neonatal, newborn, 5 and 10 day-old rats. They reported that the proliferation rate of the cartilage varied with age, and that “septal growth is more active in the early (prenatal) stages of septal development and is diminishing to a point of being almost nonexistent by the tenth day postpartum.” In the present study, I found that the septal chondrocytes of much older minipigs (4-6

months) were proliferating at a surprisingly high rate. This strongly suggests that cell proliferation contributes actively to septal growth in juvenile animals roughly equivalent in age to 6 year-old humans. These findings are in accordance with findings in chapter II that showed that the septal cartilage of minipigs of this age is interstitially expanding.

Proliferative indices reported in the current study are surprisingly high. Searls (Searls and Kinser 1972; Searls 1977; Searls 1979), using tritiated thymidine injected one hour before animal sacrifice, reported the count of positively labeled cells in a microscopic field at 480X magnification to range between 1-8 cells. Presumably, at 100 X (as used herein) there would be 23-160 per field. Similarly, Copray (1986) assessed the number of proliferating cells using tritiated thymidine administered 2 hours before sacrifice. He reported the numbers of labeled cells in a 0.25 mm^2 microscopic field to range between 2 to 10, equivalent to 5-25 cells in the larger area measured here. In this study the number of BrdU labeled cells averaged around 125 cells/ field. The apparently higher labeling can be attributed, in part, to the timing of labeling. In this study, BrdU was injected 24 hours before sacrifice. BrdU (like tritiated thymidine) is taken up by the cells undergoing DNA synthesis (S-phase of the cell cycle), therefore its presence in the blood stream for a longer time should allow more cells to incorporate BrdU into their DNA. Although its half life is short (~ 2hrs, Gilbert et al, 2005), traces of thymidine analogues are still present even after 8 hours of its injection (Hickey et al. 1983). The much longer availability of BrdU in the present study probably accounts for the higher labeling observed. Alternatively, BrdU may be a more sensitive indicator of labeling than tritiated thymidine because background noise is essentially zero. The proliferation indices of the perichondrial regions reported in this study are comparable to

those of the perichondrium of the tibial and femoral growth plates ~20 % (Schrier et al. 2006) and the indices of the periosteum in cultured rabbit tibial explants ~30 % (O'Driscoll et al. 2001).

Although the cellular proliferation rate reported in this study was surprisingly high, it comes in accordance with the rapid growth rate of the cartilage reported in chapter II and indicates that the cellular proliferation is strongly contributing to the growth of the septal cartilage.

Regional variation

Earlier studies (Kvinnsland 1977; Searls 1977; Vetter et al. 1984; Copray 1986) reported great regional variation in the chondrocytic proliferation in the septal cartilage. The highest numbers of proliferating cells were generally found in the posterior end of the cartilage near the sphenoid and ethmoid bones (Kvinnsland 1977; Searls 1977; Copray 1986), in the center (Kvinnsland 1977; Searls 1977; Vetter et al. 1984; Copray 1986), and in the most anterior tip of the cartilage (Searls 1977). Unfortunately, the posterior tail and the anterior tip could not be analyzed in the study. The part near the sphenoid bone was difficult to isolate and the anterior part (block 0 in Figure II-1) was reacted for BrdU and showed a great number of proliferating cells (Figure III-4 C), however it was not included in the statistical analysis because, in pigs, the anterior tip contains an ossification, the *os rostri* and cartilage at this area was irregular with some parts displaying signs of endochonral ossification.

The only regional variation found was the general decrease in proliferative index in the most dorsal part of the septal cartilage (dorsal perichondrial and parietotectal

cartilages). Interestingly, this region is strongly attached to the ventral portion of the nasal bone via fibrous tissue while the remaining locations of the cartilage are more separate from nearby structures. This might imply that the growth of this part is restrained by its mechanical attachment or specialization of this part of the cartilage to provide mechanical attachment rather than growth. In this regard it is interesting that the removal of the bone and nasofrontal suture that overlies the dorsal septum actually enhanced growth of the snout in rabbits (Babler et al. 1982). Thus the bones of the nasal dorsum may restrict the full growth potential of the septum. The only hint for an anterior-posterior difference was a non-significant trend for higher cellularity anteriorly (possibly indicating a more recent proliferation). Coupled with the qualitative observation of smaller cells, it is conceivable that the anterior region is slightly more important than the posterior region, but if so the difference is negligible. This corresponds well with the results of chapter II, where anterior and posterior locations elongated at the same rate, with the anterior being slightly, but not significantly faster. This tendency is probably magnified by the greater width of the anterior cartilage (chapter IV) and the greater overall size of the anterior cartilage.

Differences between perichondrial and central cartilage locations

Proliferating cells in the cartilage come from both the perichondrium and the intra-matrix chondrocytes. Examining the condylar cartilage in rats, Luder (1994) reported that the growth of the cartilage is shaped by 3 factors: perichondrial chondrocytic proliferation, cellular enlargement and matrix formation. In young animals with fast growth, the 3 factors contributed about 20%, 30% and 50% respectively.

However in older animals the proliferation of perichondrial chondrocytes contributed 75% of the growth of the cartilage, albeit that growth was less overall at this time.

The nasal septum is a very different cartilage than the mandibular condyle but nevertheless has an extensive perichondrium, capable of contributing new chondrocytes to the central cartilage. Although the proliferative index of the perichondrium was lower than that of the central cartilage, its cellularity density was higher. If both factors are considered, the number of proliferating perichondrial chondrocytes (cellular density X proliferative index) is significantly higher than the number of proliferating central chondrocytes in both anterior and posterior portion of the cartilage ($p<0.03$, paired t-test). Such a finding suggests that the perichondrium is a major source of proliferating chondrocytes in 4-6 month-old minipigs, possibly more important than the intramatrix chondrocytes, although not as dominant as in Luder's (1994) older mandibular condyles.

Summary

This chapter assessed the proliferation of the septal cartilage chondrocytes. Six animals were used for immunohistochemical evaluation of cellular proliferation using BrdU. The septal chondrocytes proliferated almost uniformly throughout the entire cartilage. In addition, the cells in the perichondrium also contributed strongly to the growth of the cartilage. Therefore, my findings suggest that the cartilage is expanding throughout its entire length at least at the cellular level.

Table III-1: Proliferative indices in the anterior part of the septal cartilage

Animal ID	Parietotectal	Central locations				Perichondrial locations				Grand average
		Dorsal	Middle	Ventral	Average central	Dorsal	Middle	Ventral	Average perichondrial	
401	0.19	0.20	0.27	0.18	0.22±0.05	0.15	0.27	0.30	0.24±0.08	0.22±0.06
402	0.07	0.20	0.22	0.26	0.23±0.03	0.13	0.28	0.31	0.24±0.10	0.21±0.09
414	0.20	0.23	0.21	0.23	0.22±0.02	0.18	0.20	0.25	0.21±0.04	0.21±0.02
415	0.19	0.14	0.19	0.22	0.18±0.04	0.18	0.19	0.14	0.17±0.03	0.18±0.03
425	0.20	0.29	0.27	0.29	0.28±0.03	0.13	0.32	0.32	0.26±0.11	0.26±0.07
426	0.20	0.26	0.27	0.23	0.25±0.02	0.10	0.24	0.17	0.17±0.07	0.21±0.06
Average±SD	0.17±0.05	0.22±0.06	0.24±0.04	0.24±0.05	0.23±0.03	0.14±0.03	0.25±0.05	0.25±0.08	0.21±0.04	0.22±0.04

Table III-2: Proliferative indices in the posterior portion of the septal cartilage

Animal ID	Parietotectal	Central locations				Perichondrial locations				Grand average
		Dorsal	Middle	Ventral	Average central	Dorsal	Middle	Ventral	Average perichondrial	
401	0.22	0.26	0.26	0.30	0.27±0.03	0.22	0.26	0.26	0.25±0.03	0.25±0.03
402	0.16	0.14	0.14	0.22	0.17±0.05	0.16	0.11	0.28	0.18±0.08	0.17±0.06
414	0.18	0.20	0.25	0.29	0.25±0.06	0.15	0.16	0.15	0.15±0.01	0.20±0.07
415	0.21	0.17	0.27	0.29	0.24±0.07	0.14	0.25	0.24	0.21±0.06	0.23+0.05
425	0.17	0.24	0.26	0.30	0.27±0.03	0.16	0.25	0.22	0.21±0.05	0.23±0.05
426	0.21	0.25	0.28	0.19	0.24±0.05	0.15	0.17	0.19	0.17±0.02	0.21±0.04
Average±SD	0.19±0.02	0.21±0.05	0.24±0.06	0.27±0.05	0.24±0.04	0.16±0.03	0.20±0.06	0.22±0.05	0.20±0.04	0.21±0.03

Table III-3: Cellular density (cells/mm2) in the anterior part of the cartilage

Animal ID		Central locations				Perichondrial locations				Grand cellular density
	Parietotectal	Dorsal	Medial	Ventral	Average central	Dorsal	Middle	Ventral	Average perichondrial	
401	1105	1183	712	612	836±305	1000	1280	996	1092±162	984±243
402	2463	645	636	672	651±90	1333	855	2570	1586±885	1311±859
414	1350	1107	953	895	985±110	1132	1489	1476	1366±202	1200±242
415	812	695	728	1095	839±222	1336	1199	1321	1285±75	1026±277
425	1325	1090	922	1411	1141±249	1492	1585	1546	1541±46	1339±248
426	1550	1060	952	1045	1019±59	1103	1209	2438	1584±742	1337±523
Average	1434±563	963±231	817±141	955±259	912±172	1233±184	1269±255	1725±634	1409±352	1199±399

Table III-4: Cellular density (cells/mm2) in the posterior part of the cartilage

Animal ID	Parietotectal	Central locations				Perichondrial locations				Grand cellular density
		Dorsal	Medial	Ventral	Central average	Dorsal	Middle	Ventral	Perichondrial average	
401	970	763	745	708	739±38	802	1204	1171	1059±223	909±208
402	1124	558	621	739	640±92	1081	1218	1807	1369±385	1021±432
414	1394	811	787	875	824±45	1025	1311	1319	1218±167	1074±262
415	1007	732	833	1011	859±141	1182	1244	1109	1178±67	1017±184
425	1283	798	894	793	828±57	1216	1022	1459	1233±219	1067±259
426	2380	1064	1038	701	934±202	1840	1833	1604	1759±135	1494±585
Average	1360±525	788±163	820±141	804±120	804±102	1191±350	1305±276	1411±266	1303±245	1097±203

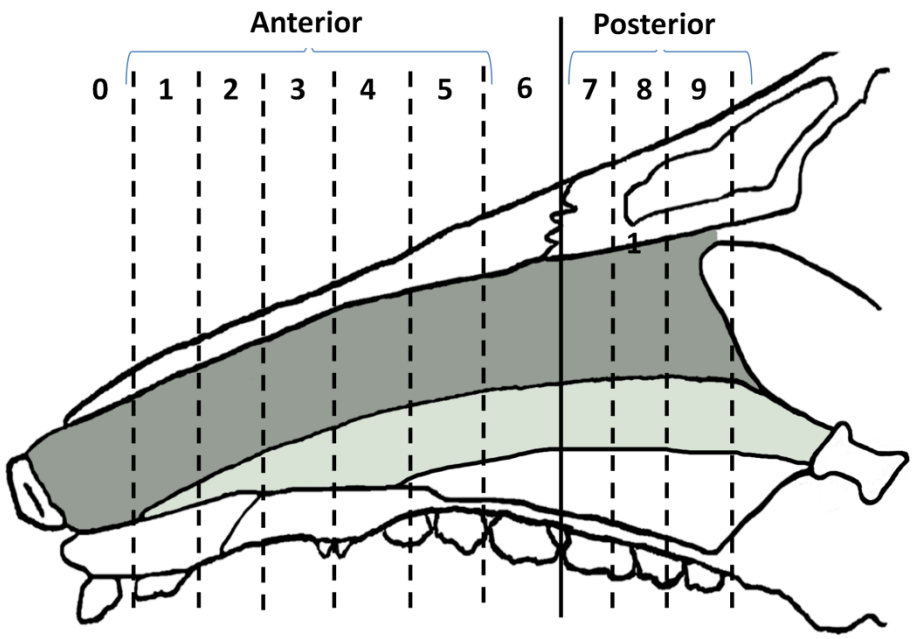

Figure III-1: Medial view of a sagittal section illustrating the position of the blocks and the anterior and posterior portions of the cartilage

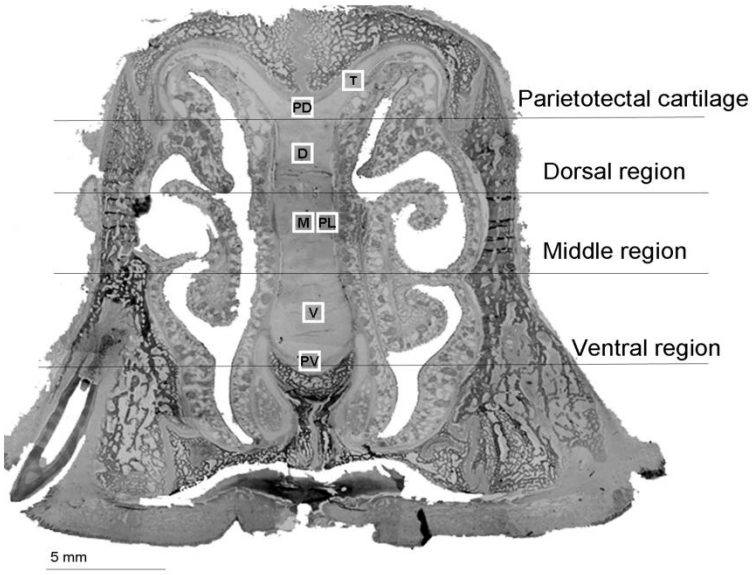

Figure III-2: Coronal view of the snout illustrating the parts of the septal cartilage that were used to measure the proliferative index. Cartilage locations: D: dorsal, M: medial, T: parietotectal, V: ventral. Perichondrial locations: PD: perichondrial dorsal, PL: perichondrial lateral, PV: perichondrial ventral

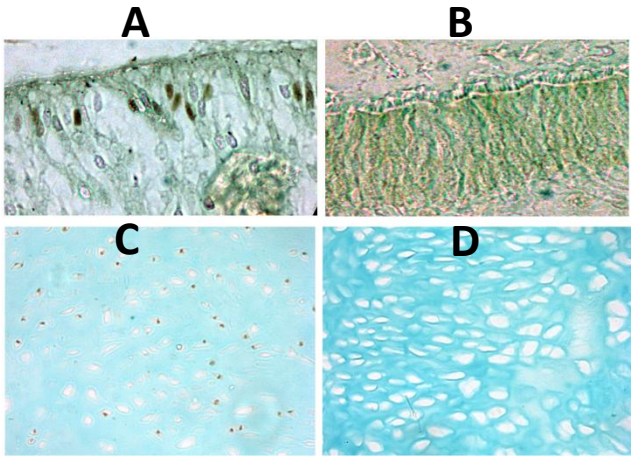

Figure III-3: Left: positive staining of the nasal epithelial cells used as positive control (A) and positively stained nasal cartilage chondrocytes (C). Right: negative control showing absence of staining in nasal epithelial cells (B) and nasal cartilage chondrocytes (D).

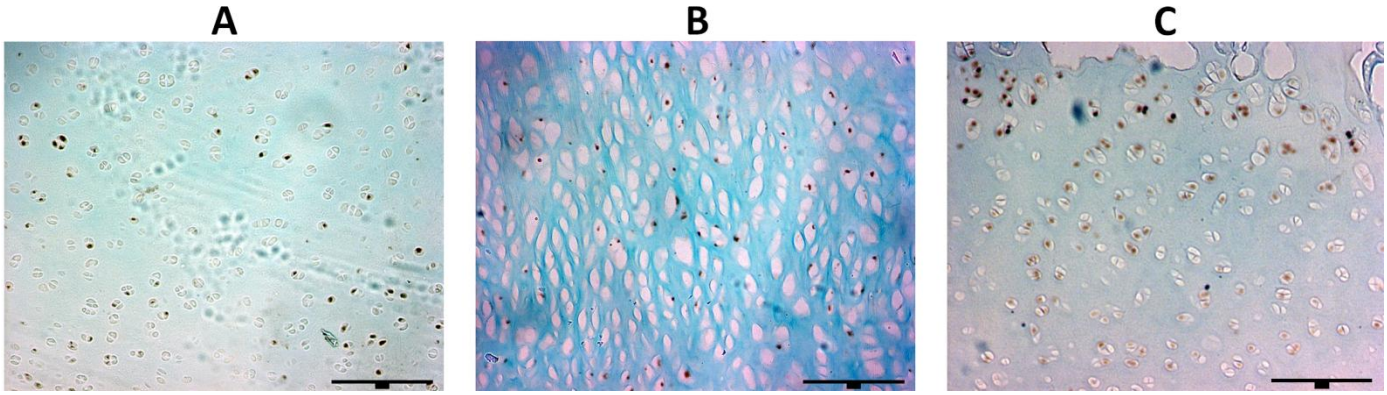

Figure III-4: A and B: The middle location in the anterior (A, block 2) and posterior portions (B, block 8) of animal 402. The cells in the posterior portion were often larger than the ones in the anterior portions. C, the nasal tip of the septal cartilage of animal 402 (block 0). Decalcified bone of the os rostri is found just above the heavily labeled chondrocytes in the dorsal part of the slide. Scale bars correspond to 200 µm.

Chapter IV: Deformation of the nasal septal cartilage during mastication

Background

The nasal septal cartilage is a midline structure stretching from the perpendicular plate of the ethmoid to the external nose. In addition to a postulated ability to apply an antero-posterior growth pressure to the snout (Sarnat and Wexler 1966; Sarnat and Wexler 1968; Kvinnsland 1973; Kvinnsland 1974; Copray 1986; Kvinnsland 1988), the septal cartilage is hypothesized to play a major role in facial integrity. For example, Badoux conceptualized the bony rostrum as an imperfect framed structure and the septal cartilage as a midline vertical strut reinforcing the pentagonal rostrum, preventing its collapse during masticatory loading (Badoux 1966; Badoux 1968). The finding that the nasal bones partially collapse after extirpation of nasal septal cartilage in young guinea pigs (Stenström and Thilander 1970) and in rats (Moss et al. 1968) has been taken as evidence of the strut-like role of the nasal septal cartilage. If this notion is correct, then the septal cartilage should bear compressive loading along the vertical axis during mastication.

The hypothesized strut role of the septal cartilage is, however, challenged by the mechanical weakness of most cartilages, especially in view of the heavy loading the snout probably receives from mastication. Cartilage in the body is usually thought to help protect the less flexible bones from overloading by shock absorption (storage of energy), load damping (absorption of energy) and/or by distributing loads over a greater

area (Kobayashi et al. 2001; Ng et al. 2003). This belief is based on experimental comparison of the viscoelastic properties of bone and cartilage (Radin and Paul 1971; Rohl et al. 1997). Recently it has been argued that despite the excellent energy absorption characteristics of cartilage, articular cartilage is too thinly layered to be the most important shock absorbing element in a typical joint (Martin 1998). This argument does not apply to the septal cartilage, which comprises a large proportion of the height of the snout skeleton. Thus the nasal cartilage might serve to store and/or absorb loads generated during mastication.

Mastication is a major source of loading of the mammalian skull, strongly influencing cranial morphology (Vilmann et al. 1989; Varrela 1990; Kiliaridis 1995; Katsaros 2001; Katsaros et al. 2002; Larsson et al. 2005; Kiliaridis 2006). Masticatory strains in the facial bones and sutures have been studied in several species using strain gages glued to the skull surface (Ross and Hylander 1996; Hylander and Johnson 1997; Rafferty and Herring 1999; Herring et al. 2001; Thomason et al. 2001; Lieberman et al. 2004; Liu et al. 2004). At least in pigs, strains are much lower in facial bones (maximally a few hundred με) compared to sutures (typically over 1000 με), suggesting that sutures are providing flexibility to the rostrum, damping loads by absorbing energy and perhaps protecting the bones from such loads (Jaslow and Biewener 1995).

To date, there are no data on the *in vivo* strain levels in the nasal septum. Strain magnitudes similar to the sutures would suggest a damping function and the orientation of those strains could either support or refute the hypothesis that the septum is a vertically compressed strut during mastication. Information on patterns of strain in the septal cartilage could also help elucidate the overall nature of rostral deformation during

chewing, specifically whether bending or torsion occurs during the power stroke (Ross and Hylander 1996; Thomason et al. 2001; Rafferty et al. 2003; Lieberman et al. 2004).

Because strain gages cannot be glued to cartilage, an alternative method must be used to assess septal strain. In this study, DVRTs (differential variable reluctance transducers) were used, which rely on barbed broaches for attachment. These transducers were developed to measure linear displacement of soft tissues (Beynnon and Fleming 1998; Fleming et al. 1999; Byl et al. 2002; Cerulli et al. 2003). Pigs were used in order to build on the body of literature already gathered, and also because their large snouts facilitate surgical access and implantation.

In this chapter the postulated role of the nasal septal cartilage as a vertical strut supporting the bony rostrum is tested by measurement of masticatory strain at the septal cartilage and nasofrontal suture were measured. Because of the difficult access to the nasal cavity, I was restricted to anteroposterior measurements of strain. Two groups were used in this study. In the first group, DVRTs were used to measure the masticatory strains at the septo-ethmoid junction and the nasofrontal suture. The measurements from this group are supplemented by observing strains in the most anterior part of the septum, but only in anesthetized animals. This portion of this chapter has been published (Al Dayeh et al. 2009). The second group comprises the animals used in the growth study (chapter II). The anteroposterior masticatory strains were measured in two intermediate positions in the cartilage, and at the nasofrontal suture. Overall, observing the masticatory strains in these two groups shows how the septal cartilage (at least the dorsal part) is deforming during mastication. The study addresses two questions: First, does the septal cartilage act as a vertical strut during mastication?

This question is answered by observing the polarity of masticatory strains in the cartilage. The vertical strut model predicts that the cartilage is vertically compressed, and, as a result of Poisson's effect, anterposteriorly tensed. Second, does the cartilage act as a stress dampener during mastication? This question is answered by measuring the magnitude of masticatory strains generated on the cartilage and nasofrontal suture. A stress dampening effect would be suggested if the septal cartilage deformation is similar in magnitude to that of the suture.

Materials and Methods

Group 1

The subjects used for this study were 10 Hanford pigs (*Sus scrofa)*, both sexes, ranging in age from 4 to 6 months and weighing 19-32 Kg. All the procedures were approved by the Institutional Animal Care and Use Committee of the University of Washington, and were carried out in Seattle in 2005-2007. The animals were trained to eat their normal diet of pelleted pig chow in the lab environment. Experiments were performed when the animals showed normal feeding behavior under experimental conditions.

On the day of the experiment, the pigs were mask-anesthetized using isoflurane/nitrous oxide and then intubated. A 3.5 cm midline incision was made to expose the frontal and nasal bones, and then a window was cut through the frontal bone just posterior to the nasofrontal suture, to reach the floor of the frontal sinus, which was removed to gain access to the posterior part of the nasal septal cartilage at the septo-ethmoid junction. A 25-gauge vertical hole was drilled in the ethmoid bone, and a

differential variable reluctance transducer (DVRT) (Microstrain Inc., Williston, VT) was implanted in an anteroposterior orientation with approximately half its length on the ethmoid and half on the cartilage (Figure IV-1). The distance between the barbs, typically 1.0-1.5 cm, was recorded. The bony window was replaced and fixed using mini-plates and screws (Mandible Trauma, SYNTHES Maxillofacial, West Chester, PA). The nasofrontal suture was instrumented lateral to the window (Figure IV-2). A second DVRT was placed on one side, and on the other the bone was cleaned, dried and prepared (M-Bond 200 catalyst, Vishay Micro-Measurements, Raleigh, NC) and then a single element strain gage (EP-08-125BT-120, Vishay) was glued (M-Bond 200, Vishay) across the suture. Fine wire electrodes for electromyography (EMG) were inserted in the masseter and temporalis bilaterally. The strain gage and DVRT signals were conditioned (Model 2120A, Vishay, and MB-STD-4, Microstrain respectively), and with the EMG signals (MEC 100, BIOPAC Systems, Santa Barbara, CA), digitized (MP100A, BIOPAC) and recorded using AcqKnowledge software (BIOPAC).

Intramuscular analgesics, buprenorphine (0.5mg/Kg, Reckitt Benckiser, Berkshire, UK) and/or ketorolac (1mg/kg, Hospira Inc., Lake Forest, IL), were injected and the animals were allowed to recover from anesthesia. Regular pig chow was offered and animals were permitted to eat for 15 minutes while signals were captured. Following that, animals were re-anesthetized; an anterior incision was made and a 4 cm window through the anterior part of one nasal bone was cut to gain access to a more anterior part of the septal cartilage (Figure IV-2). A third DVRT was placed horizontally in the dorsal part of the cartilage. Pairs of stimulating electrodes were placed in the masseters on opposite sides of the motor nerve entry point to assure stimulation of the

whole muscle. The muscles were tetanized (60 pps, 600 ms trains, 2 trains/sec) with increasing voltage until visible spread of the contraction to neighboring muscles, typically 20-60 V (S48, Grass Instruments, Warwick, RI) in the following order: left, right and both masseters. In some subjects a bite block was placed between the anterior teeth, and the above stimulation was repeated. The signals were captured as before. Finally the snout was gripped around the anterior teeth and manually manipulated: pushed anteroposteriorly and bent dorsoventrally. Lateral bending was also attempted but could not be performed consistently. After finishing the procedure, the animals were sacrificed by perfusion or by a lethal dose of pentobarbital in the ear vein. After sacrifice, the DVRTs and strain gage were visually inspected to check for positioning.

The DVRT and strain gage data were analyzed using AcqKnowledge. DVRT voltage was converted to displacement using a calibration procedure conducted prior to each experiment. DVRT strain was then calculated by dividing displacement by the measured length of the DVRT as initially placed in the tissue. Negative numbers are used to indicate compression.

Group 2

This group comprises subjects used in the growth study (chapter III). Subjects used were 10 female Hanford minipigs (*Sus scrofa*), ranging in age from 3.5 to 4.5 months and weighing 12–27 kg. Pigs were obtained as before.

Details of the surgical procedure performed on this group are described in the Materials and Method of chapter II. DVRTs (Microstrain, VT) were used to measure growth and masticatory strain at two intermediate positions in the septal cartilage

(compared to group 1) and the nasofrontal suture. The DVRT signals in this group were conditioned and amplified, then telemetered to a nearby computer with a USB Base Station (Microstrain) where the signals were captured.

During feeding, in 4 animals, the DVRT signal was recorded simultaneously with the EMG signal using same apparatus as group 1. In the remaining animals, the strains generated on the septal cartilage during mastication were recorded at 32, 64 and 658Hz, using the wireless apparatus without recording the EMG signals.

Anatomical study

To assess the anatomy of the septum and the histological nature of its attachment to the bony skeleton of the snout, additional skulls and heads of Hanford pigs of similar size were examined. Three skulls were cut parasagittally for gross examination and 4 heads were cut into 5-7 coronal blocks using a band saw. These latter 4 were a subset of the animals studied for cell replication (chapter III). Blocks were decalcified in 10% formic acid/ sodium formate, embedded in paraffin and cut at 7 μm. The sections were stained with hematoxylin and eosin, and observed by light microscopy (Nikon Eclipse E400, Tokyo, Japan); images were captured digitally (Coolsnap FX, Image Processing Solutions, North Reading Inc., MA). Histological measurements of septal cartilage width and height were made using MetaVue (Universal Imaging, Downingtown, PA)

Statistical testing (ANOVA, paired and 2-sample t-tests) was performed using Excel, GraphPad and SPSS (version 13.0) software.

RESULTS

Anatomy

The nasal septum is composed of an osseous and a cartilaginous part (Figures IV- 1, 3). The osseous portion consists of the perpendicular plate of the ethmoid posteriorly and the vomer inferiorly. The vomer, representing a fused pair of dermal bones, extends from the anterior border of the presphenoid bone to the nasal surface of the premaxillary bone; its superior surface is split to form the vomerine groove. This groove houses the inferior aspect of the nasal septal cartilage, including complete enclosure of a cylindrical posterior extension that joins the presphenoid bone (Figure IV-1). The sides of the septal cartilage are covered by an adherent perichondrium and coated with epithelium (Figure IV-3). The cartilage tapers anteriorly, with height decreasing from 20 ± 3 mm posteriorly to 12 ± 1 mm anteriorly (n = 4). Cartilage thickness varies as well (Figure IV- 3A, B), with the anterior area being thicker (4.0 ± 0.7 mm) compared to the rest of the cartilage (2.9 ± 0.2 mm), ($p = 0.01$, paired t-test). The posterior abutment of the cartilage with the perpendicular plate of the ethmoid separates easily, and its articulation with the vomerine groove is loose. However, anterior to the groove the cartilage strongly adheres to the nasal surface of the premaxillary bone. Superiorly (dorsally), the septum divides into the parietotectal cartilages, which are in tight contact with the inferior surface of the frontal and nasal bones. The septal cartilage extends 3-4 mm anterior to the tip of the nasal bones and 5-10 mm anterior to the

premaxillary bones. The most anterior part of the cartilage expands to form a wedge in which the *os rostri* ossifies (Figure IV-1).

Microscopically, the perichondrium is composed of two layers, an outer fibrous and an inner cellular layer containing flattened cells assumed to be chondroblasts. Within the cartilage matrix, chondrocytes are often arranged in nests of 2-3 cells. A few blood vessels run anteroposteriorly through the lower part of the septum, but the matrix itself is avascular. The tight superior connection of the septum and its parietotectal extensions to the nasal dorsum consists of a fibrous articulation with the frontal and nasal bones (Figure IV-3C). The tight connection of the inferior septum to the premaxillary bones is also fibrous. The loose inferior connection with the vomerine groove consists of a pad of loose connective tissue (Figure IV-3D).

Strain experiments

Group 1

The instrumentation created no problems for mastication. All animals recovered quickly from anesthesia and ate normally (Table IV-1), except for one (#415) which refused food but chewed on a rubber tube. Most instruments functioned well during mastication and muscle stimulation, but some failed sporadically during manipulation (Tables IV-2 and 3). Although these failures might simply reflect the fact that manipulations were performed last, it is likely that gripping the head and distorting the soft tissues affected the instruments, for example by preventing the DVRTs from sliding freely. I therefore have less confidence in the manipulation results.

In awake pigs, measurable displacements and strains were only seen during mastication, not during food gathering or investigative activities. During mastication, the septo-ethmoid and nasofrontal DVRTs and the nasofrontal strain gage showed peaks of displacement/strain that coincided with the end of each power stroke (Figure IV-4). The two DVRTs were usually in synchrony, and their peak displacement was slightly delayed relative to the peak measured by the sutural strain gage (53 $\pm$ 12 msec, n = 5) (Figure IV-4).

Septo-ethmoid junction DVRT

Antero-posterior strains generated during mastication at the septo-ethmoid junction were consistently compressive, averaging about -1000 $\mu\varepsilon$ (Table IV-1, Figure IV- 4). Not surprisingly for a midline recording, side of chewing made no difference in the 7 experiments with sufficiently good EMG to determine the direction of jaw movement ($p > 0.2$, paired t-test).

Although masseter stimulation was intended to mimic mastication on anesthetized animals, the results were different at the septo-ethmoid junction. Strain values were still compressive but were much lower, averaging only -73 $\mu\varepsilon$ (Table IV-1). One individual had no measurable strain (#399) and one was slightly tensed (#405, Table IV-1). There was no significant difference between bilateral, right or left masseter stimulation ($p > 0.5$, ANOVA). Insertion of a bite block between the anterior teeth in 4 animals did not cause any significant change ($p > 0.6$, paired t-test).

Strains at the septo-ethmoid junction were also usually low when the snout was manipulated (Tables IV-2 and 3). Most measurements were compressive when the

snout was forced posteriorly, with 2 individuals (#400 and #404) having magnitudes comparable to mastication. Pulling the snout anteriorly had either no effect or caused low tensile strain. Bending the snout dorsally gave very inconsistent results, whereas bending it ventrally usually caused low tension.

Anterior septal cartilage DVRT

The anterior septal DVRT was inserted after the chewing portion of the experiment, so only masseter stimulation and snout manipulation were recorded. Masseter stimulation consistently resulted in antero-posterior compression of the anterior cartilage with magnitudes greatly exceeding those of the septo-ethmoid junction even during mastication (Table IV-1). Higher compressive strains were obtained when the masseter was bilaterally stimulated (-11,271 ± 5162με, Table IV-1) than either contralateral (-6512 ± 4560 με, n = 9) or ipsilateral (-5278 ± 4684 με) stimulation; however, this difference did not reach statistical significance ($p = 0.1$, ANOVA). Block placement during bilateral stimulation resulted in a non-significant increase in strain ($p > 0.2$, paired t-test).

Pushing the snout posteriorly and pulling it anteriorly produced high magnitudes of compression and tension respectively (Table IV-2). Strong compression was recorded when the snout was bent dorsally. Only 4 successful recordings were made during ventral bending, but these were all strongly tensile (Table IV-3).

Nasofrontal suture

Recorded by strain gage, masticatory strain at the nasofrontal suture was consistently and strongly compressive, averaging over -2000 με (Table IV-1), with no significant effect of side of chewing. Recorded by DVRT, masticatory strain was still compressive, but usually less than that recorded by the strain gage (approximately -1000 με, Table IV-1) and considerably more variable, owing to very low strains in two pigs (#403 and #405).

Masseter stimulation resulted in similar sutural strain values to those recorded during mastication. Strains were usually higher for bilateral (-2666 ± 750 με and -910 ± 1019 με for strain gage and DVRT respectively, Table IV-1) followed by ipsilateral (-2059 ± 611 με for strain gage and -739 ± 897 με for DVRT) and contralateral (-1272 ± 505 με and -202 ± 270 με respectively). ANOVA on the strain gage results showed that contralateral stimulation was significantly less than bilateral and ipsilateral ($p = 0.002$), but the difference was not significant for the DVRT data ($p > 0.6$). Bite block placement did not cause any significant increase in strain with either instrument.

During manipulations, the gage and DVRT gave similar results: compression for posterior pushing and dorsal bending, and tension for anterior pulling (except the anomalous #401 DVRT) and ventral bending (Tables IV-2 and 3).

Group 2

All pigs ate normally post-surgically. In pigs with synchronized EMG signals (n=4), strains were only seen during mastication, not during food gathering or

investigative activities. During mastication, cartilage and nasofrontal suture DVRTs showed synchronous peaks of compression displacement/strain that coincided with the masseter activity at the end of each power stroke. In animals with no EMG recording, a similar pattern of compression at the three locations was also observed. Overall, compressive strains were highest on the nasofrontal suture (-4015 ± 1325με), followed by the middle septal cartilage (-2766 ± 1260με) and then the posterior septal cartilage (-1621 ± 520με) (Table IV-4). ANOVA and post hoc analysis showed that the strain at the nasofrontal suture was higher than that at the posterior cartilage ($p=0.02$); the remaining comparisons were not significant. Only two animals (412 and 417) had sufficiently good EMG recording to determine side of chewing (Table IV-5). Both animals showed a clear tendency for higher compressive strains on the ipsilateral (instrumented) side (Table IV-5). In other words, septal strains were greater when pigs chewed on the left and suture strains were greater when pigs chewed on the right. Values were statistically significant in the middle septal cartilage in both animals ($p<0.01$, paired-t), but not in the posterior septal cartilage ($p>0.5$, paired-t). Higher ipsilateral compressive strains at the nasofrontal suture reached statistical significance only in Pig 412 ($p<0.01$, paired-t). Interestingly, sutural strains recorded in group 2 were higher than strain recorded in group 1 ($p<0.001$). Similarly strains recorded at the two septal locations were significantly higher that strains recorded at the septoethmoid junction in group 1 ($p<0.04$, ANOVA with post hoc)

DISCUSSION

Functional Morphology of the Septum

The septal cartilage tightly adheres to the roof of the nasal cavity, implying that deformations should be comparable to those of the nasal dorsum. In contrast, the ventral border is tightly attached only at its anterior (premaxillary) extremity. Although the vomerine groove constrains the septal cartilage to the midline, the cartilage appears to be capable of some antero-posterior sliding within the groove. The placement of the DVRT at the anterior septum coincided (unintentionally) with the area in which the cartilage is firmly attached to its ventral boundary.

Another pertinent feature of cartilage anatomy is the fact that it is thicker anteriorly and thinner posteriorly, implying a greater ability to resist loading anteriorly. The anteroposteriorly oriented bulge in the middle (Figures IV-3A, B) also suggests the possibility of horizontal loading.

Pattern and Magnitude of Masticatory Strain in the Nasal Septum

During mastication the septo-ethmoid junction showed clear evidence of loading. Strain at the septo-ethmoid junction and the middle and posterior septal cartilage occurred at the end of each power stroke and was simultaneous with strain in the nasofrontal suture. Because the onset of strain occurred after the onset of muscle contraction, it was likely caused by occlusal force rather than being a direct result of muscle pull on the skull.

Notably, however, the compressive strain recorded was anteroposterior. If the septum behaved as a compressive strut under an idealized axial load, compression would have been dorsoventral and, based on a Poisson ratio of 0.32 in septal cartilage (Grellmann et al. 2006), I should have seen tensile strain in the anteroposterior direction. Thus these results indicate that the septal cartilage is not under simple vertical compression during mastication, as envisioned by the idealized compressive strut model. Rather, the cartilage is under anteroposterior compression caused by some aspect of occlusal loading. This is reinforced by the fact that anteroposterior compression was also the pattern of strain observed in the most anterior part of the septum during masseter muscle stimulation. In fact, the only loading regimes that produced the expected anteroposterior tension in either septal location were non-physiological manipulations that pulled the snout anteriorly (an axial tension) or bent it ventrally (placing the dorsum of the entire skull under tensile strain). I conclude that the septum does not function as a vertical strut during mastication.

It is also notable that the average magnitude of masticatory strain recorded by the septal DVRTs of both groups (around -1685$\mu\varepsilon$) was essentially the same as that recorded by the sutural DVRT in both groups (-2070 $\mu\varepsilon$). These strains are far higher than the largest principal strains observed during mastication in the nearby bones: -85 $\pm$ 12 $\mu\varepsilon$ for the nasal bone (Rafferty et al. 2003) and -53 $\pm$ 23 $\mu\varepsilon$ for the frontal bone (Herring and Teng 2000). Therefore, strain at the septum and septo-ethmoid junction is at least an order of magnitude greater than the bones. This differential suggests that the septal cartilage, like sutures, may serve to absorb energy and hence damp the forces transmitted through the skull.

Difference in sutural strain between the two groups

The magnitude of masticatory strain at the nasofrontal suture in group 2 (-4000 με, Table IV-4) was much larger than that recorded in group 1 using DVRTs (p=0.0004, 2 sample t-test). This unexpected difference can be attributed to the difference in surgical procedure between the two groups. In group 2, a larger portion of the nasal bone was reflected in order to gain access to place 2 DVRTs in the septal cartilage. This might have decreased the stiffness of the rostrum, resulting in more deformation and higher strain magnitudes at the nasofrontal suture. Masticatory strains from the septal cartilage were also high. The middle and posterior locations showed larger deformation (-2700 and -1600 με respectively, Table IV-3) than did the septo-ethmoid junction in group1 (around 1000 με). This is likely due to the fact that the septoethmoid DVRT was located across the septoethmoid junction with half of the DVRT length spanning the ethmoid bone. In addition, the surgical procedure in group 2 might have resulted in increased deformation of the cartilage during mastication.

Overall deformation: Why was the septo-ethmoid junction deformed less by stimulation and manipulation than by mastication?

Masseter stimulation was intended to mimic the power stroke of mastication in unconscious animals. In previous studies on other parts of the skull (Herring and Teng 2000), such stimulations have typically produced similar or larger strains than mastication (larger strains are explained by the more complete contraction of the muscles). Even in the present study, the instruments over the nasofrontal suture recorded higher but comparable strains to those of mastication and the DVRT in the

anterior septal cartilage registered very large compressive strains. Thus it does not seem likely that the additional surgery (cutting an anterior window in the nasal bones) somehow destroyed force transmission in the skull. Nevertheless, although strains were still compressive, the septo-ethmoid junction showed much smaller values during stimulation than during mastication (Table IV-1). Thus masseter stimulation may mimic masticatory loading of the nasofrontal suture, but it does not do so for the septo-ethmoid junction.

The discrepancy for the septo-ethmoid junction means that the skull is deformed differently during mastication and during masseter stimulation. As a working hypothesis, I propose that during masseter stimulation the snout is primarily bent and/or sheared dorsally, and that these loading regimes have minimal effects on the septo-ethmoid junction while deforming the other parts of the snout. During mastication, I propose that, additionally, the septo-ethmoid junction is axially compressed. My reasoning is as follows. Two important variables are different for these activities (mastication and masseter stimulation), the point of occlusal contact and the direction of occlusal force. Masseter stimulation applies an antero-superior force to the whole dentition, especially the anterior teeth. This occlusal force at the incisors should bend and/or shear the snout dorsally. Dorsal bending will compress the dorsum, including the nasofrontal suture and the anterior septal cartilage, but not the septo-ethmoid junction, which is located centrally in the skull, close to the presumed neutral plane (Figure IV-1). Dorsal shearing, on the other hand, will cause tensile strain along the anterodorsal-posteroventral diagonal and compressive strain along the anteroventral-posterodorsal diagonal. These opposite strains will tend to cancel out for the anteroposteriorly oriented

septo-ethmoid DVRT, but not for the sutural and the anterior septal DVRTs, which were more aligned with the compressive diagonal (Figure IV-1). Thus, both dorsal bending and dorsal shear would compress the nasofrontal suture and the anterior septum but have little effect on strain at the septo-ethmoid junction. In contrast, mastication occurs especially at the molar teeth with only fleeting contact of the premolars and incisors; further, it recruits all major jaw closing muscles, not just the anteriorly directed masseters. Molar root anatomy suggests that maxillary occlusal loads are slightly posterior in pigs (Ferrari and Herring 1995). Thus mastication would apply a posterior force to the molar teeth, compressing the septo-ethmoid junction, which is located at the level of the second molar (Figure IV-1).

The manipulation data should have tested this operating hypothesis, which predicts that posterior pushing, an axial load, will compress the septo-ethmoid junction, whereas dorsal bending/shear will have little effect. Unfortunately, the septo-ethmoid manipulation results were too poor to provide an adequate test. However, the other locations recorded did confirm that anteroposterior axial forces and dorsoventral bending/shear are capable of producing large strains on the anterior septum and the nasofrontal suture, and the strains are in the expected directions. Thus the hypothesis that during mastication the snout is axially compressed as well as bent or sheared dorsally is plausible but still lacks a definitive test.

High strain magnitudes in the anterior septal cartilage: flexibility or loading?

The pattern of strain recorded in the anterior cartilage during masseter stimulation was anteroposterior compression, the same as for the septo-ethmoid

junction and the nasofrontal suture. Interestingly, the magnitude of strain (over 11,000 με, Table IV-1) was much higher than the rest of the cartilage and the nasofrontal suture in both groups ($p = 0.0008$, 2-sample t-test) and vastly greater than the septo-ethmoidal junction and the masticatory values for the middle and posterior cartilage locations in group 2 ($p < 0.0001$, 2-sample t-test). Clearly, strain distribution in the cartilage is not uniform.

The load responsible for the deformation of the anterior septal cartilage is not obvious. The anterior septum also showed high strain magnitudes with very consistent directionality when the snout was manipulated (Table IV-2). Compression due to posterior pushing was not significantly different from that seen during masseter stimulation ($p = 0.34$, paired t-test) but both were greater than that seen for dorsal bending ($p = 0.01$ and 0.008, paired t-tests). This suggests (but does not prove) that masseter stimulation includes a component of anteroposterior axial compression on the anterior septum (but not the septo-ethmoid junction, as discussed above). One possible source is from contraction of the robust facial muscles which move the rhinarium in pigs; stimulation of the facial nerve could not be avoided during masseter tetanus because the nerve overlies the muscle. If this scenario is correct, then the facial muscles compress the cartilage axially rather than bending it laterally, because right and left masseter stimulations resulted in similar compressive values rather than causing compression on one side and tension on the other. However, it is unlikely that this particular strain pattern would have been seen during natural mastication, which does not involve the rhinarial muscles.

Regardless of the source of load to the anterior cartilage, the question remains as to why the observed strains were so large. This part of the septum is actually relatively thick (Figure IV-3), and mechanical testing (chapter V) indicates that its elastic moduli in compression and tension are higher than the rest of the cartilage. Therefore, the larger strains in the anterior cartilage do not arise from greater flexibility of this region. A possible explanation is that this area was still firmly attached to surrounding tissue and would have to follow all snout deformations. The anterior surgical window was unilateral and the cartilage retained a part of its dorsal attachment. The anterior septum is the only part of the cartilage that is firmly attached by fibrous tissue to both the nasal dorsum and the nasal floor at the premaxillary bone. In contrast, the septo-ethmoid junction DVRT location is less well moored to the skull. First, the symmetrical access window removed the dorsal attachment entirely. Second, more posterior areas of the cartilage (including the septo-ethmoid junction) sit on a pad of loose connective tissue in the vomerine groove which may partially insulate them from masticatory strains. Finally, inasmuch as the snout tapers anteriorly, higher stress concentrations may occur anteriorly. In summary, high strains in the anterior septum are probably related to its anatomical position, not to a low modulus of elasticity. The particularly high compression seen during masseter stimulation was partially due to facial muscle contraction.

Nasofrontal suture and the relative performance of DVRT and strain gage

In a previous study on intact pigs (Rafferty and Herring 1999), strain gage readings from the nasofrontal suture were similar in pattern but somewhat smaller in magnitude (masticatory strain -1583 $\pm$ 506 $\mu\varepsilon$) than in the present work (-2252 $\pm$ 826 $\mu\varepsilon$). The

difference is statistically insignificant ($p = 0.11$), but if real, can probably be ascribed to the presence of the bone window in the present study, which would have reduced the stiffness of the region.

In theory, DVRTs and strain gages should give the same results for the nasofrontal suture, and this comparison was intended as a validation test for the DVRT. However, the DVRT projected several millimeters above the skull surface, a position that could accentuate its response to dorsoventral bending, but which was also vulnerable to interference from overlying skin. This is the most likely explanation for the fact that the DVRT measurements of the nasofrontal suture were more variable than those of the strain gage. The DVRT strain magnitudes were also significantly less than those measured by strain gages in group 1(paired t-test for mastication data, $p = 0.024$). Likely causes for the difference in magnitude include (1) several extremely low DVRT values that probably indicate the device was hung up (for example, #403, Tables IV-1 and 3) and (2) a relatively greater amount of bone included in the span of the DVRT compared to the strain gage.

The short lag of about 50 msec in the peak of DVRT displacement relative to the peak of strain measured by the strain gage (Figure IV-4) must have been due to the instrumentation, since placement on the suture was similar. The frequency response for DVRT is reported as 7 kHz by the manufacturer (*vs.* 100 kHz for the strain gage conditioners), and thus is not likely to have caused a lag of this magnitude. Rather, the lag of the DVRT may relate to the time taken for the barbs of the DVRT, sitting in drilled holes, to engage the tissue, i.e. a compliance issue. Although the DVRT is a less exact instrument than the strain gage, in the context of the present study it was useful to have

both on the suture, because this comparison enabled us to determine that the septo-ethmoid junction and the suture deformed simultaneously.

Mastication in pigs and bilateral symmetry of strain

Because the septo-ethmoid junction was instrumented in the midline, no differences due to side of chewing or stimulation were expected, and none were seen. The nasofrontal suture is bilateral, but as in previous studies it did not show an effect of chewing side, presumably because chewing in pigs involves muscles of both sides and possibly bilateral tooth contact (Herring et al. 2001; Rafferty et al. 2003). Asymmetry of sutural strain was seen for unilateral masseter stimulations. Whereas bilateral and ipsilateral masseter stimulations produced similar levels of compression, levels were decreased 50% or more for contralateral stimulations. This suggests that in addition to the dorsal bending produced by the masseter, unilateral contraction adds an element of lateral bending or twisting. Lateral bending toward the more strongly contracted side is also suggested by the mastication data of group 2, in which the transversely placed DVRTs were positioned to be sensitive to lateral deformation. Albeit only 2 pigs had appropriate data, both showed higher compression for chewing on the DVRT side, suggesting that the septum bends laterally in the ipsilateral direction. However, this asymmetry in group 2 also might have been due to the surgical weakening of the ipsilateral skeletal framework.

The anterior septal cartilage was instrumented from the side, so it should also have reflected lateral bending caused by unilateral muscle contraction. However, identical strong compressive strains of the anterior septum were observed for

contralateral and ipsilateral stimulations. Notably, the anterior septum is far anterior to the anterior origin of the masseter muscles. Probably the lateral deviation toward the contracting masseter is a local effect that does not impinge on the anterior snout.

Summary

Returning to the two questions discussed in the background section, the finding of anteroposterior compression in the nasal septum is inconsistent with the expectations for an idealized vertical strut. I conclude that the septum does not function in this manner during mastication. Strain magnitudes in the septum are at least an order of magnitude higher than local bone strain, suggesting that the septal cartilage may help to absorb energy and dampen masticatory loads. The septum is probably capable of some limited sliding movement in the vomerine groove but is elsewhere firmly attached to the rostrum. The strain patterns observed suggest that during masticatory power stroke, the pattern of deformation of the snout is a combination of anteroposterior compression superimposed on dorsal bending and/or shearing.

Table IV-1: Peak anteroposterior strain during mastication and masseter stimulation in group 1 (με)

Pig#	Septo-ethmoid junction DVRT		Anterior cartilage DVRT	Nasofrontal suture DVRT		Nasofrontal suture strain gage	
	Mastication	Stimulation*	Stimulation*	Mastication	Stimulation*	Mastication	Stimulation*
398	-1224 ± 132 (n=18)	-216 ± 61 (B)	-4291 ± 124 (B)	-2168 ± 166 (n=6)	ND	-2257 ± 779 (n=24)	-1915 ± 61 (B)
399	-1815 ± 195 (n=18)	0	ND	-1671 ± 94 (n=24)	-757 ± 71 (B)	-1650 ± 392 (n=24)	-2157 ± 59 (B)
400	-301 ± 57 (n=9)	-119 ± 7 (R)	ND	-743 ± 182 (n=24)	-1354 ± 184 (B)	-2892 ± 737 (n=24)	-2093 ± 51 (B)
401	-1031 ± 215 (n=24)	-111 ± 23 (B)	-6411 ± 662 (B)	-1052 ± 224 (n=24)	-3239 ± 227 (B)	-2533 ± 251 (n=30)	-3086 ± 265 (B)
402	-1194 ± 234 (n=24)	-109 ± 13 (R)	-10,215 ± 101 (B)	-1434 ± 399 (n=24)	-788 ± 37 (B)	ND	-3880 ± 28 (B)
403	-196 ± 12 (n=3)	-24 ± 2 (B)	-7307 ± 890 (B)	-79 ± 6 (n=18)	-12 ± 6 (C)	-2866 ± 389 (n=24)	-2240 ± 595 (B)
404	-877 ± 145 (n=12)	-132 ± 40 (B)	-17,480 ± 372 (B)	-213 ± 4 (n=12)	-1439 ± 188 (I)	-682 ± 73 (n=18)	ND
405	-52 ± 5 (n=12)	18 ± 3 (R)	-11,325 ± 1250 (B)	-81 ± 20 (n=24)	-273 ± 22 (I)	-2885 ± 668 (n=24)	-3295 ± 193 (B)
414	-992 ± 392 (n=24)	-20 ± 6 (L)	-17,711 ± 136 (B)	-566 ± 200 (n=18)	-242 ± 45 (B)	ND	ND
415	-2150 ± 140 (n=3)†	-19 ± 3 (R)	-15,430 ± 1041(B)	-2005 ± 156 (n=6)†	-427 ± 137 (B)	ND	ND
Grand Mean	**-983 ± 677**	**-73 ± 75**	**-11,271 ± 5162**	**-1001 ± 788**	**-948 ± 988**	**-2252 ± 826**	**-2666 ± 750**

mean ± standard deviation; n= number of chewing strokes; negative values indicate compressive strain). ND: no data

* The values listed are the maximum strain recorded during masseter stimulation regardless of side stimulated. The letter in parentheses indicates the stimulation condition producing this maximum: B - bilateral; R - right; L - left; C - contralateral; I - ipsilateral masseter stimulation. Stimulation averages are for 3 repetitions at supramaximal tetanus.

† Chewing on a rubber tube

Table IV-2: Antero-posterior strain during anterior (axial tension) and posterior (axial compression) manipulations (με)

Pig#	Septo-ethmoid DVRT		Anterior cartilage DVRT		Nasofrontal suture DVRT		Nasofrontal suture strain gage	
	Posterior	**Anterior**	**Posterior**	**Anterior**	**Posterior**	**Anterior**	**Posterior**	**Anterior**
398	-27	0	-3818	1296	ND	ND	-431	547
399	ND	0	ND	ND	ND	538	ND	943
400	-408	0	-1860	716	-1209	716	-1376	995
401	0	16	-8734	4512	-2957	-1177	-1449	710
402	ND	ND	-12,911	340	-159	223	-2236	1455
403	-21	23	-6132	1670	ND	70	-1639	994
404	-985	ND	-14,170	1135	-1028	1490	ND	ND
405	-15	10	-15,407	318	-603	9700	-3298	ND
414	0	0	-7376	5213	-1044	75	ND	ND
415	ND	ND	-5363	ND	ND	60	ND	ND
Grand Mean	**-208 ± 373**	**7 ± 10**	**-8419 ± 4770**	**1900 ± 1895**	**-1167 ± 957**	**1299 ± 3228**	**-1738 ± 961**	**941 ± 309**

Three identical strokes were analyzed for each manipulation.

ND: no data

Table IV-3: Antero-posterior strain during manipulated dorsal and ventral bending of the snout (με)

Pig #	Septo-ethmoid DVRT		Anterior cartilage DVRT		Nasofrontal suture DVRT		Nasofrontal suture strain gauge	
	Dorsal	Ventral	Dorsal	Ventral	Dorsal	Ventral	Dorsal	Ventral
398	-30	-29	-3314	1470	ND	ND	-1300	1800
399	ND	ND	ND	ND	-1550	ND	-2300	2200
400	70	0	ND	ND	-2340	1460	-1800	2900
401	7	50	-2985	1480	-4560	2280	-1700	1000
402	500	ND	-1750	2290	-1416	1770	-1400	2500
403	-7	34	-3600	1090	ND	ND	-2000	3500
404	1370	0	-2300	ND	-3820	1620	ND	ND
405	-30	10	-3360	ND	-1430	ND	-3500	4000
414	0	10	ND	ND	-93	800	ND	ND
415	-140	221	-518	ND	-270	690	ND	ND
Grand Mean	**193±477**	**37±78**	**-2547±1108**	**1583±505**	**-1935±1579**	**1437±603**	**-2000±744**	**2557±1018**

Three identical strokes were analyzed for each manipulation.

ND: no data

Table IV-4: Strains recorded during mastication in group 2 (με)

Animal ID	Middle cartilage DVRT (με)	Posterior cartilage DVRT	Nasofrontal suture DVRT*
411†	-3748 ± 625 (6)	-1495 ± 498 (6)	-1831 ± 166 (6)
412†	-517 ± 91 (8)	-1903 ± 446 (7)	-5985 ± 570 (8)
413†	-3978 ± 199 (7)	-988 ± 494 (7)	- 1295 ± 199 (6)
417†	-2161 ± 830 (8)	-2646 ± 624 (6)	-3803 ± 1170 (8)
422	ND	-1787 ± 73 (4)	ND
427	-2798 ± 662 (6)	-1142 ± 143 (6)	-4173 ± 695 (6)
430	-2221 ± 328 (8)	-1605 ± 231 (6)	-4270 ± 817 (7)
431	-3939 ± 492 (7)	-1386 ± 594 (6)	-3837 ± 460 (6)
Grand mean	**-2766 ± 1260**	**-1621 ± 520***	**-4015 ±1325***

Mean ± SD. The number of chewing cycles analyzed is between parentheses. ND: no data

* Strain recorded at the nasofrontal suture was significantly higher than that recorded at the posterior septal cartilage, p=0.02

† Animals with simultaneous EMG

Table IV-5: Strain recorded by the DVRTs in group 2 during ipsilateral (side of the DVRT) and contralateral (opposite side) chewing

	412			417		
	Anterior cartilage DVRT (με)	Posterior cartilage DVRT (με)	Nasofrontal suture DVRT (με)	Anterior cartilage DVRT (με)	Posterior cartilage DVRT (με)	Nasofrontal suture DVRT (με)
Ipsilateral	-549 ±16 (3)	-2209 ± 68 (3)	-3605 ± 260 (3)	-2854 ± 515 (4)	-3092 ± 96 (4)	-4687 ± 1039 (4)
Contralateral	-452 ± 13 (3)	-1598 ± 461 (3)	-2179 ± 256 (3)	-1469 ± 150 (4)	-2237 ± 646 (4)	-2920 ± 110 (4)
P (paired-t)	< 0.01	NS	< 0.01	< 0.01	NS	NS

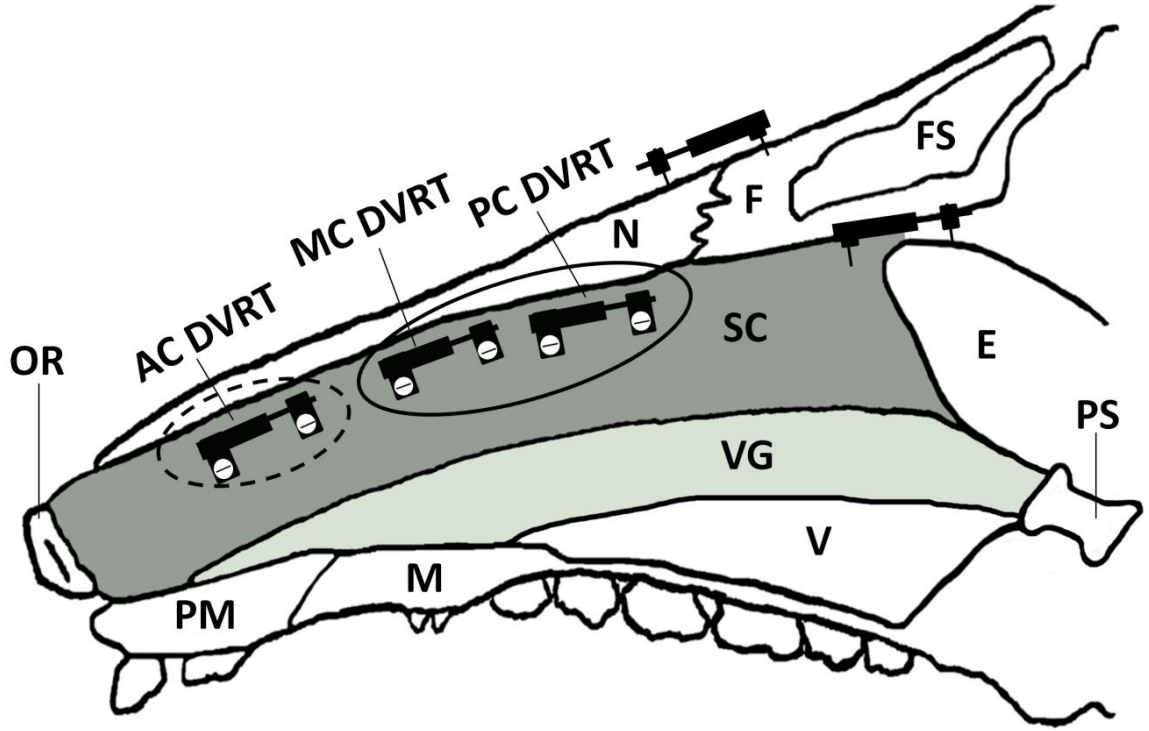

Figure IV-1: Sagittal section of a pig skull illustrating the anatomy of the nasal septal cartilage, its relations to surrounding structures, and the location of the cartilage DVRTs in both groups. E, perpendicular plate of ethmoid bone; F, frontal bone; FS, frontal sinus; M, palatal process of maxillary bone; OR: os rostri; PM, premaxillary bone; PS, presphenoid bone; SC, septal cartilage; V, body of the vomer; VG: vomerine groove which contains the lower portion of the septal cartilage. The DVRTs implanted in group 2 are surrounded with a solid circle. AC DVRT: anterior cartilage DVRT (inserted before masseter stimulation and manipulation), SE DVRT: septo-ethmoid junction DVRT, NF DVRT: nasofrontal suture DVRT. Group 2 cartilage DVRTs: MC DVRT, middle cartilage DVRT; PC DVRT: posterior cartilage DVRT.

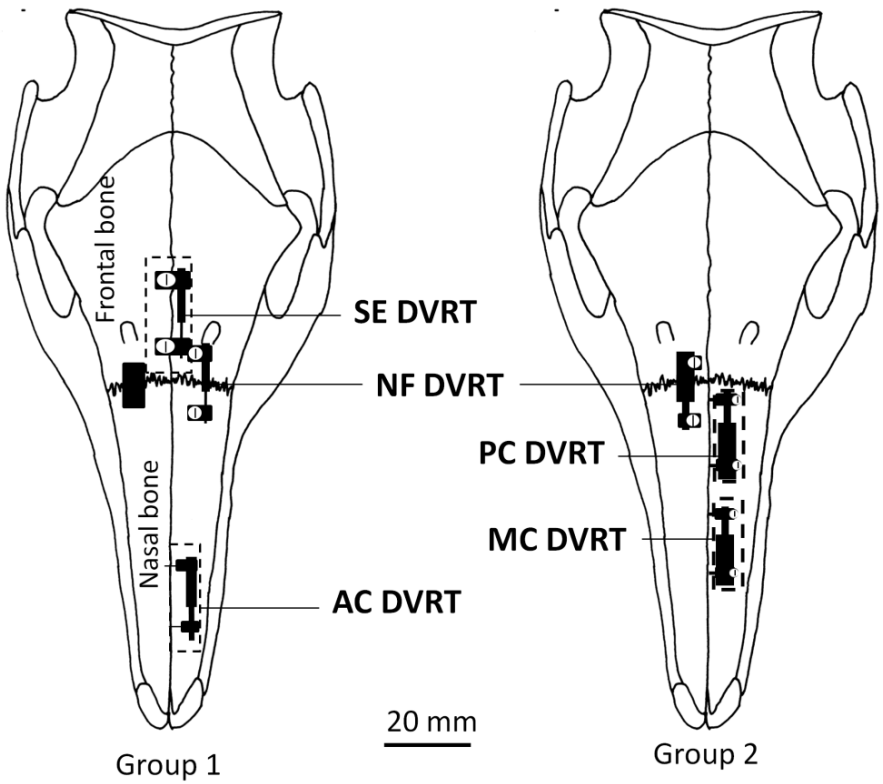

Figure IV-2: Sagittal view of the pig skull illustrating the surgical access windows (dashed boxes) in both groups and the sensors location. Abbreviations are as is figure IV-1

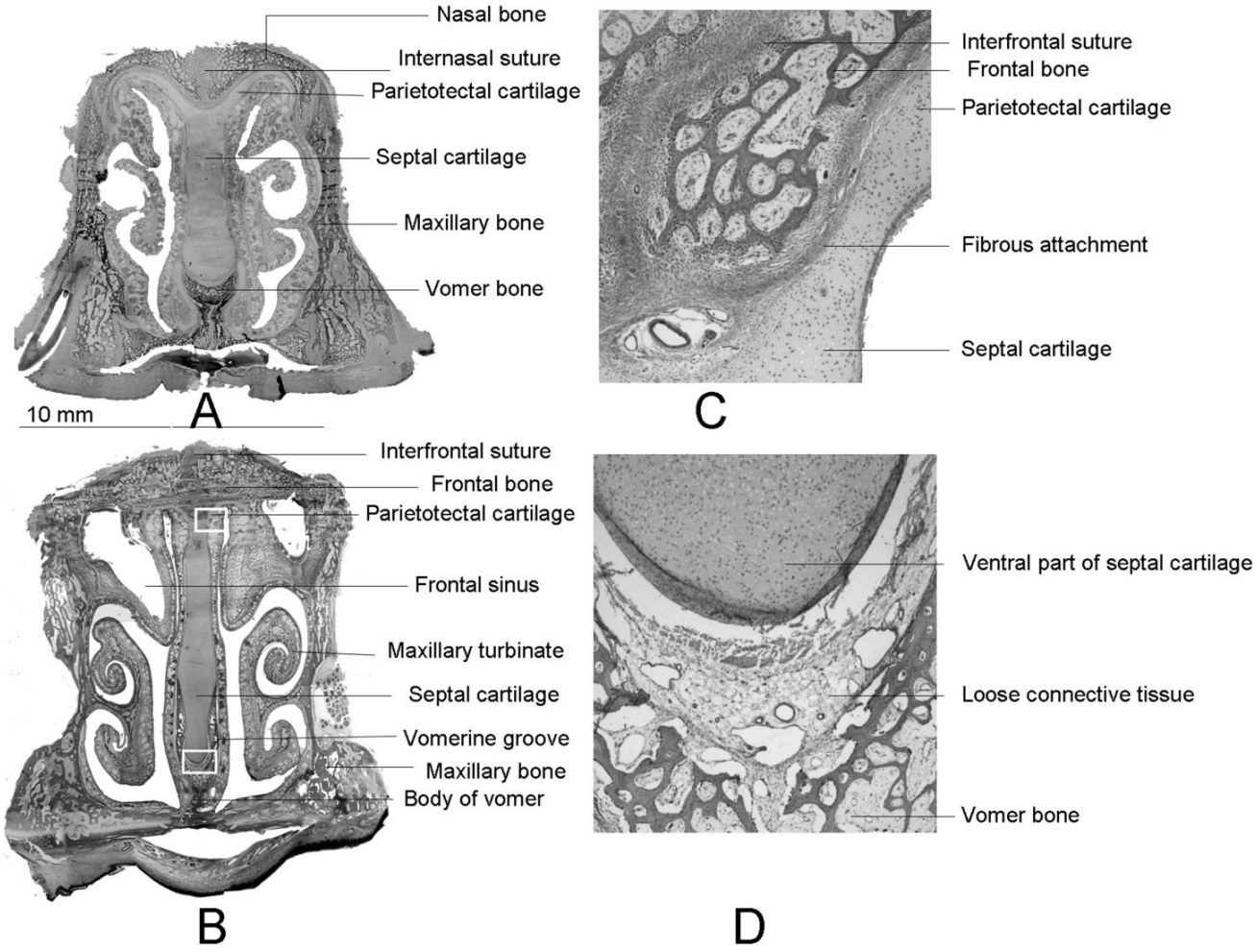

Figure IV-3: Coronal sections of the snout (hematoxylin and eosin stain) showing the nasal septal cartilage (A) at the location where the anterior DVRT was implanted and (B) close to the septo-ethmoid junction where the septo-ethmoid DVRT was implanted. Dorsally the cartilage splits into two parietotectal cartilages that underlie the nasal and frontal bones. C and D are enlargements of the boxed areas in B. The parietotectal cartilages are tightly connected to the overlying bones by fibrous tissue as seen in C. The ventral part of the cartilage lies on a pad of loose connective tissue in the vomerine groove as seen in D. The vomerine groove depth increases posteriorly (compare A and B). The break between the palate and the palatal mucosa in both A and B is artifactual

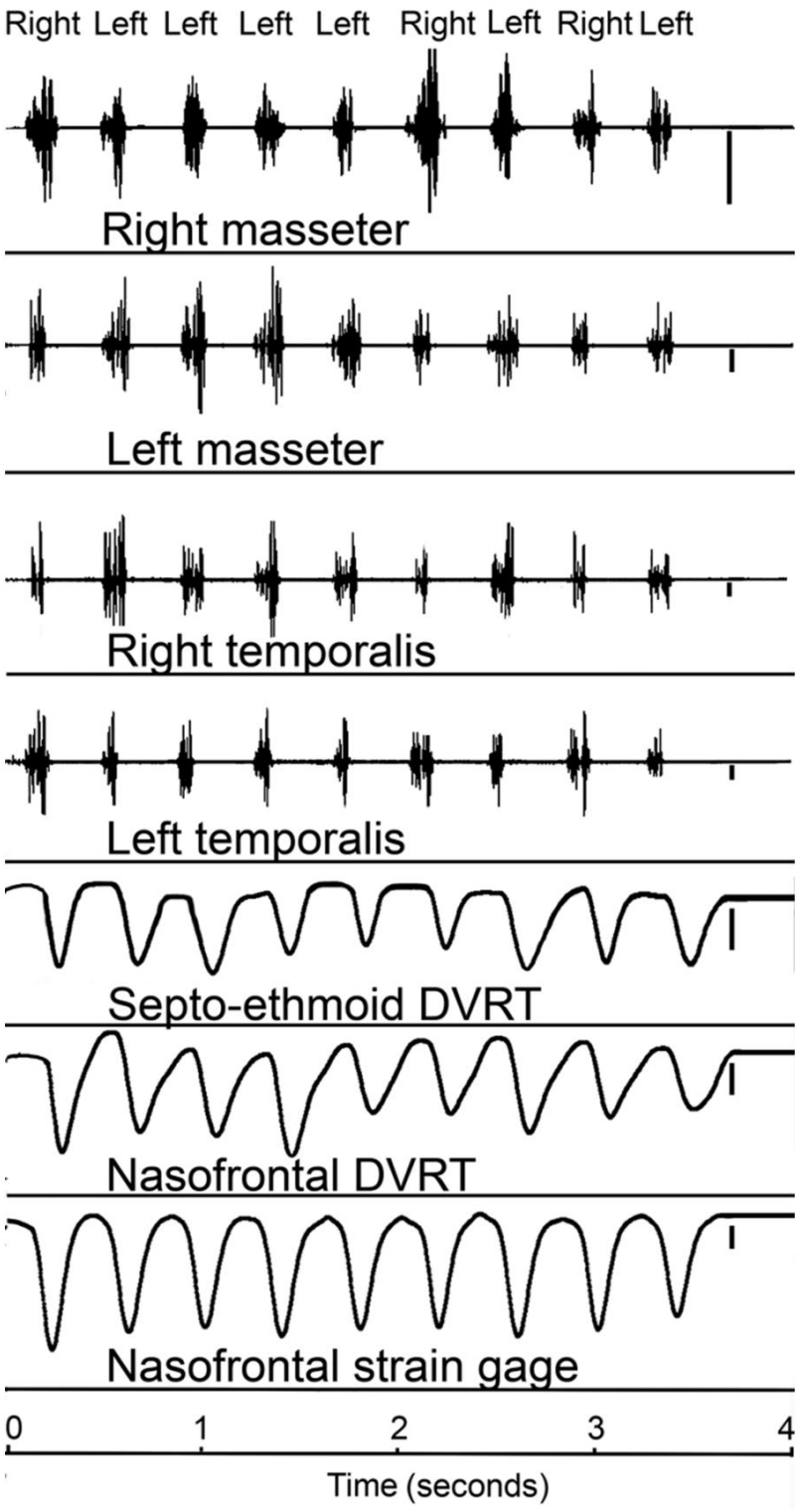

Figure IV-4: Recording from subject 401 (group 1) during mastication illustrating EMG of right and left masseter and temporalis synchronized with the nasofrontal and septo-ethmoid DVRTs and nasofrontal strain gauge. The side of chewing is indicated at the top. Scale bars correspond to 30 mV for masseter and 100 mV for temporalis, 500 με for the DVRTs and strain gauge

Chapter V: Mechanical properties of the nasal septal cartilage and its physiologic implications

Background

The septal cartilage is hypothesized to act as a primary growth center of the midface, with expansion of the cartilage separating the facial bones at the suture (Scott 1951; Scott 1953). As discussed earlier, general support of this role is furnished by retardation of midfacial growth after septal cartilage extirpation in some animal experiments (Sarnat and Wexler 1966; Kvinnsland 1974). However, an alternative explanation is that the extirpation of the nasal septum resulted in collapse of the nasal bone rather than a direct growth effect (Moss et al. 1968; Stenström and Thilander 1970). This reasoning was based on theoretical studies that modeled the snout as an imperfect framed structure requiring a midline strut, the nasal septum, to prevent its collapse under masticatory loading (Badoux 1966; Badoux 1968). In chapter II, I reported that in pigs the septum was compressed anteroposteriorly during mastication. This does not support the idea of the cartilage acting as a vertical strut, although it might function as an anteroposterior strut. I further suggested that the septal cartilage acts a stress dampener, absorbing and dissipating loads generated on the snout during masticatory strokes. Unlike articular cartilage (Martin et al. 1998), the septal cartilage has substantial volume and could contribute substantially to the absorption of loads as sutures are thought to do (Jaslow and Biewener 1988). On the other hand, if the septum is acting as a strut, the cartilage should be stiff enough to withstand loads generated during mastication.

The role of the septal cartilage either as a growth center or as a strut is challenged by its likely mechanical weakness. If cartilage expansion is tensing the facial sutures, then the resistance of the sutures must place the cartilage under compression. In order to resist such loads, the cartilage stiffness in compression would have to be higher than that of the sutures in tension. On the other hand, if the septum is acting as a strut, or has any mechanical role during mastication, the cartilage should be stiff enough to withstand loads generated by feeding activities. In addition, the cartilage might show directional and regional adaptations to its loading regime (Figure V-1).

Cartilage is an almost avascular tissue that is composed predominately of matrices rich in type II collagen and large proteoglycan aggregates known as aggrecans. The proteoglycan molecule consists of a central hyaluronic acid polymer and side chains of chondroitin and keratan sulfates. This arrangement results in a high negative charge and high water content (Mow and Wang 1999). The aggrecans and fibers together with the fluid content provide the cartilage with its strength (Huang et al. 2001; Naumann et al. 2002). This complex composition gives rise to a well documented nonlinear response to load and a viscoelastic mechanical behavior (Langelier and Buschmann 2003, Huang et al., 2001). The intrinsic compressive properties are dictated by the proteoglycan and water content while the tensile properties are dictated by the collagen content (Huang et al. 2001). Thus, direction of loading, loading rate (DiSilvestro et al. 2001; Langelier and Buschmann 2003; Li and Herzog 2004), loading time and hydration (Race et al. 2000) are all important determinants of the mechanical properties of cartilage. Loading rate is especially important in considering the possible roles of the septal cartilage in growth (slow loading) versus mastication (fast loading).

Although the septum is often used as a source for the measurement of the mechanical properties of cartilage (Wong et al. 2001; Naumann et al. 2002; Rotter et al. 2002; Chao et al. 2003; Gaon et al. 2003; Richmon et al. 2005; Grellmann et al. 2006; Grellmann et al. 2006; Richmon et al. 2006; Westreich et al. 2007), these studies have not systematically investigated directional and regional differences. Additionally, the perichondrium was excised in most cases, a procedure that results in a 50% decrease in the elastic modulus of auricular cartilage (Roy et al. 2004).

Thus, the overall aim of this chapter is to measure the mechanical properties of the nasal septal cartilage in compression and tension, with particular attention to the effects of regional variation and loading rate. Pig septa were used, to allow comparison to previous data on in vivo bone and suture strain (Rafferty and Herring 1999; Rafferty et al. 2003) and on the mechanical properties of the nasofrontal suture (Popowics and Herring 2007) which overlies the septum. The ultimate goal is to shed light on the role of the septal cartilage in facial growth and integrity.

Materials and Methods

Compression tests:

Pig heads (n=18) were obtained from a local abattoir (Kapowsin Meat, Graham, WA), age, sex and breed unknown. Nasal septa were extracted and stored frozen in 4% phosphate buffered saline (PBS) until samples were tested. Freezing was necessitated by the duration of the testing, but thawed cartilage is less stiff than fresh (~ 30%, calculated from Langelier and Buschmann, 2003), a factor that probably affected the results.

On the day of measurement, septa were thawed and six 9-10 by 9 mm rectangular samples were cut from the cartilage as shown in Figure V-2: 2 vertical (one anterior and one posterior) and 4 horizontal (3 dorsal and one ventral). Natural thickness with the perichondrium in place was preserved and measured. Samples were compressed in long-axis orientation (Figure V-2). The 2 vertical and 2 of the horizontal samples (dorsal middle and ventral) were loaded at 1%/s (equivalent to ~0.1 mm/sec) while the remaining 2 horizontal (dorsal anterior and posterior) samples were loaded at 0.1%/s (equivalent to ~0.01 mm/sec). The fast strain rate was chosen to mimic the low end of the masticatory loading range (Chapter IV). I intended to use a strain rate of about 0.01 %/sec to mimic growth loads (Chapter II), but the testing machine proved to be unreliable at rates lower than 0. 1%/sec. So, this rate was used as the closest approximation to growth loads. Sandpaper was glued to the compression platens in order to keep samples in place during testing. All tests were made in an MTS/Sintech 2 Testing Machine (Raleigh, NC) with saline immersion to keep the samples hydrated.

Samples were preloaded to 1.5 or 2.5 N, and the resultant deformation was defined as 0% strain. Subsequently, samples were loaded to strain points 2, 4, 6, 8 and 10% in random order, and the strain was held for a relaxation time of 120 sec. A two-minute rest period separated each loading to allow cartilage rehydration. Finally, samples were loaded until failure.

Deformation was converted to strain by dividing by the recorded length of the cartilage sample between compression platens before loading. Load was converted to stress by dividing by the sample cross-sectional area calculated from the recorded thickness and width of the sample before the test. Throughout each test, stress and

strain were continuously recorded at 50 Hz. Stress-strain and stress-time graphs were plotted. Samples that showed buckling or instability during testing were discarded.

For each test, stiffness (elastic modulus) was calculated as the slope of the linear region of the stress-strain curve (Figure V-3): Stiffness (slope) = $\frac{\quad}{\quad}$. Relaxation stress was measured at 0, 10, 30 and 120 seconds (Figure V-3). The percentage drop in the relaxation stress between each time interval was calculated as an indication of stress absorption by the cartilage. The final failure test was used to measure the ultimate stress and strain of the cartilage.

The effect of loading rate was tested by comparing dorsal samples loaded at high speed (DH) with samples loaded in the same direction at low speed (DH (a) and DH (p)) (Figure V-2), using ANOVA for repeated measures. To assess whether the septum showed greater compressive stiffness and strength vertically (vertical strut) or anteroposteriorly (corresponding to in vivo strain), vertical vs. horizontal loading directions were compared (AV, PV vs. DH and VH, Figure V-2) using ANOVA for repeated measures with paired t-tests used to compare individual pairs to identify source of significance. The effect of location was assessed by using paired t-tests to compare the anterior and posterior vertical samples (AV vs. PV in Figure V-2), the dorsal and ventral horizontal samples (DH vs. VH in Figure V-2) and the anterior and posterior samples loaded at low speed (DH (a) vs. DH (p) in Figure V-2). All statistical tests were performed using SPSS v13.0.

Tension tests:

Pig heads (n=22) were obtained as before; nasal septa were extracted and stored in saline at 4°C. On the day of testing, four hourglass-shaped samples approximately 10x20mm, were cut (Figure V-2), 2 vertical (anterior and posterior) and 2 horizontal (dorsal and ventral).

Each sample was fitted into a pair of acrylic grips. Metallic blades and rubber bands were used to allow compression free mechanical retention of the samples (Figure V-2). The length and the width of the exposed sample were measured prior to each experiment; final dimensions of the exposed cartilage averaged 4.2x5.1 mm. The acrylic grip/sample assembly was loaded into pneumatic clamps and mounted in the MTS/Sintech2. Throughout the testing, samples were kept hydrated using saline immersion. Samples were pre-loaded to 1.5 or 2.5 N, and the resultant deformation was defined as 0% strain. Because septum is not thought to be tensed by growth, no slow loading rate was used. The fast rate of 10%/sec was used for all samples. Although much faster than the fast compressive loading rate of 1%/sec, this rate is still probably in the masticatory range. Five strain points were used: 2, 4, 6, 8 and 10% in random order; a ten-minute rest period separated each loading to allow cartilage rehydration. Finally, samples were loaded until failure. Recording parameters were the same as for compression testing, as was calculation of stress, strain, elastic modulus (stiffness), and percentage drop in relaxation stress (Figure V-3), except that the time points for relaxation were 0, 10 and 30 seconds.

Although septal growth is expected to cause only compression, masticatory loading could cause some regions to undergo tensile strain, compensated by increased tensile stiffness. If the septum is subject to compressive loading during mastication, adaptations for tensile stiffness might be expected in the orthogonal direction owing to a Poisson effect. Therefore the vertically and horizontally loaded samples were compared using ANOVA for repeated measures followed by paired t-tests to detect the source of significant difference. Alternatively, if the septum undergoes dorsal flexion, then the ventral horizontal location might show greater tensile stiffness than the dorsal location (Figure V-1). This was tested using paired t-tests. Finally, the anterior site, which is attached to the mobile snout disc, is more subject to deflection than the more protected posterior region, which might be associated with enhancement of anterior stiffness. The anterior vertical location was compared to posterior vertical to test this possibility, again using paired t-tests.

Results

Compression results:

No significant difference in mechanical properties was present between samples preloaded at 1.5 and 2.5N, so values were averaged. The cartilage displayed a non-linear compression behavior, with stiffness increasing with increased strain (Figure V-4). Values ranged from 1.6 ± 0.6 MPa (DH (a), 2% strain) to 5.4 ± 1.8 MPa (DH, 10% strain). Consequently, stiffness and relaxation stress had to be analyzed separately for each strain level. Results were similar at all strain levels, but statistical significance was usually present only for the higher strains of 6, 8 and 10%.

Loading rate was an important determinant of the compressive stiffness of the cartilage for all strain levels, as seen in Figure V-4 bottom. Dorsal horizontal samples loaded at high speed (DH) were stiffer than nearby samples loaded at low speed (DH (a) and DH (p), $p<0.01$, repeated measures ANOVA).

Among the 4 regions tested at 1%/sec, there were also significant differences ($p=0.03$, repeated measures ANOVA). However, these did not correspond with the vertical or horizontal orientation of the compressive load. Post hoc testing showed that the posterior vertical samples were significantly less stiff than the other regions for almost all comparisons. The dorsal horizontal region was usually stiffer than ventral horizontal, but the differences were not statistically significant ($p=0.1$, paired t-test at 10% strain)

Stress absorption, here defined as percent loss of stress, mainly occurred during the first 10 seconds of relaxation (Figure V-5, Table V-1), for specimens loaded at 1%/ sec, but was much more gradual, and less overall, for specimens loaded at 0.1 %/sec ($p<0.01$, repeated measures ANOVA). Stress absorption in the samples loaded at 1%/sec showed regional differences ($p=0.03$, repeated measures ANOVA). Although horizontally loaded specimens tended to have greater absorption (i.e. more stress relaxation), significant differences were confined to the AV site, which exhibited less absorption compared to DH and VH, with consistent statistical significance at all strains except 2%.

Several samples buckled during failure testing, resulting in smaller sample sizes for ultimate strain and stress (Table V-2). Ultimate strain averages ranged from 25%

(DH) to 34% (AV) and did not differ for loading rate, orientation of load or location. Ultimate stress (strength) also did not depend on loading rate, although values for samples loaded at 0.1%/ sec (1.4-1.5 MPa, Table V-2) usually were lower than those loaded at 1%/sec (1.6-3.3 MPa, Table V-2). However there were regional differences among the locations tested at 1%/ sec, specifically, the AV had significantly greater strength that the other three locations ($p=0.01$, repeated measures ANOVA).

Tensile results:

Unlike the findings from compression, a preload of 1.5 vs. 2.5N affected tensile results. Since relatively few samples had been preloaded to 2.5N (between 2 and 7 for each location), results of this group were discarded and only the 1.5N preloaded specimens are reported. Another contrast with the compression results is that strain level (2%, 4%, 6%, 8%, and 10%) was not related to stiffness (Figure V-6). Therefore, averaged tensile stiffness could be calculated, simplifying statistical treatment. As illustrated in Figure V-6, tensile stiffness ranged from 0.49 MPa in the anterior vertical specimens to 0.79 MPa in the posterior vertical specimens. Overall, tensile stiffness varied by region but not by orientation. Specifically, the anterior vertical specimens had lower tensile stiffness than the other regions ($p<0.01$, repeated measures ANOVA).

Tensile stress relaxation totaled 40-50% over the 30 sec holding period, with most of the drop (32-39%) occurring in the first 10 seconds (Figure V-7 and Table V-3). There were no differences associated with strain level (2%-10%) or with region.

Failure testing (Table V-4) showed that the ultimate strains ranged from 110% in PV to 160% in AV. Although the AV specimens showed the highest ultimate strain, the

difference was not statistically significant (p=0.1, repeated measures ANOVA). Ultimate stress (strength) ranged from 1.1-2.0 MPa and showed regional differences (p<0.01. repeated measures ANOVA). In pairwise comparisons, the AV specimens were stronger than all other locations. In addition, tensile strength was higher in DH than in VH specimens (p=0.01, paired t-test).

Discussion

Limitations

The compressive and tensile properties reported here are not fully comparable. First, the tensile tests were performed at 10%/sec, where as the compressive tests were performed at 0.1 and 1%/sec. The rate for tension was chosen because pilot studies indicated high consistency at 10%/sec. Later, however, I became aware that this rate was somewhat faster than the typical physiological loading rate during mastication. Because the purpose of the study was to understand the biological role of the nasal septum, I chose to conduct the compressive tests at 0.1% and 1%/sec rather than using the same rate. However, since the cartilage is a viscoelastic material, higher strain rates result in higher stiffness (DiSilvestro et al. 2001; Langelier and Buschmann 2003; Li and Herzog 2004). Thus the stiffness values in the tension experiments are overestimated. Second, tension samples were stored at 4^{o}C whereas compression samples were frozen. Freezing decreases the mechanical properties of cartilage (around 30%, calculated from Langelier and Buschmann, 2003). Thus, the compressive values are underestimated. Even with tensile values overestimated and compressive values underestimated, compressive stiffness (2-6 MPa, Figure V-3) was much greater than tensile stiffness (0.4-0.9 MPa, Figure V-6) supporting the well-known fact that

cartilages are adapted to compressive rather than tensile loads. Despite the probable underestimation of compressive properties, my results are comparable to those of porcine septal cartilage reported from bending tests (Wong et al. 2001; Gaon et al. 2003), and higher than the equilibrium modulus (0.2-0.7 MPa) found with confined compression on cartilage samples extracted from humans (Rotter et al. 2002; Richmon et al. 2005; Richmon et al. 2006). On the other hand, despite likely overestimation, my tensile stiffness values are lower than those reported in humans (around 3-8 MPa, (Richmon et al. 2005; Grellmann et al. 2006).

Loading order could have affected the results if higher strain points (i.e. 8 or 10%) came early, resulting in cartilage damage. Previous reports suggested that strain amplitudes higher than 5% may result in weakening and permanent damage of the cartilage (Morel and Quinn 2004). This is especially important since some of the compressed cartilage samples started to show signs of failure at 20-30% strain. However, a post-hoc comparison of samples loaded first at 2 and 4% versus those loaded first at 8 or 10%, showed no difference ($p>0.3$, t-test), so I conclude that the non-failure testing did not damage the tissue.

Overall comparison of compressive and tensile properties

Although the difference in the compression and tension protocols prevents definitive conclusions, consistent patterns are clear. The septal cartilage is stiffer under compression than under tension regardless of location, loading speed or strain (Figure V-3 vs. Figure V-6). In part because the initial tensile stiffness is low stress relaxation is less dramatic for tension than for compression (Table V-1 vs. Table V-3). Further tensile stress relaxation appears to have reached an asymptote by 30 sec, whereas

compression relaxation was still dropping at 120 sec (Figure V- 5 vs. Figure V-7). The final relaxation stress measured was similar for both types of loading (0.03-0.09 MPa, Figures V-5 and V-7).

The septal cartilage was weaker under tension (ultimate stress 1.1-2.0 MPa) than under compression (1.6-3.3 MPa) as well as less stiff (Tables V-2 and V-4). However, it was strikingly more deformable, stretching to more than twice its original length during failure tests (Table V-4), as opposed to the 30% strain typically seen during compression failure (Table V-2). It is conceivable that the perichondrium contributed substantially to these high tensile ultimate strains, for example by first aligning and then stretching the collagen fibers.

Loading rate and strain amplitude

Strain rate (loading speed) and strain level were important determinants of the compressive stiffness of the cartilage. Cartilage was consistently stiffer at higher compressive strain and faster loading. These results are in accordance with previous studies on articular cartilage (DiSilvestro et al. 2001; Langelier and Buschmann 2003; Li and Herzog 2004). Such nonlinearity to strain level was not present in tensile tests; tensile stiffness was not affected by the strain level (rate was not tested). The sensitivity to compression rate and level can be attributed to the fact that cartilage compressive properties are mainly dictated by the water and proteoglycan content. As the amplitude of the strain increases, the load is increasingly resisted by the fluid component of the cartilage. In addition, higher strain rate results in increased drag forces and less time for fluid to flow through the porous proteoglycans, causing increased fluid pressure and

“self stiffening” of the cartilage (Langelier and Buschmann 2003; Li and Herzog 2004). This phenomenon might help to protect the chondrocytes against fast impact loads (Quinn et al. 2001). In contrast, tensile properties are dictated by resistance of collagen fibers to stretch (Mow and Wang 1999; Huang et al. 2001; Quinn et al. 2001), a phenomenon that is not affected by strain amplitude once the elastic portion of the cartilage is reached.

Does the cartilage act as a strut or as a stress dampener during mastication?

The strut model envisions that the cartilage is stiff in order to resist masticatory loads. The cartilage does not seem well adapted for this role. The compressive stiffness values recorded, while typical for cartilage, (Mow and Wang 1999), are certainly much lower than the elastic moduli of bone (20,000 MPa, Carter and Beaupre, 2001). Thus I conclude that the septal cartilage is not stiff enough to act as a strut resisting loads generated during mastication, either in the vertical or anteroposterior direction. Cartilage moduli reported here are comparable to those of the sutures between bones (McLaughlin et al. 2000; Tanaka et al. 2000; Radhakrishnan and Mao 2004; Popowics and Herring 2007). In addition, the cartilage displayed notable compressive stress relaxation, especially at the faster strain rate, suggesting that the septal cartilage is well suited to absorb impact loads, such as those during mastication. These findings, together with findings in chapter IV, suggest that the septal cartilage, together with sutures (Jaslow and Biewener 1995), helps to dampen the loads generated during mastication. Although such a role for the articular cartilage (Kobayashi et al. 2001) has been thought improbable because the articular cartilage is too thin to function as a

stress absorber in the joint (Martin 1998), this argument does not apply to the septal cartilage which comprises a large volume of the snout.

Septal cartilage adaptation to loading regimes

If the snout is dorsally flexed during mastication (Rafferty and Herring 1999; Rafferty et al. 2003), then regional adaptation to dorsal compression and ventral tension is expected. On the other hand, if the cartilage is anteroposteriorly compressed during mastication, adaptation of the dorsal and ventral locations to horizontal compression would be expected. Evidence for dorsal flexion was weak. There was a tendency for increased compressive stiffness of the dorsal location (Figure V-4), but it was not statistically significant. The ventral location showed no tendency for greater tensile stiffness (Figure V-6). These results do not refute the existence of dorsal flexion, but do not strongly support it either. The results also do not support an adaptation for anteroposterior compression. The difficulty here is that the anterior and posterior vertical locations differed whereas the compression model predicts them to be the same. The posterior vertical location shows the pattern expected-- relatively flexible under compression (Figure V-4) and relatively stiff under tension (Figure V-6). The anterior vertical location, clearly unique, displayed higher stiffness in compression and lower stiffness in tension, a pattern more suggestive of a vertical compression, except that the location is unusually strong in both directions of loading (Tables V-2 and V-4). These findings suggest some specialization of the anterior part of the cartilage rather than simple planar deformation. This part is relatively thick (chapter IV), and is firmly attached to the mobile snout disc as well as the premaxillary and nasal bones, rendering it more subject to non-masticatory loadings, such as digging. In chapter IV, ,

much higher magnitudes of strain during masseter stimulation were seen in the anterior as compared to the posterior septum. Taken together, these findings indicate that the anterior location is adapted to withstand increased physiologic loading in a variety of directions.

Growth role

If the septal cartilage plays an active role in midfacial growth, then the growth pressure of the septal cartilage should be sufficient to stretch and separate the facial sutures, and the cartilage should be stiff enough to withstand the recoil pressure of the sutures. The fact that the cartilage is an efficient stress absorber might weaken the ability of cartilage to separate the sutures, as the stresses generated during growth might be absorbed rather than transmitted to separate the sutures. However, a trend toward decreased stress absorption and increased residual stress in the cartilage with decreased strain rate was observed in this study (Figure V-5). Thus, it is possible that the residual stress might be sufficient to separate the sutures, depending on the resistance of the sutures. The most relevant sutural data are for the nasofrontal suture in pigs (Popowics and Herring 2007) measured using similar methods as in this chapter. The suture stiffness was an order of magnitude higher than the stiffness of the septal cartilage measured in this study, thus undermining the postulated growth role of the septum in separating the sutures. Stress absorption in the suture was less (approximately 40%, compared to 70% in the cartilage) which also argues against growth role. However, the values reported for the suture are not strictly comparable to those for the cartilage. The samples used to test the sutural properties consisted of not

only sutural tissue but included much of the nasal and frontal bones. Because the suture is more flexible than the surrounding bones, it is expected that most of the strain was concentrated on the suture; however the sample length used to calculate strain and later stiffness included the combined length of the suture and adjoining bones. If only the suture gap length is used to calculate the stiffness, stiffness is an order of magnitude lower, because the estimated suture length (around 340 μm, Popowics and Herring, 2007) is 10 times smaller than average sample length used (3.4 mm). This calculation results in stiffness values that are comparable to those of the horizontally loaded cartilage under similar speed, and suggests that the septal cartilage is stiff enough to withstand the resistance of the suture, especially given the fact that residual stress decays slowly, and not to zero under compression.

Summary

The compressive and tensile mechanical properties of the nasal septal cartilage were investigated in order to shed light on the role of the cartilage in facial integrity and midfacial growth. The cartilage is stiffer and stronger under compression than under tension and shows regional variations that suggest specialization of the anterior region. The results suggest that the septal cartilage acts as a stress dampener helping to dissipate loads generated during mastication. In addition, the septal cartilage may be mechanically capable, under slow loading rates, of separating facial sutures, thus playing an active role in midfacial growth.

Table V-1: Compression relaxation stress at 0 second, and percent loss at 10, 30 and 120 seconds after holding strain at 2, 6 and 10%. Results were similar for the intermediate times and strains. See Figure V-2 for locations and abbreviation

	2%				6%				10%			
	Relaxation stress at 0 sec (MPa)	% loss at 10 sec	% Loss at 30 sec	% loss at 2 min	Relaxation stress at 0 sec (MPa)	% loss at 10 sec	% Loss at 30 sec	% loss at 2 min	Relaxation stress at 0 sec (MPa)	% loss at 10 sec	% Loss at 30 sec	% loss at 2 min
AV† (1%/sec)	0.08±0.02	30.8±7.6	42.8±9.2	54.0±13.7	0.26±0.09	38.9±7.2	49.9±10.1	71.0±9.6	0.50±0.20	42.2±9.7	50.7±10.0	77.7±9.2
PV (1%/sec)	0.08±0.02	31.0±12.4	45.9±13.8	61.7±14.8	0.19±0.05	41.8±10.5	59.2±10.6	75.2±10.0	0.36±0.12	45.9±9.3	64.3±13.3	80.7±8.9
DH*† (1%/sec)	0.10±0.03	35.7±9.5	49.7±11.2	62.9±17.5	0.28±0.09	47.1±12.4	66.6±13.4	81.8±10.1	0.55±0.17	50.8±13.0	69.3±12.3	84.1±10.2
VH† (1%/sec)	0.08±0.01	38.9±11.1	45.8±10.6	71.0±13.2	0.24±0.08	49.6±10.4	67.5±9.5	81.5±8.2	0.50±0.14	54.9±12.1	74.5±13.9	87.2±8.1
DH (a)* (0.1%/sec)	0.06±0.02	16.2±8.3	29.1±9.5	43.4±17.1	0.16±0.04	24.3±10.3	41.9±12.2	61.9±13.5	0.29±0.12	23.9±8.2	43.3±11.3	66.4±11.1
DH (p)* (0.1%/sec)	0.07±0.02	19.5±6.9	33.9±8.6	51.6±14.7	0.15±0.06	27.3±10.1	46.3±11.2	67.2±11.6	0.24±0.11	24.0±6.8	44.5±9.7	68.0±8.9

†Horizontal samples showed higher stress relaxation than the anterior vertical samples ($p<0.03$, repeated measures ANOVA) for all strain levels (except 2% dorsal horizontal)

**Dorsal horizontal samples loaded at faster speed showed higher stress relaxation than samples loaded at low speed ($p<0.05$, repeated measures ANOVA).*

Table V-2: Ultimate compressive stress and strain of the septal cartilage

	1%/sec loading rate				0.1%/sec loading rate	
Orientation	**Anterior vertical** n=16	**Posterior vertical** n=17	**Ventral horizontal** n=16	**Dorsal horizontal** n=14	**Dorsal horizontal (a)** n=13	**Dorsal horizontal (p)** n=8
Ultimate stress (MPa)	**3.3±1.4***	**1.6±0.4***	**2.2±0.8***	**1.9±0.6***	**1.5±0.6**	**1.4±0.3**
Ultimate strain (%)	**33.9±9.4**	**32.5±6.6**	**29.3±11.4**	**25.3±4.4**	**33.8±5.5**	**32.9±10.9**

** The anterior vertical samples had higher ultimate stress than the posterior vertical samples ($p<0.001$, paired t-test), and the dorsal and ventral horizontal samples loaded at 1%/sec ($p<0.01$, repeated measures ANOVA).*

Table V-3: Tensile relaxation stress at 0 seconds, and percent loss at 10and 30 seconds after holding the strain at 2, 6 and 10%. Results were similar for the intermediate times and strains

	2%			6%			10%		
	Relaxation stress at 0 sec (MPa)	% loss at 10 sec	% Loss at 30 sec	Relaxation stress at 0 sec (MPa)	% loss at 10 sec	% Loss at 30 sec	Relaxation stress at 0 sec (MPa)	% loss at 10 sec	% Loss at 30 sec
Anterior vertical *	0.05±0.02	35.1±7.2	45.4±9.4	0.08±0.04	37.5±8.0	46.4±10.9	0.11±0.06	39.1±9.2	50.1±10.8
Posterior vertical	0.06±0.02	35.8±8.1	47.0±10.1	0.10±0.03	36.4±7.8	48.2±9.2	0.14±0.06	35.1±8.6	47.4±11.2
Dorsal horizontal	0.06±0.02	34.5±8.3	44.7±9.9	0.09±0.04	34.6±6.6	44.1±9.6	0.15±0.05	33.9±5.7	45.4±6.8
Ventral horizontal	0.06±0.02	33.4±5.8	44.5±7.4	0.09±0.04	32.2±10.7	40.4±13.5	0.13±0.05	34.4±6.2	46.0±7.1

** The anterior vertical samples had lower tensile stiffness than the other locations*

Table V-4: Ultimate tensile stress and strain of the septal cartilage

Orientation	Anterior vertical (n=14)	Posterior vertical (n=18)	Dorsal horizontal (n=15)	Ventral horizontal (n=13)
Ultimate stress (MPa)	2.0±0.7*	1.1±0.4*	1. 4±0.5†	1.1±0.4†
Ultimate strain (%)	157.2±72.5	105.8±42.0	126.4±56.4	122.7±60.0

** Anterior samples were significantly stiffer than posterior samples*

† Dorsal samples were significantly stiffer than ventral samples

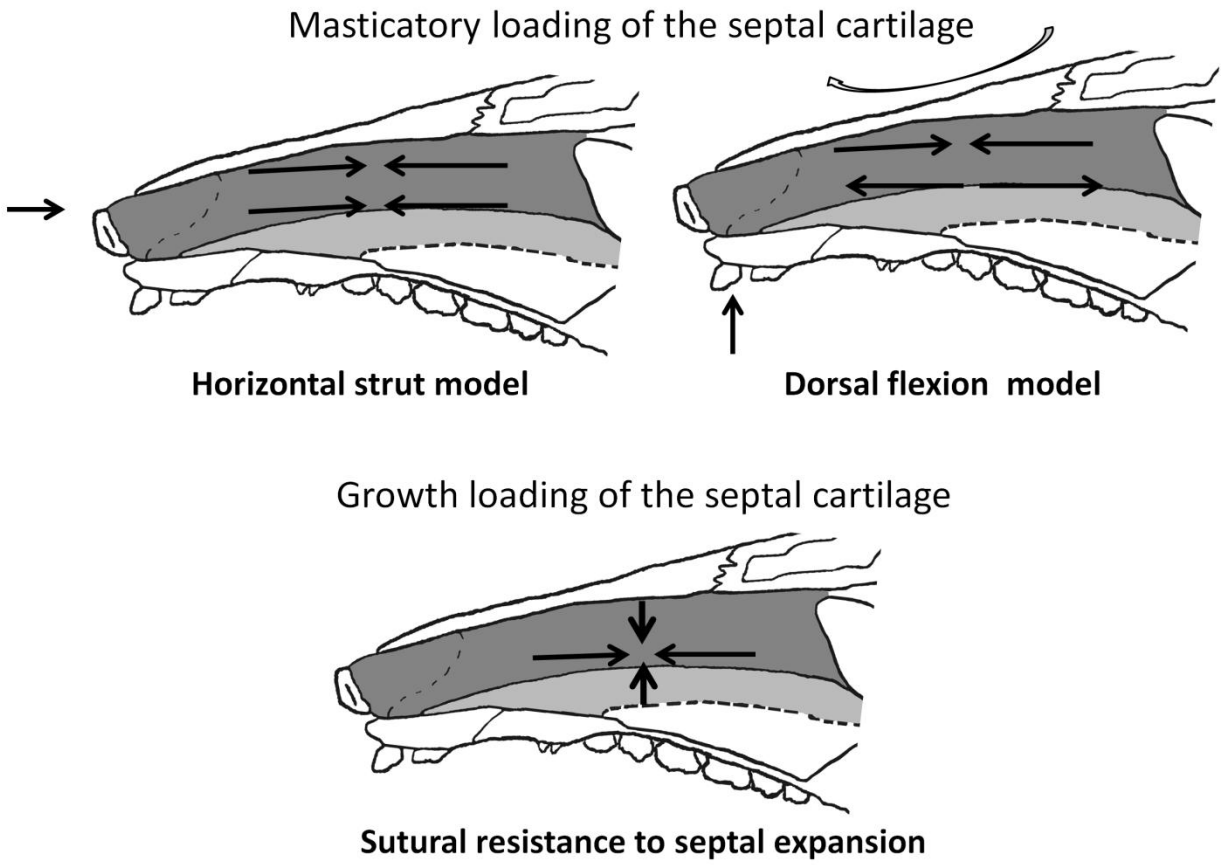

Figure V-1: Medial view of the pig nasal septal cartilage illustrating possible patterns of loading during mastication (top row) and during growth (bottom). Both the horizontal strut model and the dorsal flexion model are consistent with in vivo data which show that the dorsal region of the septum and snout show anteroposterior compression strain during mastication (Al Dayeh et al, 2009; Rafferty et al, 2003)

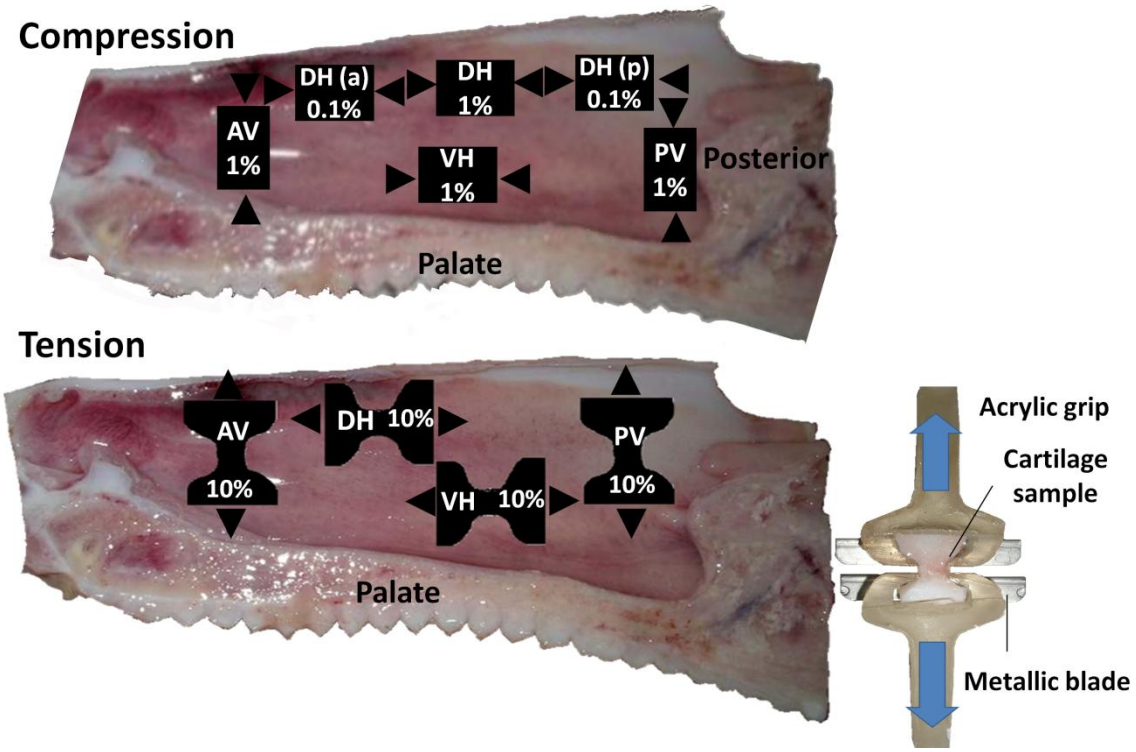

Figure V-2: Medial view of the septal cartilage illustrating the location of the tested samples in compression (top) and in tension (bottom). Loading direction is designated by arrows. Numbers indicate loading speed in %length/ sec. AV: anterior vertical, VH: Ventral horizontal, DH: Dorsal horizontal, PV: Posterior vertical. DH (a): dorsal horizontal anterior, DH (p): dorsal horizontal posterior. Right: During tension experiments the cartilage samples were placed in acrylic grips and kept aligned by metallic blades.

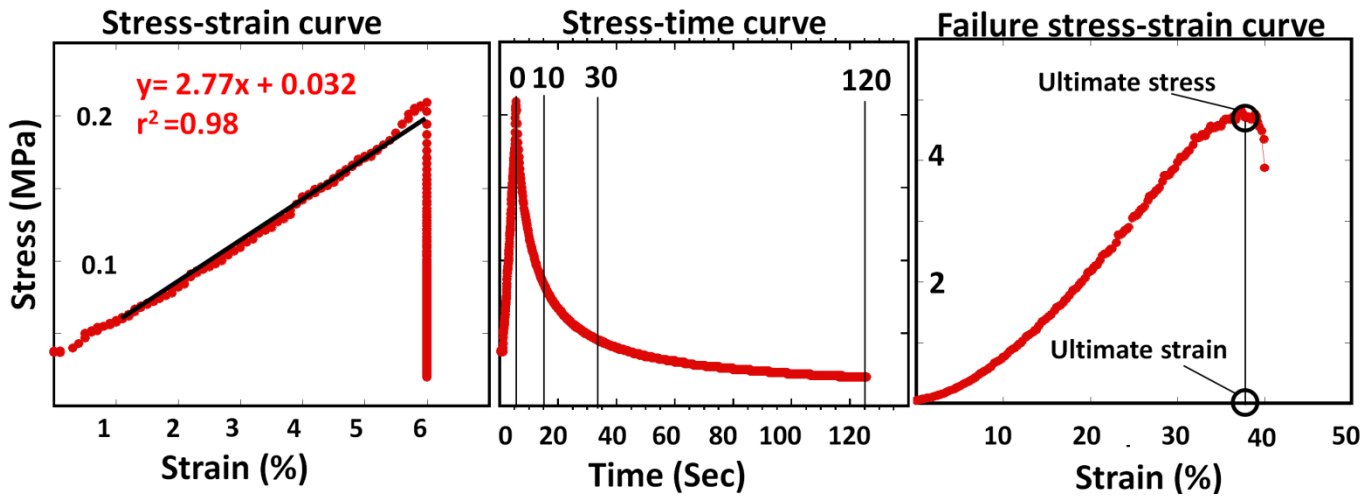

Figure V-3: Examples of mechanical tests. Left: Stress-strain curve illustrating stiffness calculation. This sample was vertically compressed at 1%/s until 6% strain was reached. Center: Stress-time plot of the same sample. After 6% strain was reached, strain was held for 120 seconds for relaxation (30 seconds in tension experiments). Relaxation stress was measured at 0, 10, 30, and 120 seconds (0, 10 and 30 seconds in tension). Drop in stress between these time points was used as an indication of the stress dissipation of the cartilage. Right: Failure stress-strain curve for same sample, showing the ultimate stress and strain.

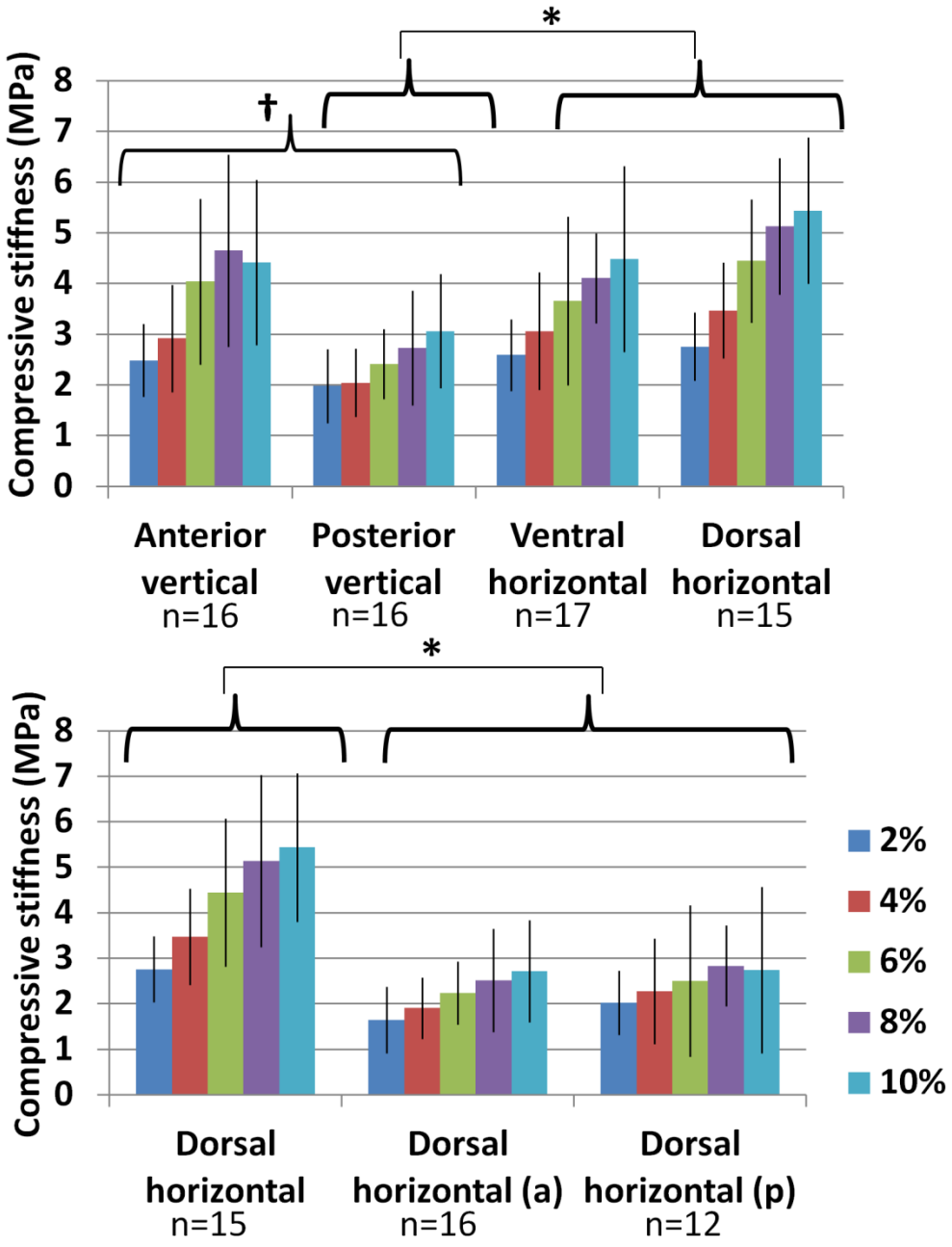

Figure V-4: Compressive stiffness (Young's elastic modulus) of the nasal septum. Increased strain level and rate both resulted in increased stiffness. Locations are illustrated in Figure V-2. Top: Samples loaded at 1%/sec. The anterior vertical and dorsal horizontal samples were stiffer than the posterior vertical samples at all strains. The ventral horizontal samples were stiffer than the posterior vertical samples at 6, 8 and 10% strain. Bottom: The dorsal horizontal samples loaded at 1%/sec were stiffer than nearby samples loaded horizontally at 0.1%/sec at all strains

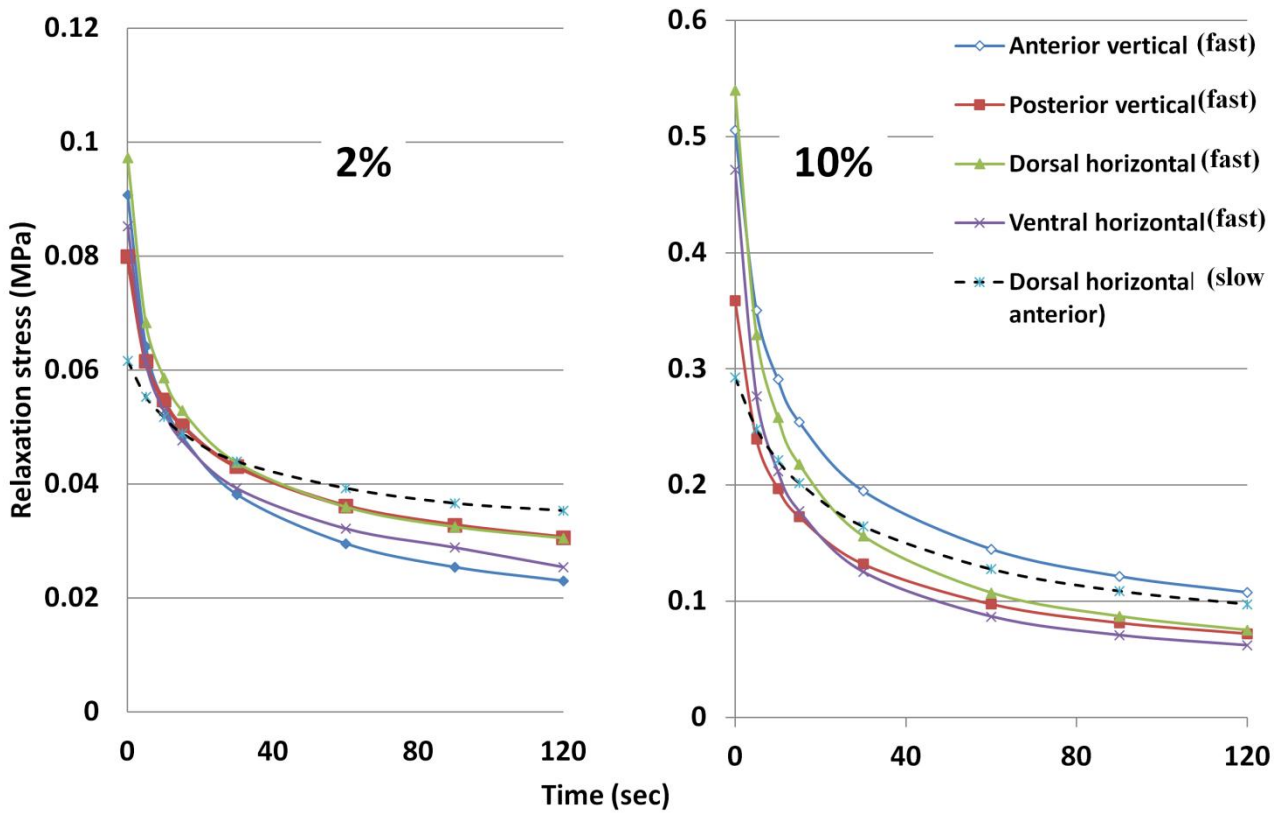

Figure V-5: Drop in compression relaxation stress for nasal septum samples loaded at 2 and 10% strain. Intermediate strain points followed similar patterns and are omitted for clarity. One slowly loaded (0.1%/sec) location (DH (a), dashed line) is contrasted with the four locations loaded at 1%/sec. Greater drops in relaxation stress were consistently seen in the samples loaded at the faster rate. Although the stress in the slowly loaded locations is very low at time 0, the residual stress at 120 sec is as high (10% strain) or higher (2% strain) than that for the faster loaded locations.

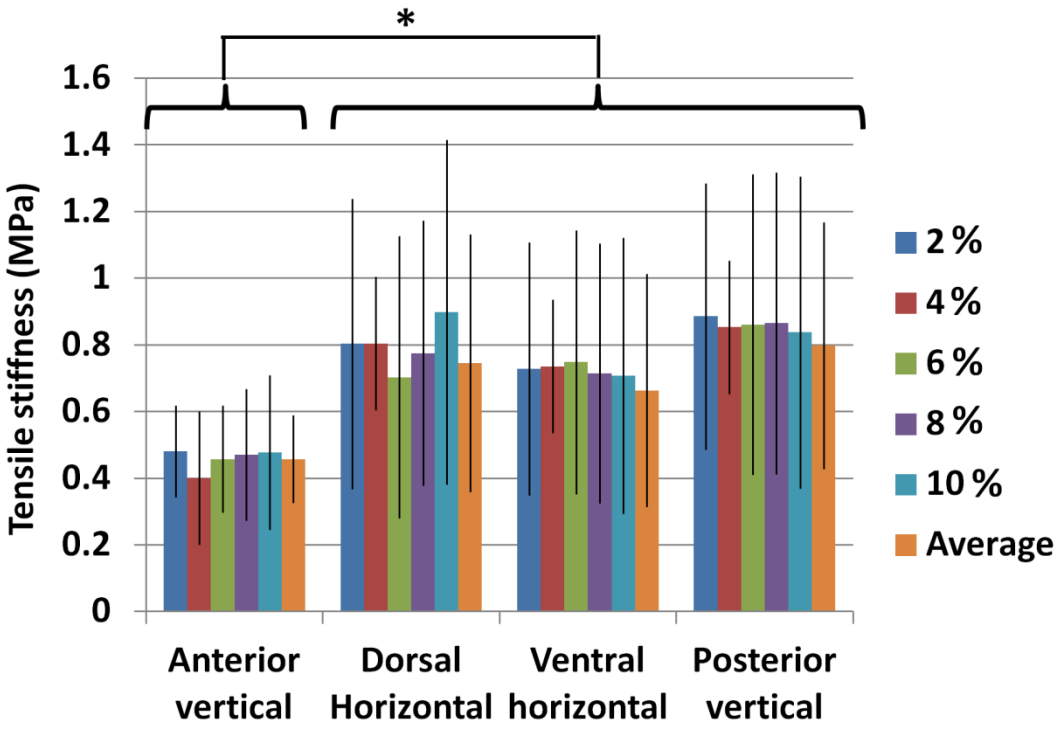

Figure V-6: Tensile stiffness (Young's elastic modulus) of the nasal septum. In contrast to compression stiffness, tensile stiffness was relatively constant regardless of magnitude of strain. The anterior vertical samples were less stiff than the remaining locations

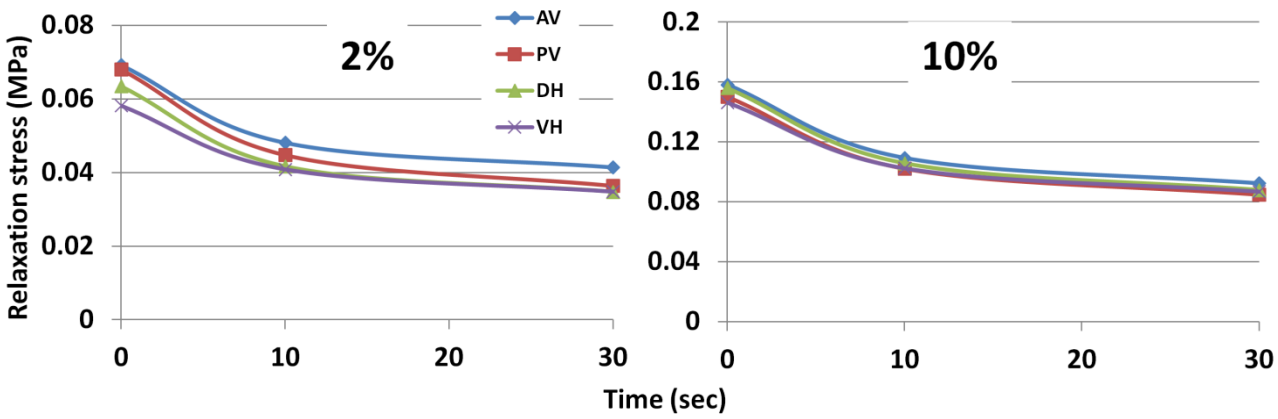

Figure V-7: Drop in tensile relaxation stress for septal samples loaded at 2% and 10% strain. Intermediate strain points followed similar patterns and are not shown for clarity.

Chapter VI: General discussion

Craniofacial anomalies are among the most common birth defects, appearing in approximately 1 out of 2000 newborns. They range in severity from simple clefts to more severe syndromes that affect large areas of the craniofacial apparatus. These defects invariably include the nasal septum, which articulates with the palatal midline. Treatment of such anomalies is complicated by lack of knowledge of the biologic processes controlling facial growth and maintaining its mechanical integrity. Some aspects of facial deformity, such as midfacial hypoplasia, may actually get worse after surgical treatment. Interference with septal growth is one possible contributing factor. Better knowledge of facial growth processes could provide enormous improvements to the fields of orthodontics and dentofacial orthopedics.

This thesis had two main goals. The first goal was to determine whether the nasal septal cartilage acts as a “growth center” that separates midfacial sutures and resulting in suture growth. The second goal was to determine whether the septum acts as a biomechanical strut supporting the face and maintaining its integrity during physiologic loading. The first goal was addressed in chapters II, III and V. In chapter II, the growth of the septal cartilage in minipigs was measured in vivo and compared to the separation of the nasofrontal suture. This suture was chosen as a representative of the midfacial sutural system because of ease of surgical access, and the presence of previous data concerning the bone apposition rate at this suture (Rafferty and Herring 1999). This chapter was supplemented by observing the proliferation of the septal chondrocytes in minipigs of similar strain and age (chapter III). Finally, the mechanical

properties of the nasal septal cartilage and nasofrontal suture were studied to determine whether the postulated growth role of the cartilage is mechanically feasible. The second goal of the study, addressed in chapters IV and V, was to determine the biomechanical role of the septal cartilage in the midface. This was approached by measuring the deformation (polarity and magnitude) of the septal cartilage and nasofrontal suture during mastication (chapter IV). This chapter was supplemented by measuring the mechanical properties of the septal cartilage under loading rates that mimic those encountered during mastication in order to determine if the cartilage is adapted to any particular pattern of loading that could support the observed in vivo deformation (chapter V).

Pigs were used as the animal model throughout this thesis. They were chosen for various reasons: (1) their ample size facilitated surgical procedures and instrument implantation, (2) the existence of a large body of literature concerning the mineral apposition rate at the nasofrontal suture (Rafferty and Herring 1999), mechanical properties of the nasofrontal suture (Popowics and Herring 2007) and in vivo masticatory strain in pigs of similar strain to the ones used in this study (Rafferty and Herring 1999; Rafferty and Herring 2002; Rafferty et al. 2003). Therefore, this study will fit into the “big picture” of the overall growth and biomechanics of the midface in pigs.

Growth of the nasal septal cartilage and nasofrontal suture:

Technical considerations:

Because of its deep location, very few attempts have been made to measure the in vivo growth of the nasal septal cartilage. Most previous studies focused on determining the role of the nasal cartilage in midfacial development by utilizing indirect approaches such as observing midfacial growth after septal cartilage extirpation (Moss et al. 1968; Sarnat and Wexler 1968; Stenström and Thilander 1970; Kvinnsland 1974) and studying the growth of the septal cartilage in culture (Copray 1986). Such studies are limited by indirect assessment of growth (extirpation studies) and the artificial culture environment. In this study, I utilized a novel approach to monitor the growth of the septal cartilage directly and continuously at one-minute intervals over a period of several days. The procedure involved the use of a linear displacement transducer (DVRT) to measure the growth of the nasal septal cartilage and the nasofrontal suture. The main advantage of using the DVRT was its reliance on barbs for mechanical attachment to the cartilage, and screws for attachment to the nasal and frontal bones. Furthermore, the same general methodology could be used to record masticatory mechanics. However, the use of the DVRTs introduced some unavoidable limitations. The mechanical attachment of the DVRT (the barbs and screws) causes unavoidable injury to the cartilage, in the form of small holes which could potentially widen with the forces of growth and function. This might have resulted in some minor instability of the DVRTs. However, the overall recordings showed steady growth and reproducible masticatory patterns.

Growth of the septal cartilage

The growth of the septal cartilage was evaluated by measuring the separation between the DVRT barbs. This approach did not measure the cartilage growth in the form of matrix formation and cellular proliferation; rather it is a measure of interstitial expansion. Although other factors might contribute to cartilage expansion beside growth, such as water absorption, their effect would have been minimalized by the long period of time over which growth was monitored. Thus I believe that the expansion of the cartilage measured by the DVRTs was a good estimate of its growth. My results indicate that the septal cartilage lengthens at a rate of 0.07%/hr. This value compares favorably with rates reported for organ culture of 4-day-old albino rat septal fragments (0.08-0.13%, calculated from Copray 1984). Implanting two DVRTs in the cartilage was intended to test if expansion of the cartilage is uniform. However, because of surgical accessibility, the two DVRTs were implanted close to each other, thus growth reported might not represent that of the entire cartilage. Nonetheless, no difference in growth rate was found between the two sites. Assuming that the cartilage is expanding at a uniform rate, then these results indicate that the cartilage doubles in length in 2.5 months, a plausible estimates for pigs.

Cellular proliferation, matrix formation and a growth plate at the caudal end of the cartilage might be all contributing to growth of the cartilage. In this study, I attempted to study one of these factors: chondrocytic proliferation. Results clearly indicated that the septal chondrocytes are proliferating at a high rate (around 20%/day). This fast proliferation rate coincides with the high expansion rate recorded by the DVRTs. In addition, the relative uniformity noticed in the proliferation of the septal cartilage support

the finding of no difference in growth recorded by the two cartilage DVRTs. These results clearly indicate that the cellular proliferation contributes strongly to the overall growth of the cartilage. Furthermore, proliferation of the septal chondrocytes is supplemented by proliferation of the septal chondrocytes is supplemented by proliferation of septal perichondrial cells, some of which likely have a chondrocytic fate.

Growth of the nasofrontal suture

The growth of the nasofrontal suture recorded by the DVRT reflects the separation of the nasofrontal suture, not bone formation at the sutural edges. The nasofrontal suture was found to separate at an approximate rate of 0.03%/hr (~80 μm/day). This exceeds the mineral apposition rate measured previously at the suture (around 50-60 ±15-20 μm/day for the entire suture; calculated from Rafferty and Herring, 1999). This suggests that tissue separation of the suture is faster than bone formation at the suture and is consistent with the idea that the suture growth starts by separation of the sutural tissue followed by bone formation at the sutural edges

Does the nasal septal cartilage play an active role in midfacial growth?

The finding that the growth rate of the septal cartilage was more than double that of the suture coupled with the fact that the overall volume of the cartilage is larger than the suture (Figure II-1), clearly support the idea that the growth of the nasal septal cartilage could lead to separation of the suture as suggested by Scott (1953). Moreover, the results of the cross-correlation analysis in chapter II showed that the expansion of the cartilage is simultaneous with or precedes the separation of the suture. On the other hand, the suggestion that the growth of the cartilage is causing separation of the

nasofrontal suture is challenged by the mechanical nature of the cartilage. In order for the cartilage to act as a growth center, then expansion of the cartilage should be capable of separating the midfacial sutures, including the nasofrontal suture. The main aim of chapter V was to investigate if the cartilage is mechanically suited for such a role. If the septal cartilage is truly separating the nasofrontal suture then the recoil pressure of the sutural tissue will place the cartilage under anteroposterior compression. In order for separation to occur the stiffness of the cartilage under compression should be greater than the stiffness of the nasofrontal suture under tension. My findings were not conclusive, but suggest that the stiffness of the septal cartilage under compression is at least comparable to the stiffness of the nasofrontal suture under tension, not contradicting an active role of the nasal septal cartilage in midfacial growth. In addition, one of the important findings of chapter V is that under low strain rate, the cartilage tended to store (rather than dissipate) the loading energy (Figure V-5). This finding, if true, buttresses the probability that under slow loading rate (as seen during growth) the cartilage could store enough loading energy to separate the sutures.

The role of the nasal septal cartilage in facial integrity

Technical considerations

The role of the nasal septal cartilage in facial integrity was assessed by measuring the directionality and deformation of the nasal septal cartilage during mastication. Traditionally, strain gages were used to measure the deformation of various skull bones and sutures. Unfortunately, strain gages cannot be glued to the nasal cartilage, so an alternative approach was needed. In this study I utilized DVRTs

attached to the septal cartilage using barbs. As mentioned above, this attachment probably introduced some “play” between the DVRT and the cartilage tissue. Another limitation with the use of the DVRTs is the fact that they measure linear displacement. Thus they are only accurate in measuring the deformation along their long axis. Deformation that is not in line with the long axis of the DVRT will be underestimated. In addition, the surgical access to the nasal cavity might have affected the integrity of the snout, resulting in exaggerated deformation values. Nonetheless, the consistent findings of these experiments suggest that despite limitations, the results are still valid and reproducible.

Does the nasal septal cartilage act as a vertical strut during mastication?

If the cartilage is a vertical strut supporting the nasal cavity and preventing the collapse of the nasal bone under masticatory loading, then the cartilage should be compressed vertically, and as a result of Poisson’s effect, tensed horizontally during mastication. In addition, the strut role predicts that the cartilage is stiff enough to withstand loads. Such claims were not supported. The strain polarity reported in this study indicated that the cartilage was compressed anteroposteriorly, which does not support the vertical strut role of the cartilage. Furthermore, the magnitude of the strain was high, indicating that the cartilage is not designed to act as a strut. Thus, the vertical strut role of the septal cartilage (Badoux 1968; Moss et al. 1968) was rejected.

High deformability of the cartilage and the stress dampener role

The fact that the strain magnitude in the cartilage was similar to strain magnitude at the nasofrontal sutures suggests that the cartilage, like sutures, functions as a stress

breaker/dampener helping to dissipate and absorb loads generated during mastication. This stress dampener role is supported by the excellent energy absorption properties of the cartilage, especially under fast strain rates (chapter V).

General conclusions and future research interests

In this study the role of the nasal septal cartilage in midfacial growth and in facial integrity was investigated. The role of the nasal septal cartilage in midfacial growth was addressed by measuring and comparing the growth of the septal cartilage and nasofrontal suture. Furthermore the cellular proliferation in the septal cartilage was assessed. This was further supplemented by studying the mechanical properties of the cartilage under testing conditions that attempted to mimic the in vivo growth loads. The role of the septal cartilage in preserving the facial integrity was assessed by measuring the deformation of the nasal septal cartilage and nasofrontal suture during mastication. This was further supplemented by measuring the mechanical properties of the septal cartilage under loading rates and conditions that mimicked those encountered during mastication.

The findings generally supported the idea that the nasal septal cartilage plays an active role in midfacial growth and that the growth of the cartilage causes expansion and resulting in bone formation at the suture (Scott 1951). Mechanical testing of the septal cartilage was less clear but did not rule out such a role. The determination of substantial cellular proliferation everywhere in the septum was also consistent with active, expansive and relatively uniform growth of the septal cartilage.

The septal cartilage was found to be compressed anteroposteriorly during mastication. The magnitude of the strain was relatively high and approximated the magnitude of strain recorded at the nasofrontal suture. Thus, neither the directionality nor the magnitude of strain supported the idea that the cartilage acts as a vertical strut during mastication (Moss et al. 1968). Rather, show that the excellent energy absorption indicated by mechanical testing, coupled with high strain during mastication suggest that the cartilage acts as a stress dampener dissipating impact loads and protecting the more rigid bones.

Future research must include an understanding of the interaction of the nasal septal with additional facial sutures, especially the premaxillary-maxillary and the zygomatico-maxillary sutures. Understanding the mechanical relationship between the septum and all the facial sutures will offer a unique opportunity to identify the determinants of midfacial growth, and how they can be utilized to develop therapeutic approaches to address deformities such as midfacial retrognathia. The general strategy of utilizing DVRTs in order to study growth and mechanics of several structures simultaneously was very successful in this thesis and could be used on other parts of the midface. Ultimately, the strategy could be employed to examine the effects of various treatment regimens (such as protraction) on growth phenomena.

Chapter VII: References

Al Dayeh, AA, KL Rafferty, M Egbert and SW Herring (2009). "Deformation of nasal septal cartilage during mastication." Journal of Morphology **270**(10): 1209-1218.

Alford, FP, HWG Baker and HG Burger (1973). "Secretion rate of human growth-hormone .1. Daily secretion rates, effect of posture and sleep." Journal of Clinical Endocrinology & Metabolism **37**(4): 515-520.

Arbona, JR, DN Marple, RW Russell, CH Rahe, DR Mulvaney and JL Sartin (1988). "Secretory patterns and metabolic clearance rate of porcine growth hormone in swine selected for growth." Journal of Animal Science **66**(12): 3068-3072.

Babler, WJ, JA Persing, KM Persson, HR Winn, JA Jane and GT Rodeheaver (1982). "Skull growth after coronal suturectomy, periostectomy, and dural transection." Journal of Neurosurgery **56**(4): 529-535.

Babula, WJ, GR Smiley and AD Dixon (1970). "Role of cartilaginous nasal septum in midfacial growth." American Journal of Orthodontics **58**(3): 250-263.

Badoux, DM (1966). "Framed structures in the mammalian skull." Acta Morphol Neerl Scand. 1966;6(3):239-50.

Badoux, DM (1968). "Cremona diagrams of framed structures in skull of canis familiaris and sus scrofa scrofa." Proceedings of the Koninklijke Nederlandse Akademie Van Wetenschappen Series C-Biological and Medical Sciences **71**(3): 229-244.

Beynnon, BD and BC Fleming (1998). "Anterior cruciate ligament strain in-vivo: A review of previous work." Journal of Biomechanics **31**(6): 519-525.

Bujia, J, P Pitzke, E Kastenbauer, E Wilmes and C Hammer (1996). "Effect of growth factors on matrix synthesis by human nasal chondrocytes cultured in monolayer and in agar." European Archives of Oto-Rhino-Laryngology **253**(6): 336-340.

Byl, C, C Puttlitz, N Byl, J Lotz and K Topp (2002). "Strain in the median and ulnar nerves during upper-extremity positioning." The Journal of Hand Surgery **27**(6): 1032-1040.

Cerulli, G, DL Benoit, M Lamontagne, A Caraffa and A Liti (2003). "In vivo anterior cruciate ligament strain behaviour during a rapid deceleration movement: Case report." Knee Surgery, Sports Traumatology, Arthroscopy **11**(5): 307-311.

Chao, KKH, KHK Ho and BJF Wong (2003). "Measurement of the elastic modulus of rabbit nasal septal cartilage during nd : Yag (lambda=1.32 mu m) laser irradiation." Lasers in Surgery and Medicine **32**(5): 377-383.

Claus, R, A Bingel, S Hofacker and U Weiler (1990). "24 hour profiles of growth-hormone (gh) concentrations in mature female and entire male domestic pigs in comparison with mature wild boars (sus-scrofa l)." Livestock Production Science **25**(3): 247-255.

Copray, J (1986). "Growth of the nasal septal cartilage of the rat invitro." Journal of Anatomy **144**: 99-111.

Cupero, TM, CE Middleton and AB Silva (2001). "Effects of functional septoplasty on the facial growth of ferrets." Archives of Otolaryngology-Head & Neck Surgery **127**(11): 1367-1369.

Delaire, J and D Precious (1986). "Influence of the nasal-septum on maxillonasal growth in patients with congenital labiomaxillary cleft." Cleft Palate Journal **23**(4): 270-277.

Delaire, J and D Precious (1987). "Interaction of the development of the nasal-septum, the nasal pyramid and the face." International Journal of Pediatric Otorhinolaryngology **12**(3): 311-326.

DiSilvestro, MR, Q Zhu and J-KF Suh (2001). "Biphasic poroviscoelastic simulation of the unconfined compression of articular cartilage: Ii---effect of variable strain rates." Journal of Biomechanical Engineering **123**(2): 198-200.

Dubreuil, P, H Lapierre, G Pelletier, D Petitclerc, Y Couture, P Gaudreau, J Morisset and P Brazeau (1988). "Serum growth-hormone release during a 60-hour period in growing-pigs." Domestic Animal Endocrinology **5**(2): 157-164.

Enlow and Hans (1996). Essentials of facial growth. Philadelphia, Saunders.

Ferrari, CS and SW Herring (1995). "Use of a bite-opening appliance in the miniature pig: Modification of craniofacial growth." Acta Anatomica **154**(3): 205-215.

Fleming, BC, BD Beynnon, PA Renstrom, RJ Johnson, CE Nichols, GD Peura and BS Uh (1999). "The strain behavior of the anterior cruciate ligament during stair climbing: An in vivo study." Arthroscopy: The Journal of Arthroscopic & Related Surgery **15**(2): 185-191.

Gaon, MD, KHK Ho and BJF Wong (2003). "Measurement of the elastic modulus of porcine septal cartilage specimens following nd : Yag laser treatment." Lasers in Medical Science **18**(3): 148-153.

Garrett, BJ, JM Caruso, K Rungcharassaeng, JR Farrage, JS Kim and GD Taylor (2008). "Skeletal effects to the maxilla after rapid maxillary expansion assessed with cone-beam computed tomography." American Journal of Orthodontics and Dentofacial Orthopedics **134**(1).

Grellmann, W, A Berghaus, EJ Haberland, Y Jamali, K Holweg, K Reincke and C Bierogel (2006). "Determination of strength and deformation behavior of human cartilage for the definition of significant parameters." Journal of Biomedical Materials Research Part A **78A**(1): 168-174.

Grellmann, W, A Berghaus, EJ Haberland, Y Jamali, K Holweg, K Reincke and C Bierogel (2006). "Determination of strength and deformation behavior of human cartilage for the definition of significant parameters (vol 78a, pg 168, 2006)." Journal of Biomedical Materials Research Part A **79A**(3): 758-758.

Hans, MG, L Scaletta and JC Occhino (1996). "The effects of antirat nasal septum cartilage antisera on facial growth in the rat." American Journal of Orthodontics and Dentofacial Orthopedics **109**(6): 607-615.

Herring, SW, KL Rafferty, ZJ Liu and CD Marshall (2001). "Jaw muscles and the skull in mammals: The biomechanics of mastication." Comparative Biochemistry and Physiology a-Molecular & Integrative Physiology **131**(1): 207-219.

Herring, SW, KL Rafferty, ZJ Liu and CD Marshall (2001). "Jaw muscles and the skull in mammals: The biomechanics of mastication." Comparative Biochemistry and Physiology - Part A: Molecular & Integrative Physiology **131**(1): 207-219.

Herring, SW and SY Teng (2000). "Strain in the braincase and its sutures during function." American Journal of Physical Anthropology **112**(4): 575-593.

Hickey, TL, DR Whikehart, CA Jackson, PF Hitchcock and JD Peduzzi (1983). "Tritiated-thymidine experiments in the cat - a description of techniques and experiments to define the time-course of radioactive thymidine availability." Journal of Neuroscience Methods **8**(2): 139-147.

Huang, CY, VC Mow and GA Ateshian (2001). "The role of flow-independent viscoelasticity in the biphasic tensile and compressive responses of articular cartilage." Journal of Biomechanical Engineering-Transactions of the Asme **123**(5): 410-417.

Huggare, J and O Rönning (1995). "Growth of the cranial vault - influence of intracranial and extracranial pressures." Acta Odontologica Scandinavica **53**: 192-195.

Hylander, WL and KR Johnson (1997). "In vivo bone strain patterns in the zygomatic arch of macaques and the significance of these patterns for functional interpretations of craniofacial form." American Journal of Physical Anthropology **102**(2): 203-232.

Ingervall, B and B Thilander (1972). "Human spheno-occipital synchondrosis .1. Time of closure appraised macroscopically." Acta Odontologica Scandinavica **30**(3): 349-356.

Jaslow, CR and AA Biewener (1988). "Strain patterns in cranial bones and sutures during impact loading." American Zoologist **28**(4): A175-A175.

Jaslow, CR and AA Biewener (1995). "Strain patterns in the horncores, cranial bones and sutures of goats (capra hircus) during impact loading." Journal of Zoology **235**(2): 193-210.

Kasai, K, T Moro, E Kanazawa and T Iwasawa (1995). "Relationship between cranial base and maxillofacial morphology." European Journal of Orthodontics **17**(5): 403-410.

Katsaros, C (2001). "Masticatory muscle function and transverse dentofacial growth." Swedish Dental Journal Suppl. 2001;(151):1-47.

Katsaros, C, R Berg and S Kiliaridis (2002). "Influence of masticatory muscle function on transverse skull dimensions in the growing rat." Journal of Orofacial Orthopedics/Fortschritte der Kieferorthopädie **63**(1): 5-13.

Kiliaridis, S (1995). "Masticatory muscle influence on craniofacial growth." Acta Odontologica Scandivica. 1995 Jun;53(3):196-202.

Kiliaridis, S (2006). "The importance of masticatory muscle function in dentofacial growth." Seminars in Orthodontics **12**(2): 110-119.

Kobayashi, K, H Mishima, S Hashimoto, RS Goomer, FL Harwood, M Lotz, H Moriya and D Amiel (2001). "Chondrocyte apoptosis and regional differential expression of nitric oxide in the medial meniscus following partial meniscectomy." Journal of Orthopaedic Research **19**(5): 802-808.

Kvinnsland, S (1973). "Growth potential of autografts of cartilage from nasal septum in rat." Plastic and Reconstructive Surgery **52**(5): 557-561.

Kvinnsland, S (1974). "Autogenous transplantation of nasal-septum cartilage in rat." Archives of Oral Biology **19**(9): 767-770.

Kvinnsland, S (1974). "Partial resection of cartilaginous nasal-septum in rats - its influence on growth." Angle Orthodontist **44**(2): 135-140.

Kvinnsland, S (1977). "Regional variations in cell-proliferation and matrix formation in cartilaginous nasal-septum of rat - [thymidine-h-3] and [sulfate-s-35] incorporation studies." Growth **41**(2): 85-93.

Kvinnsland, S (1988). "Invitro growth of the nasal septal cartilage of the rat in a serum-free culture-medium - [h-3]-thymidine incorporation studies." Acta Anatomica **131**(3): 231-234.

Langelier, E and MD Buschmann (2003). "Increasing strain and strain rate strengthen transient stiffness but weaken the response to subsequent compression for articular cartilage in unconfined compression." Journal of Biomechanics **36**(6): 853-859.

Larsson, E, B Ogaard, R Lindsten, N Holmgren, M Brattberg and L Brattberg (2005). "Craniofacial and dentofacial development in pigs fed soft and hard diets." American Journal of Orthodontics and Dentofacial Orthopedics **128**(6): 731-739.

Li, LP and W Herzog (2004). "Strain-rate dependence of cartilage stiffness in unconfined compression: The role of fibril reinforcement versus tissue volume change in fluid pressurization." Journal of Biomechanics **37**(3): 375-382.

Lieberman, DE, GE Krovitz, FW Yates, M Devlin and MS Claire (2004). "Effects of food processing on masticatory craniofacial growth in a retrognathic strain and face." Journal of Human Evolution **46**(6): 655-677.

Liu, ZJ, JR Green, CA Moore and SW Herring (2004). "Time series analysis of jaw muscle contraction and tissue deformation during mastication in miniature pigs." Journal of Oral Rehabilitation **31**(1): 7-17.

Long, R, RC Greulich and BG Sarnat (1968). "Regional variations in chondrocyte proliferation in the cartilaginous nasal septum of the growing rabbit." Journal of Dental Research **47**(3): 505-505.

Luder, HU (1994). "Perichondrial and endochondral components of mandibular condylar growth - morphometric and autoradiographic quantitation in rats." Journal of Anatomy **185**: 587-598.

Martin , BD, Sharkey N. (1998). Skeletal tissue mechanics. New York, Springer

Mathews, MB and L Decker (1977). "Comparative studies of water sorption of hyaline cartilage." Biochimica et Biophysica Acta (BBA) - General Subjects **497**(1): 151-159.

McComb, H and KE Salyer (1990). "Primary repair of the bilateral cleft lip nose: A 15-year review and a new treatment plan." Plastic and Reconstructive Surgery **86**(5): 890-893.

McLaughlin, E, Y Zhang, D Pashley, J Borke and J Yu (2000). "The load-displacement characteristics of neonatal rat cranial sutures." Cleft Palate-Craniofacial Journal **37**(6): 590-595.

Morel, V and TM Quinn (2004). "Cartilage injury by ramp compression near the gel diffusion rate." Journal of Orthopaedic Research **22**(1): 145-151.

Mosher, TJ, H Smith, BJ Dardzinski, VJ Schmithorst and MB Smith (2001). "Mr imaging and t2 mapping of femoral cartilage." American Journal of Roentgenology **177**(3): 665-669.

Moss, ML (1964). "Vertical growth of human face." American Journal of Orthodontics and Dentofacial Orthopedics **50**(5): 359-576.

Moss, ML, BE Bromberg, IC Song and G Eisenman (1968). "Passive role of nasal septal cartilage in mid-facial growth." Plastic and Reconstructive Surgery **41**(6): 536-&.

Moss, ML, BE Bromberg, IG Song and G Eisenman (1968). "The passive role of nasal septal cartilage in mid-facial growth." Plastic and Reconstructive Surgery **41**(6): 536-542.

Mow, VC and CCB Wang (1999). "Some bioengineering considerations for tissue engineering of articular cartilage." Clinical Orthopaedics and Related Research **367**: S204-S223.

Muskhelishvili, L, JR Latendresse, RL Kodell and EB Henderson (2003). "Evaluation of cell proliferation in rat tissues with brdu, pcna, ki-67(mib-5) immunohistochemistry and in situ hybridization for histone mrna." Journal of Histochemistry & Cytochemistry **51**(12): 1681-1688.

Naumann, A, JE Dennis, A Awadallah, DA Carrino, JM Mansour, E Kastenbauer and AI Caplan (2002). "Immunochemical and mechanical characterization of cartilage subtypes in rabbit." Journal of Histochemistry & Cytochemistry **50**(8): 1049-1058.

Ng, LJ, KS Tai, A Plaas, AJ Grodzinsky and C Ortiz (2003). "Ultrastructure and nanomechanics of biological tissues: Cartilage and bone." Abstracts of Papers of the American Chemical Society **225**: 303-PMSE.

Nie, XG (2005). "Cranial base in craniofacial development: Developmental features, influence on facial growth, anomaly, and molecular basis." Acta Odontologica Scandinavica **63**(3): 127-135.

O'Driscoll, SWM, DBF Saris, Y Ito and JS Fitzimmons (2001). "The chondrogenic potential of periosteum decreases with age." Journal of Orthopaedic Research **19**(1): 95-103.

Ogle, RC, SS Tholpady, KA McGlynn and RA Ogle (2004). "Regulation of cranial suture morphogenesis." Cells Tissues Organs **176**(1-3): 54-66.

Opperman, LA (2000). "Cranial sutures as intramembranous bone growth sites." Developmental Dynamics **219**(4): 472-485.

Persing, JA, EP Morgan, AJ Cronin and WP Wolcott (1991). "Skull base expansion - craniofacial effects." Plastic and Reconstructive Surgery **87**(6): 1028-1033.

Persson, KM, WA Roy, JA Persing, GT Rodeheaver and HR Winn (1979). "Craniofacial growth following experimental craniosynostosis and craniectomy in rabbits." Journal of Neurosurgery **50**(2): 187-197.

Pirinen, S (1995). "Endocrine regulation of craniofacial growth." Acta Odontologica **53**(3): 179-185.

Pirinen, S, A Majurin, HL Lenko and K Koski (1994). "Craniofacial features in patients with deficient and excessive growth-hormone." Journal of Craniofacial Genetics and Developmental Biology **14**(3): 144-152.

Popowics, TE and SW Herring (2007). "Load transmission in the nasofrontal suture of the pig, sus scrofa." Journal of Biomechanics **40**(4): 837-844.

Quinn, TM, RG Allen, BJ Schalet, P Perumbuli and EB Hunziker (2001). "Matrix and cell injury due to sub-impact loading of adult bovine articular cartilage explants: Effects of strain rate and peak stress." Journal of Orthopaedic Research **19**(2): 242-249.

Rabie, ABM, MJM Tsai, U Hagg, X Du and BW Chou (2003). "The correlation of replicating cells and osteogenesis in the condyle during stepwise advancement." Angle Orthodontist **73**(4): 457-465.

Race, A, ND Broom and P Robertson (2000). "Effect of loading rate and hydration on the mechanical properties of the disc." Spine **25**(6): 662-669.

Radhakrishnan, P and JJ Mao (2004). "Nanomechanical properties of facial sutures and sutural mineralization front." Journal of Dental Research **83**(6): 470-475.

Radin, EL and IL Paul (1971). "Importance of bone in sparing articular cartilage from impact." Clinical Orthopaedics and Related Research(78): 342-&.

Rafferty, KL and SW Herring (1999). "Craniofacial sutures: Morphology, growth, and in vivo masticatory strains." Journal of Morphology **242**(2): 167-179.

Rafferty, KL and SW Herring (2002). In vivo biomechanics of the snout.

Rafferty, KL, SW Herring and CD Marshall (2003). "Biomechanics of the rostrum and the role of facial sutures." Journal of Morphology **257**(1): 33-44.

Richmon, JD, A Sage, VW Wong, AC Chen, RL Sah and D Watston (2006). "Compressive biomechanical properties of human nasal septal cartilage." American Journal of Rhinology **20**(5): 496-501.

Richmon, JD, AB Sage, VW Wong, AC Chen, C Pan, RL Sah and D Watson (2005). "Tensile biomechanical properties of human nasal septal cartilage." American Journal of Rhinology **19**(6): 617-622.

Rohl, L, F Linde, A Odgaard and I Hvid (1997). "Simultaneous measurement of stiffness and energy absorptive properties of articular cartilage and subchondral trabecular bone." Proceedings of the Institution of Mechanical Engineers Part H-Journal of Engineering in Medicine **211**(3): 257-264.

Rönning, O (1995). "Basicranial synchondroses and the mandibular condyle in craniofacial growth." Acta Odontologica Scandinavica **53**(3): 162-166.

Rosenberg, P, HR Arlis, RD Haworth, L Heier, L Hoffman and G LaTrenta (1997). "The role of the cranial base in facial growth: Experimental craniofacial synostosis in the rabbit." Plastic and Reconstructive Surgery **99**(5): 1396-1407.

Ross, CF and WL Hylander (1996). "In vivo and in vitro bone strain in the owl monkey circumorbital region and the function of the postorbital septum." American Journal of Physical Anthropology **101**(2): 183-215.

Rotter, N, G Tobias, M Lebl, AK Roy, MC Hansen, CA Vacanti and LJ Bonassar (2002). "Age-related changes in the composition and mechanical properties of human nasal cartilage." Archives of Biochemistry and Biophysics **403**(1): 132-140.

Roy, R, SS Kohles, V Zaporojan, GM Peretti, MA Randolph, JW Xu and LJ Bonassar (2004). "Analysis of bending behavior of native and engineered auricular and costal cartilage." Journal of Biomedical Materials Research Part A **68A**(4): 597-602.

Sarnat, BG (1980). "Eye volume in young and adult-rabbits." Acta Anatomica **106**(4): 462-467.

Sarnat, BG and MR Wexler (1966). "Growth of face and jaws after resection of septal cartilage in rabbit." American Journal of Anatomy **118**(3): 755-767.

Sarnat, BG and MR Wexler (1968). "Postnatal growth of nose and face after resection of septal cartilage in rabbit." Oral Surgery Oral Medicine Oral Pathology Oral Radiology and Endodontics **26**(5): 712-727.

Schrier, L, SP Ferns, KM Barnes, JAM Emons, EI Newman, O Nilsson and J Baron (2006). "Depletion of resting zone chondrocytes during growth plate senescence." Journal of Endocrinology **189**(1): 27-36.

Scott, JH (1951). "The cartilage of the nasal septum and facial growth." Journal of Anatomy **85**(4): 434-434.

Scott, JH (1953). "The cartilage of the nasal septum." British Dental Journal **95**: 37-40.

Searls, JC (1975). "Radioautographic study of chondrocytic proliferation in nasal septal cartilage of the 5-day-old rat." 291-298.

Searls, JC (1976). "Autoradiographic study of chondrocytic proliferation in nasal septal cartilage of prenatal rat." Cleft Palate Journal **13**(OCT): 330-341.

Searls, JC (1977). "Autoradiographic comparison of nasal septal growth in prenatal, newborn, 5-day-old and 10-day-old rats." Journal of Dental Research **56**(7): 874-874.

Searls, JC (1979). "Comparative autoradiographic study of chondrocytic proliferation in nasal septal cartilage of the 5-day-old rat, rabbit, guinea-pig and beagle." American Journal of Anatomy **154**(3): 437-445.

Searls, JC and DD Kinser (1972). "Autoradiographic study of chondrocytic proliferation in nasal septal cartilage of 10-day-old rat." Journal of Dental Research **51**(3): 812-818.

Seinsheimer, F and CB Sledge (1981). "Parameters of longitudinal growth-rate in rabbit epiphyseal growth plates." Journal of Bone and Joint Surgery-American Volume **63**(4): 627-630.

Siegel, MI, MP Mooney, JW Eichberg, T Gest and DR Lee (1992). "Nasal capsule shape changes following septopremaxillary ligament resection in a chimpanzee animal-model." Cleft Palate-Craniofacial Journal **29**(2): 137-142.

Sirianni, JE and RW Goy (1987). "Role of androgens in establishing macaque dentofacial size and morphology." International Journal of Primatology **8**(5): 507-507.

Stenström and Thilander (1972). "Healing of surgically created defects in septal cartilages of young guinea-pigs." Plastic and Reconstructive Surgery **49**(2): 194-199.

Stenström, SJ and BL Thilander (1970). "Effects of nasal septal cartilage resections on young guinea pigs." Plastic and reconstructive surgery **45**(2): 160-170.

Sun, ZY, E Lee and SW Herring (2007). "Cell proliferation and osteogenic differentiation of growing pig cranial sutures." Journal of Anatomy **211**(3): 280-289.

Takigawa, M, M Okada, T Takano, H Ohmae, M Sakuda and F Suzuki (1984). "Studies on chondrocytes from mandibular condylar cartilage, nasal septal cartilage, and spheno-occipital synchondrosis in culture .1. Morphology, growth, glycosaminoglycan synthesis, and responsiveness to bovine parathyroid-hormone (1-34)." Journal of Dental Research **63**(1): 19-22.

Tanaka, E, Y Miyawaki, R del Pozo and K Tanne (2000). "Changes in the biomechanical properties of the rat interparietal suture incident to continuous tensile force application." Archives of Oral Biology **45**(12): 1059-1064.

Thilander, B (1995). "Basic mechanisms in craniofacial growth." Acta Odontologica Scandinavica **53**(3): 144-151.

Thomason, JJ, LE Grovum, AG Deswysen and WW Bignell (2001). "In vivo surface strain and stereology of the frontal and maxillary bones of sheep: Implications for the structural design of the mammalian skull." Anatomical Record **264**(4): 325-338.

Tokimasa, C, T Kawata, T Fujita, M Kaku, S Kawasoko, S Kohno and K Tanne (2000). "Effects of insulin-like growth factor-i on nasopremaxillary growth under different masticatory loadings in growing mice." Archives of Oral Biology **45**(10): 871-878.

Van Cauter, E, M Kerkhofs, A Caufriez, A Van Onderbergen, MO Thorner and G Copinschi (1992). "A quantitative estimation of growth hormone secretion in normal man reproducibility and relation to sleep and time of day." Journal of Clinical Endocrinology and Metabolism **74**(6): 1441-1450.

Varrela, J (1990). "Effects of attritive diet on craniofacial morphology - a cephalometric analysis of a finnish skull sample." European Journal of Orthodontics **12**(2): 219-223.

Verwoerd, CDA, NAM Urbanus and GJ Mastenbroek (1980). "The influence of partial resections of the nasal septal cartilage on the growth of the upper jaw and the nose - an experimental-study in rabbits." Clinical Otolaryngology **5**(5): 291-302.

Vetter, U, W Heit, G Helbing, E Heinze and W Pirsig (1984). "Growth of the human septal cartilage - cell-density and colony formation of septal chondrocytes." Laryngoscope **94**(9): 1226-1229.

Vetter, U, G Helbing, W Heit, W Pirsig, K Sterzig and E Heinze (1985). "Clonal proliferation and cell-density of chondrocytes isolated from human-fetal epiphyseal, human adult articular and nasal septal cartilage - influence of hormones and growth-factors." Growth **49**(2): 229-245.

Vetter, U, W Pirsig and E Heinze (1984). "Postnatal-growth of the human septal cartilage - preliminary-report." Acta Oto-Laryngologica **97**(1-2): 131-136.

Vilmann, H, S Kirkeby and ML Moss (1989). "Skull development in the muscular dystrophic mouse." European Journal of Orthodontics **11**(3): 206-213.

Wealthall, RJ and SW Herring (2006). "Endochondral ossification of the mouse nasal septum." Anatomical Record Part a-Discoveries in Molecular Cellular and Evolutionary Biology **288A**(11): 1163-1172.

Westreich, RW, HW Courtland, P Nasser, K Jepsen and W Lawson (2007). "Defining nasal cartilage elasticity - biomechanical testing of the tripod theory based on a cantilevered model." Archives of Facial Plastic Surgery **9**(4): 264-270.

Wong, BJF, KKH Chao, HK Kim, EA Chu, X Dao, M Gaon, CH Sun and JS Nelson (2001). "The porcine and lagomorph septal cartilages: Models for tissue engineering and morphologic cartilage research." American Journal of Rhinology **15**(2): 109-116.

Wong, KK, S Filatov and DJ Kibblewhite (2010). "Septoplasty retards midfacial growth in a rabbit model." The Laryngoscope **120**(3): 450-453.